ACSNANO

www.acsnano.org

REVIEW

Triboelectric Nanogenerators-Based Therapeutic Electrical Stimulation on Skin: from Fundamentals to Advanced Applications

Weijiang Wang,[Φ] Wentao Sun,[Φ] Yanfeng Du, Wenbin Zhao, Lijun Liu, Yong Sun,* Dejuan Kong, Hongfei Xiang,* Xiaoxiong Wang,* Zhou Li,* and Qingming Ma*

Cite This: https://doi.org/10.1021/acsnano.3c01634

ABSTRACT: Discovery of the amazing and vital therapeutic roles of electrical stimulation (ES) on skin has sparked tremendous efforts to investigate ES suppliers. Among them, triboelectric nanogenerators (TENGs), as a self-sustainable bioelectronic system, can generate self-powered and biocompatible ES for achieving superior therapeutic effects on skin applications. Here, a brief review of the application of TENGs-based ES on skin is presented, with specific discussions of the fundamentals of TENGs-based ES and its feasibility to be applied for adjusting physiological and pathological processes of skin. Then, a comprehensive and in-depth depiction of emerging representative skin applications of TENGs-based ES is categorized and reviewed, with particular descriptions about its therapeutic effects on achieving antibacterial therapy, promoting wound healing, and facilitating transdermal drug delivery. Finally, the challenges and perspectives for further advancing TENGs-based ES toward a more powerful and versatile therapeutic strategy are discussed, particularly regarding opportunities in fundamental multidisciplinary research and biomedical applications.

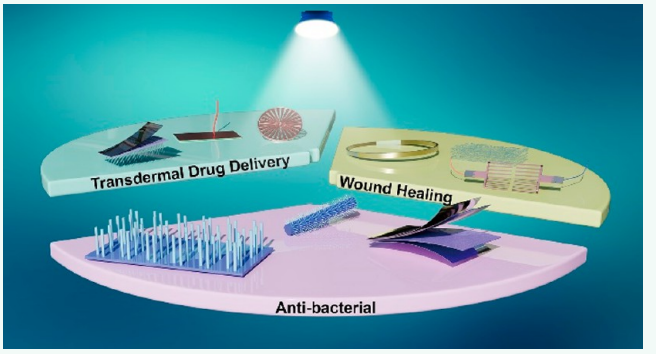

KEYWORDS: *triboelectric nanogenerators, electric stimulation, transdermal drug delivery, antibacterial, wound healing, skin, therapeutic applications, energy conversion*

The skin serves as a crucial barrier that protects the human body from external elements and substances while also regulating body temperature and reducing water loss.[1,2] Additionally, the skin has been utilized as an effective route for delivering drugs to treat various diseases through transdermal drug delivery, as it offers an alternative to traditional injection or oral administration methods. By avoiding first-pass metabolism and providing sustained drug release over time, transdermal drug delivery holds great promise.[3,4] Nevertheless, the skin, as the largest organ on the body surface, can be easily compromised by accidents or external insults, resulting in skin diseases like bacterial infection and skin wound and leading to the loss of their functions of transdermal drug delivery.[5]

Over the past decades, many physiotherapeutic strategies, such as electrical stimulation (ES), ultrasonication, and heating,[6−9] have been directly engineered as therapeutic agents for skin diseases, including treating bacterial infection and promoting wound healing.[10−12] Among these approaches, ES has gained significant attention due to its multifaceted therapeutic effects, including reducing bacterial adhesion, improving cellular immunity, increasing perfusion, and accelerating wound healing.[13,14] Not only can ES reduce bacterial infection and avoid antibiotic resistance by altering the permeability of the bacterial cell membrane, it can also enhance tissue regeneration by promoting the migration of fibroblasts to the wound site.[15,16] Furthermore, ES can facilitate transdermal drug delivery through iontophoresis and electroporation, allowing for the enhanced penetration of drugs across the skin barrier.[17,18] Despite the advancements in applying ES on skin, several challenges remain in the practical application.[19,20] For

Received: February 20, 2023
Accepted: May 24, 2023

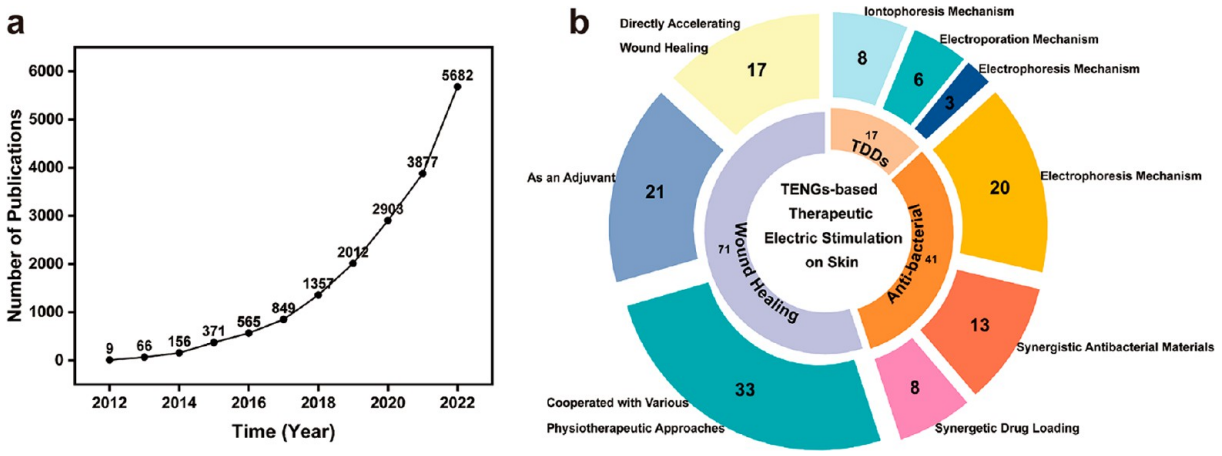

Figure 1. a) Growth in the number of publications in the field of TENGs reflecting the increasing interest in TENGs research. b) Summary of the number of publications when the words "triboelectric nanogenerator" and "electrical stimulation" are combined with common words related to therapeutic skin applications, including "antibacterial", "wound healing", and "transdermal drug delivery". Data were extracted from Scopus search in February 2023 for the appearance of these common words in title, abstract, and keywords of publications when combined with the words "triboelectric nanogenerator" and "electrical stimulation". This shows the continued growth of this field.

instance, traditional power supplies for ES tend to be bulky and have poor stability, and the requirement for battery replacement and the associated costs from device aging limit its widespread use.[21,22] To address these challenges and fully realize the potential of ES on skin, the development of a self-sustaining bioelectronic system that provides therapeutic ES would represent a valuable strategy.[23]

Recently, the advent of triboelectric nanogenerators (TENGs) has resulted in the creation of self-powered and biocompatible ES for improved therapeutic effects on skin.[24] Originally proposed by Professor Z. Wang in 2012, TENGs utilize triboelectrification and electrostatic induction to convert mechanical energy into electrical energy.[25,26] Since then, the number of publications about TENGs each year increases significantly according to the analysis of the published literature from the citation database Scopus (Figure 1a). Particularly, the features of TENGs, including high charge density, flexible structure, low cost, and broad applicability, make them ideal for powering ES on the body's surface.[27] Furthermore, the electrical properties of TENGs-based ES match the requirements for the physiological and pathological processes of the skin, thus offering a highly effective means of treating skin diseases such as bacterial infections and promoting wound healing.[28−32] Additionally, TENGs-generated electricity can be used to enhance transdermal drug delivery for the treatment of various diseases.[33] Overall, TENGs-based ES is linked to the growing field of achieving therapeutic effects on skin applications as reflected in the data extracted from Scopus (Figure 1b). Significant progress has been made in applying TENGs for generating therapeutic electrical impulses on skin,[34] which calls for a comprehensive depiction of its whole scene, from fundamentals to various advanced applications.

In this review, we highlight up-to-date progress in TENGs-based therapeutic ES for different skin applications (Figure 2). First, the fundamentals of TENGs-based ES, including the working mechanism of TENGs and their operating modes for generating ES, are introduced. Then, the relationship between the characteristics of TENGs-based ES and the electrophysiological process of skin is interpreted in depth, demonstrating the feasibility of applying TENGs-based ES on skin. Afterward, emerging skin applications benefits from the TENGs-based ES are systematically reviewed into three major categories, including antibacterial, wound healing, and transdermal drug delivery, highlighting the beauty of fundamental science and envision of therapeutic applications. The challenges and perspectives on developing TENGs-based ES with innovative applications are proposed and discussed in the end.

TRIBOELECTRIC MATERIALS SELECTION CRITERIA

TENGs represent a technology for converting biomechanical energy into electrical energy.[43,44] In biomedical applications, TENGs-based ES can be used for skin therapeutic roles, such as antibacterial therapy, promoting wound healing, and facilitating transdermal drug delivery. TENGs utilize the coupling effect of triboelectricity (TE) and electric induction.[45] In other words, the basic working mechanism of TENGs is considered to be a combination of two materials separated by a gap that works like a capacitor. It was found by Wang et al. that, when focusing on the nanoscale, TE can be seen to control the electron transfer mechanism.[45] TENGs typically work in four different modes: Contact Separation Mode, Lateral Sliding Mode, Single Electrode Mode, and Free-standing Triboelectric Layer Mode.[46,47] The output performance of TENGs is mainly affected by the material surface charge properties and environment impacts. The characteristics of the material's surface potential, roughness, and composition are crucial in determining the TENGs output performance. Additionally, the external elements, such as motion parameters, temperature, and humidity, can also influence the output performance of TENGs. Among these factors, the material surface potential properties are particularly important for the output characteristics of TENGs. In Figure 3a, AlphaLab constructed a series of triboelectric materials used to guide the development of high-performance TENGs.[48,49] Materials that are spaced widely apart or at the other end of the triboelectric series have been shown to make high-performance devices. Recently, some high-performance triboelectric materials like RSSP, Ecoflex-B, and fluorinated ethylene propylene (FEP) have been developed for application in the field of TENGs.[50,51] In addition to possessing good triboelectric properties, these materials must also possess certain levels of biocompatibility, antibacterial effectiveness, and other qualities to be used on human skin. Thus, careful materials

https://doi.org/10.1021/acsnano.3c01634
ACS Nano XXXX, XXX, XXX−XXX

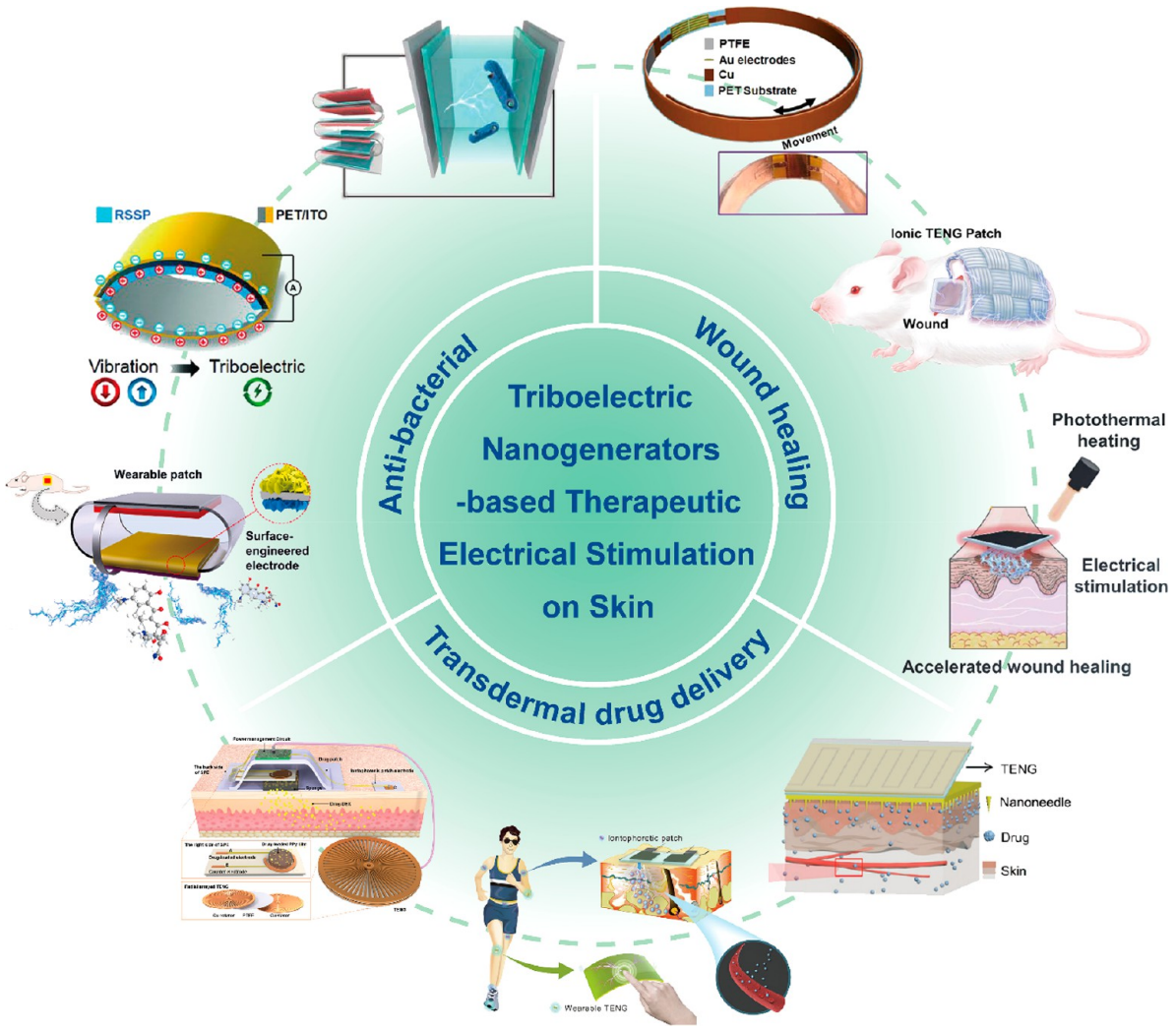

Figure 2. TENGs-based therapeutic electric stimulation for different applications on skin, including antibacterial, wound healing, and transdermal drug delivery. Reproduced with permission from ref.[35] Copyright 2018 Elsevier. Reproduced with permission from ref.[36] Copyright 2018 Wiley-VCH. Reproduced with permission from ref,[37] Copyright 2021 Elsevier. Reprinted with permission under a Creative Commons ACS Author Choice License from ref.[38] Copyright 2018 Yin Long et al., published by American Chemical Society. Reproduced with permission from ref.[39] Copyright 2020 Elsevier. Reproduced with permission from ref.[40] Copyright 2021 Elsevier. Reproduced with permission from ref.[41] Copyright 2019 Elsevier. Reproduced with permission from ref.[42] Copyright 2019 Wiley-VCH. Reproduced with permission from ref.[33] Copyright 2019 Wiley-VCH.

selection is required when designing TENGs for these applications. Furthermore, each specific application requires materials with distinct features and electric parameters tailored to meet those particular purposes. Here in this section, we summarize the specific criteria for selecting triboelectric materials for antibacterial therapy, wound healing, and transdermal drug delivery. We also offer some insights into the selection criteria of TENGs triboelectric materials.

Triboelectric Materials for Antibacterial Therapy. In order to achieve the desired bactericidal effect, the electrical output performance must be maintained at a high level.[52] Thus, to improve the output performance of TENGs, the two triboelectric materials should have electrical properties that are noticeably opposite to one another. Current antibacterial TENGs use triboelectric materials with significant variations in surface potential properties as friction layers to achieve high output performance. Examples of such materials include PDMS, gelatin/glycerol (G/G) film, RSSP, PET, PTFE, and Mg−Al LDH@Al film.[35,37,53] Furthermore, modifying the nanofibers on the electrode can further enhance the electric field. In addition to boosting electrical output performance, the triboelectric materials can also perform synergistic bactericidal functions. For instance, recombinant spider silk proteins (RSSP), which is a triboelectric material and antibacterial substance, can simultaneously act as a friction layer and sterilize bacteria, thereby enhancing the antibacterial effect.[36] Additionally, Mg−Al LDH@Al film can also be used as a friction layer and a drug container to play a synergistic antibacterial role under electric stimulation. In summary, choosing triboelectric materials with high-voltage performance and synergistic antibacterial capabilities is an appealing choice for antibacterial applications.

Triboelectric Materials for Wound Healing. Similar to antibacterial, the electrical output performance of triboelectric materials is also essential for wound healing. Appropriate voltage and current density can facilitate cell migration and proliferation, which is the cellular foundation of wound healing. Besides, the flexibility of friction layers is especially essential for wounds. Ionic patch, Ecoflex-B, nylon-coated cloth, and leather are all

https://doi.org/10.1021/acsnano.3c01634
ACS Nano XXXX, XXX, XXX−XXX

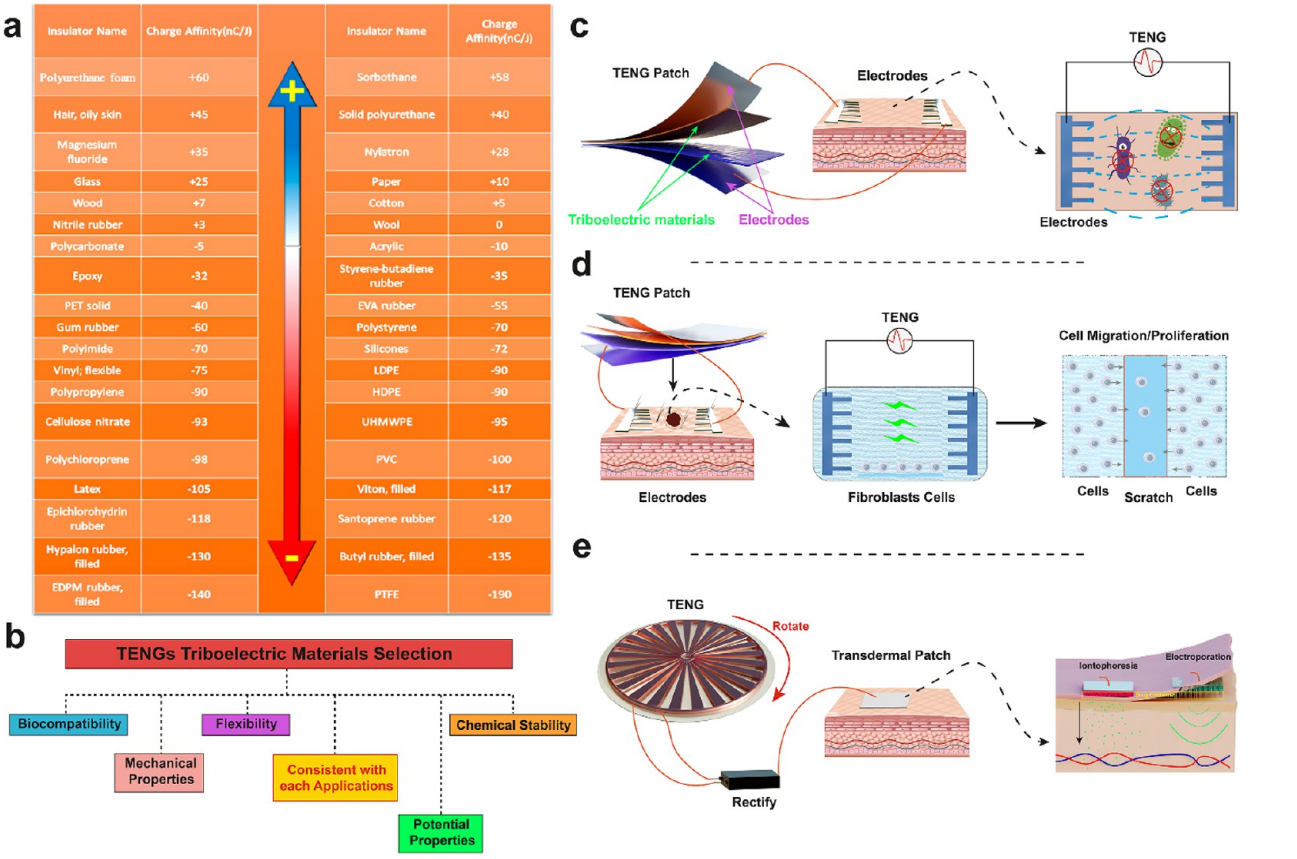

Figure 3. Illustration of the materials selection criteria and model systems of TENGs for different skin applications. a) Triboelectric series developed by AlphaLab (© 2009). Reproduced with permission from ref.[57] Copyright 2017 Cell Press. b) Proposed general criteria for TENGs triboelectric materials selection to facilitate therapeutic roles of TENGs-based ES in targeting biomedical applications. c–e) Model systems to illustrate the generation and propagation of TENGs-based ES through skins for playing therapeutic roles on (c) antibacterial therapy, (d) wound healing, and (e) transdermal drug delivery.

flexible triboelectric materials with excellent surface potential properties and wound compatibility, preventing further harm for wound from the hard friction layers.[39,54,55] Select triboelectric materials for wound healing that can provide adequate electrical performance as well as superb flexibility is critical. Besides, it is also possible to enhance the skin comfort of nonflexible materials by incorporating triboelectric materials into textile fabrics.[56] Furthermore, hydrogel has been proved to have the effect of promoting wound convergence in wound healing.[12] Making the friction materials as the hydrogel or combining the hydrogel with the friction layer represents the promising directions for the future development of TENGs for wound healing. In summary, it is essential to consider both the compatibility of the materials with the wound and the output performance for promoting wound healing.

Triboelectric Materials for Transdermal Drug Delivery. Current systems developed for transdermal drug delivery are primarily made up of TENGs, a rectifier bridge, and transdermal electrode patch. By changing the drug repository, patients can prolong the service life of the product without having to replace TENGs. In addition, most TENGs devices are wearable due to being required to satisfy patient self-controlled release needs. Under these circumstances, the human skin environment, such as temperature, humidity, and slight acidity, must be considered when choosing triboelectric materials. These traits present various requirements for triboelectric materials, such as oxidation resistance, surface potential stability, and a portion corrosion protection. Furthermore, the TENGs friction layer coupled with antibacterial materials will improve patient compliance even further.

Moreover, some general criteria for the selection of TENGs triboelectric materials to achieve higher effectiveness and performance are listed below (Figure 3b).

1. Biocompatibility: To avoid adverse reactions when materials come into contact with biological tissues or fluids, TENG materials should be biocompatible. Safe materials with a long history of medical device usage, such as silicone, polyethylene, and polypropylene, are excellent options for TENGs.
2. Mechanical Properties: Materials used in TENGs should have adequate mechanical properties to endure repeated mechanical stimulation. They should be flexible, durable, and have a high tensile strength. Common TENG materials with good mechanical properties include polydimethylsiloxane (PDMS), polyurethane (PU), and poly(ethylene terephthalate) (PET).
3. Surface Potential Properties: To guarantee high amounts of charge transmission and high output performance, it is suggested to choose two kinds of triboelectric materials with substantial potential properties differences if at all feasible.
4. Flexibility: Wearable techniques are increasingly being used by TENGs devices to accomplish application effects, which can significantly improve user compliance and will

https://doi.org/10.1021/acsnano.3c01634
ACS Nano XXXX, XXX, XXX−XXX

add additional requirements for triboelectric materials selection.

5. Chemical Stability: TENGs triboelectric materials should be chemically stable to avoid degradation when exposed to biological fluids or environmental factors, especially for wearable TENGs devices.
6. Additional Features Consistent with the Applications: As we discussed above, different applications of TENGs-based ES require distinct triboelectric materials requirements. For antibacterial purpose, the friction materials output performance qualities and synergistic antibacterial function are the main factors that should be considered. For wound healing, the most significant factors are the flexibility of triboelectric materials and the compatibility with the wound sites. So far as transdermal drug delivery, the first consideration is various stability factors. When choosing TENGs materials, it is critical to consider the application in its entirety.

In conclusion, by considering these criteria, researchers can choose appropriate materials for developing TENGs to facilitate therapeutic roles of TENGs-based ES in targeting biomedical applications, such as wound healing, antibacterial, and transdermal drug delivery.

FEASIBILITY OF APPLYING TENGS-BASED ES TO REGULATE THE PHYSIOLOGICAL AND PATHOLOGICAL PROPERTIES OF THE SKIN

In this section, we present a systematic demonstration of the feasibility of applying TENGs-based ES to regulate the physiological and pathological properties of the skin. First, we provide model systems to briefly explain the generation and propagation of TENG-based ES through skin for therapeutic purposes, including antibacterial therapy, wound healing, and transdermal drug delivery. We then discuss in detail the underlying mechanisms of how the skin-propagated TENG-based ES promotes these functions.

For antibacterial therapy, wearable TENG patches are frequently used as surface antibacterial devices. These patches consist of two triboelectric materials placed next to each other, covered by electrodes on both sides that can be embedded in garments or affixed to the skin surface. The TENG patch electrodes connect to outer electrodes attached to the skin, allowing charge transfer between the two triboelectric materials via one working mechanism while voltage is transmitted to the skin through electrodes and wires. This creates an electric field between the skin electrodes, which exerts bactericidal effects through various mechanisms, such as electroporation and formation of hydrogen peroxide (HP), as shown in Figure 3c. Similarly, TENG patches for wound healing are wearable at the wound site, with external electrodes connected to the TENG patch placed on both sides of the wound to provide sufficient electric stimulation. The electric field between the two electrodes triggers diverse positive alterations in wound healing, such as cell migration and proliferation, as shown in Figure 3d. For transdermal drug delivery, TENGs patch can be designed to be self-regulating or wearable to meet distinctive requirements, such as continuous therapy and real-time regulated release. To integrate voltage, most TENGs transdermal devices use a rectifier bridge, which converts bidirectional pulse current (PC) and alternating current into direct current (DC) for transdermal patches.[41,42] The wires transmit the voltage produced by TENG to the rectifier, which is then rectified and sent to the transdermal patch (Figure 3e). The transdermal patch utilizes electrical stimulation to enhance the skin's permeability for drugs through various mechanisms, such as iontophoresis, electroporation, and electrophoresis. It is worth noting that the proposed model systems are not comprehensive enough to fully illustrate the generation and propagation of TENGs-based ES through skins for playing therapeutic purposes, and a more sophisticated and general model system is highly desired in the future.

In the following part, we will discuss the deeper mechanism of how the skin-propagated TENGs-based ES produces distinctive functions, such as improving antibacterial capacity, accelerating wound healing, and promoting transdermal drug delivery.

Mechanism of TENGs-Based ES for Promoting Transdermal Drug Delivery. *Iontophoresis.* Iontophoresis, a technology that facilitates the introduction of ionic medications into the body through the application of low-voltage current to the skin, has been shown to achieve high-efficiency transdermal drug delivery.[29] For transdermal drug delivery, iontophoresis refers to the application of a moderate electric stimulation.[58] The mechanism of ion transport across the skin and into the bloodstream during iontophoresis is primarily through two processes: electromigration and electroosmosis. Electromigration refers to the movement of ions, where negatively charged anions are attracted to the cathode and positively charged cations are attracted to the anode.[59] Conversely, electroosmosis involves the convection motion of water induced by electric stimulation and is particularly beneficial for neutral drug molecules that do not ionize when exposed to electric current. Furthermore, TENGs-based devices have been demonstrated to play a significant role in transdermal efficiency and compliance by converting biomechanical energy into moderate pulse current and direct current through a rectifier bridge. In PC iontophoresis, skin depolarization after each pulse treatment leads to a reduction in skin irritation and impedance, ensuring continuous transdermal drug delivery.[60] In DC iontophoresis, TENGs charged for 3 min can provide available electric stimulation for 20 min due to capacitive storage of electricity. These findings demonstrate that TENGs-based electric stimulation is well-suited for iontophoresis due to its moderate electric stimulation, stability, and high compliance.

Electroporation. The utilization of electroporation in transdermal drug delivery involves the application of high-voltage pulses, typically in the range of 100 V, to create aqueous pores for the introduction of a diverse range of drugs into deeper layers of the skin.[30] The TENG equipment is capable of producing voltage exceeding 100 V, meeting the demands of this process. Furthermore, the current generated by TENGs is generally below 100 μA, ensuring a relatively safe electroporation process. Compared to iontophoresis, electroporation not only enables transdermal drug delivery but also enables the introduction of viral drug molecules into various cell types through the creation of cell membrane apertures. However, electroporation, like most intracellular delivery techniques that rely on membrane rupture, is faced with the challenge of post-treatment cell death, which may result from electroporation, lysis, or severe thermal damage.[61,62] To mitigate this challenge, electroporation is being investigated in conjunction with microneedles arrays, as demonstrated by Liu et al.[33] The utilization of TENGs-based microneedles arrays limits the electrical stimulation to the tip of the needles, resulting in an enhanced electrical field of 2800 V cm^{-1} and reduced applied voltage and cellular damage. Thus, TENGs-based electrical

https://doi.org/10.1021/acsnano.3c01634
ACS Nano XXXX, XXX, XXX−XXX

stimulation satisfies the voltage requirements and can improve the output and reduce cellular damage by combining with microneedles.

Mechanism of TENGs-Based ES for Accelerating Wound Healing. *Recruitment of Immunocytes.* Accelerating the recruitment of immunocytes and cytokines plays a function in enhancing wound healing during the early phase of inflammation. For the duration of the inflammatory phase, the acceleration of recruitment is advantageous for accelerating the wound healing process. According to studies, macrophages, lymphocytes, and neutrophils move to the site in response to endogenous electrical stimulation.[63]

Resolution of Inflammation. It is well-established that the recruitment of immunocytes and cytokines in the early stage of inflammation can have a positive impact on wound healing. However, the duration of the inflammatory response can also have a significant impact on the rate of wound healing. If the levels of cytokines persist for an extended period, it can negatively impact the overall wound healing process.[64] To mitigate this effect, TENGs-based ES has been proposed as a method to reduce the amounts of immunocytes and cytokines present in the body during the late phase of the inflammatory response. By resolving the inflammation, TENGs-based ES has the potential to play a key role in the wound healing process.

Antibacterial. When the number of bacteria exceeds a certain threshold, the inflammatory cells may no longer be able to effectively eliminate the microbes, leading to infection and prolonging the wound healing process.[65] To address this issue, wound sterilization has been proposed as a means to shorten the time required for wound healing. Wolcott et al. were pioneers in investigating the impact of exogenous ES on *in vivo* antibacterial activity.[31] In their study, they used negative polarity DC to treat chronic wounds infected with Proteus and Pseudomonas species. They found that the wounds were free of infection a few days later, demonstrating the efficacy of exogenous ES in sterilizing skin wounds. The mechanism behind the direct antibacterial activity of ES is believed to involve two processes: electroporation effects and the formation of hydrogen peroxide. TENGs have been shown to generate sufficient voltage to support these processes and promote antibacterial activity.

Migration and Proliferation of Cells. During the proliferative phase of wound healing, the formation of new granulation tissue and epithelium is a key aspect. Research has revealed that fibroblasts, endothelial cells, and epithelial cells respond to electrical impulses during this phase.[64] The electric field generated by electrical stimulation has been shown to provide directional signals to cells and override other directional cues, such as chemokine gradients and pressures.[66] This effect of electrical stimulation on cell migration cannot be replicated by other therapeutic options. Numerous studies have demonstrated that exogenous electrical stimulation can promote cell proliferation and accelerate the wound healing process. These findings highlight the potential of electrical stimulation as a therapeutic tool in the management of wounds.[67]

The rate of wound closure in epithelial cells is found to be positively correlated with the rate of recovery.[68] The mechanism of the basal skin potential has a significant impact on the migration and proliferation of these cells.[69] The application of a DC electric field has been shown to enhance the endogenous electric field recovery, thus promoting faster wound healing. In particular, research has demonstrated that the application of a DC electric field as low as 10 mV mm^{-1} is sufficient to induce directional migration of keratinocytes.[70]

The impact of direct current (DC) electrical stimulation on fibroblast development was investigated by Dunn et al. in 1988. The study utilized carbon fiber electrodes impregnated with collagen sponge matrix and observed directional migration of fibroblasts toward the anode.[71] This migration was believed to be mediated by the activation of the phosphoinositide 3-kinase (PI3K) and the Na+/H+ exchange isomer 1 (NHE1) signaling pathways.[72] Subsequent research by Konstantinos et al. has revealed that the levels of scratch closure and proliferation in fibroblasts can be dramatically increased by ES.[73] They hypothesized that microcurrents may play a role in accelerating cell migration and proliferation by phosphorylating mitogen-activated protein kinase (MAPK). In conclusion, the results of these studies suggested that TENGs-based ES can promote the migration and proliferation of fibroblasts, thus promoting the formation of granulation tissue and wound healing. This mechanism of promoting fibroblast migration and proliferation is considered to be the most important and widely used approach for TENGs-based ES in wound healing.

Angiogenesis is a crucial aspect of the proliferation phase and a vital component of granulation tissue formation in wound healing. Rapid induction of vascular endothelial growth factor (VEGF) after injury is known to stimulate the migration, proliferation, and vascularization of endothelial cells.[74] Recent research has established that exogenous ES can enhance the production of VEGF at the wound site, which may represent one of the pathways by which electrical stimulation promotes vascularization.[75,76] These findings suggest that, by promoting the migration and vascularization of endothelial cells, TENGs-based ES may accelerate the pace of wound healing.

Mechanism of TENGs-Based ES for Improving Antibacterial Therapy. The direct antibacterial mechanism created by ES is thought to be composed of two components: electroporation and the formation of a significant amount of hydrogen peroxide (HP) through electrolysis. Electroporation requires a high-voltage electric field greater than 100 V delivered in a pulse, while the production of H_2O_2 is enhanced with extended ES application of more than 8 h. This results in H_2O_2 buildup in the wound area, reaching a concentration of approximately 6−15 mmol L^{-1} at 24 h, which is capable of effectively inhibiting and killing bacteria such as *Staphylococcus aureus* and *Escherichia coli*.[37] The mechanism behind this antibacterial activity is believed to be DNA strand breakage caused by the oxidation of DNA by reactive oxygen species (ROS) released by the decomposition of HP.[77] ROS are oxygen-containing molecules with unpaired electrons (free radicals). TENGs devices are an excellent choice for delivering high-voltage pulse ES required for the aforementioned processes. In addition to the direct antibacterial effects, TENGs-based ES can also indirectly inhibit bacterial growth by attracting neutrophils and macrophages.[28] Furthermore, TENGs-based ES may also reduce bacterial adhesion, thus lowering the likelihood of biofilm development in chronic wounds, where bacteria can form antibiotic-resistant polymicrobial biofilms.[78]

APPLYING TENGS-BASED ES FOR ANTIBACTERIAL THERAPY

Cutaneous bacterial infection has persisted as a major threat to public health during the last several decades.[79] *Staphylococcus aureus* and *Escherichia coli*, respectively, belong to species of Gram-positive and Gram-negative bacteria and may transmit illness in a variety of different ways.[80−82] Particularly, skin is a vulnerable target of bacterial infection, due to the fact that skin is

https://doi.org/10.1021/acsnano.3c01634
ACS Nano XXXX, XXX, XXX−XXX

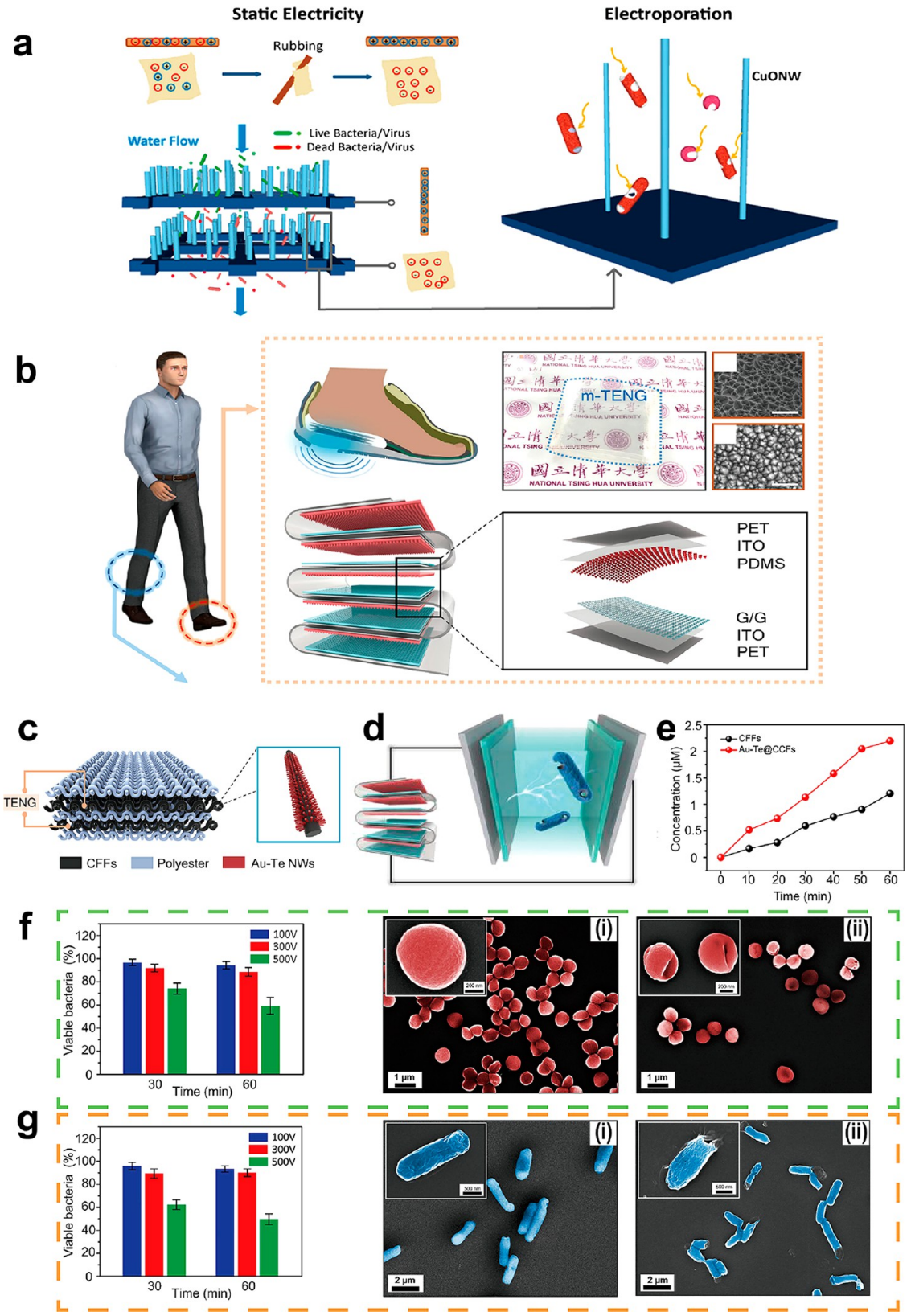

Figure 4. Schematics of CuONW filtration device during operation powered by static electricity and m-TENG-based ES for wearable disinfection system. a) Filtration apparatus based on CuONW. Reproduced with permission from ref.[53] Copyright 2014 American Chemical Society. b) Arrangement of the components that make up the wearable, self-powered sterilization system. b) A wearable fiber-based electroporation device's schematic design. d) The experimental setup is shown schematically. e) Different periods of operation result in different amounts of H_2O_2 being produced by the self-powered disinfection system. f, g) Before-and-after SEM images of S. aureus and *E. coli* before (f) and after (g) being subjected to m-TENG-based ES, as well as quantitative maps of each virus inventory at various voltages. Reproduced with permission from ref.[35] Copyright 2018 Elsevier.

https://doi.org/10.1021/acsnano.3c01634
ACS Nano XXXX, XXX, XXX−XXX

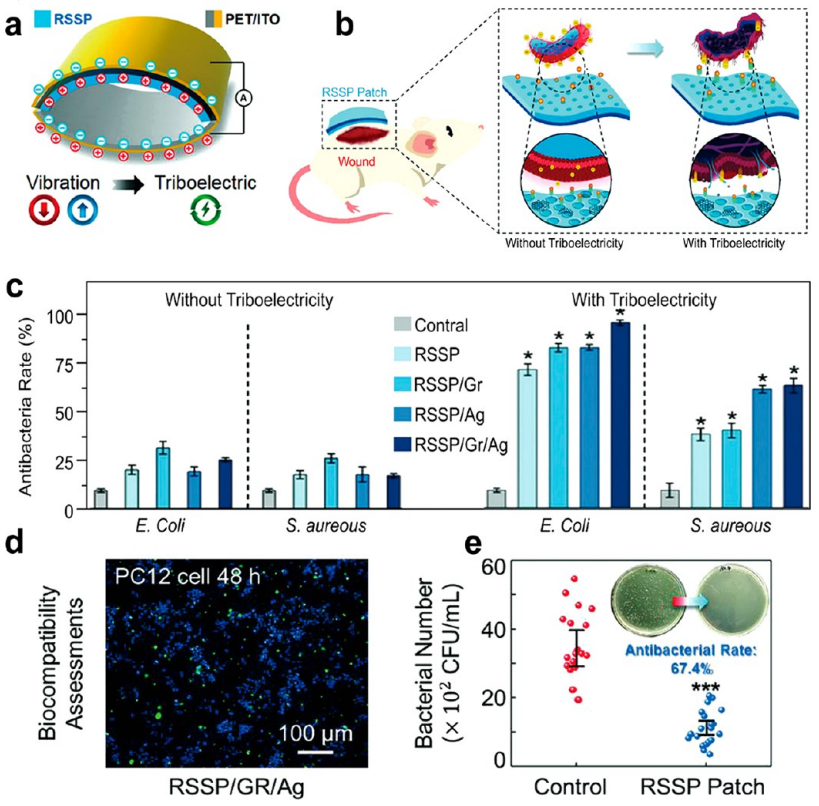

Figure 5. As an antibiotic-free antibacterial patch, nanocomposites based on RSSPs seem promising. a) Depiction of the basic operating principle of RSSP-TENG, showing how efficiently RSSP may lose electrons upon contact with PET. b) The antibacterial defense mechanism diagram. c) Both the RSSP patch and the RSSP-doped patch showed promising antibacterial activity against *E. coli* and S. aureus. d) Neuronal PC12 cells cultured *in vitro* for 48 h on an RSSP/GR/Ag substrate showed excellent biocompatibility. e) The RSSP patch inhibited *S. aureus in vivo*, as evidenced by bacteria counts in the infected site. Reproduced with permission from ref.[36] Copyright 2018 Wiley-VCH.

in constant contact with the clothing which absorbs and holds onto moisture, and such condition is conducive to the growth of microbes.[83] Antibiotics are by far the most popular method used in the battle against cutaneous bacterial infection, but the administration of antibiotics over an extended period may lead to a rise in antibiotic resistance. Electrical stimulation (ES) has been shown to be an equally effective therapeutic agent of reducing growth of the bacteria as the use of antimicrobial drugs.[84−87] The electroporation effect[88] caused by the high-voltage electric field and the formation of a great deal of hydrogen peroxide by electrolysis[89,90] are now thought to be the two parts of the antibacterial mechanism created by ES. Since the antibacterial mechanism of ES generally does not cause resistance in bacteria, it is anticipated that ES can be applied as an effective therapeutic strategy for bacterial infections. Multiple works have been conducted by applying TNEGs-generated ES to treat cutaneous bacterial infection. For instance, a fast water disinfection device was successfully developed using copper oxide nanowires and static electricity, which can achieve complete disinfection at a high rate.[91] As shown in Figure 4a, static electricity can be generated by an external TENG and applied to the two parallel copper oxide nanowire (CuONW) electrodes, which were compressed inside an in-line filter holder. Though copper oxide nanowire, a localized increased electric field can be produced, which enabled fast water disinfection. Raw water from the tap and lake water were both completely disinfected of harmful germs and viruses with a single filter at a rate of 3000 L per minute per square meter. The disadvantage should be noted that, even though this apparatus could eliminate waterborne microorganisms, widespread usage on the skin is unlikely until the TENGs that produce therapeutic ES can be miniaturized.[36,92]

To realize miniaturization of therapeutic TENGs-based ES, trials have been attempted. For instance, a motion-activated self-powered active disinfection system was developed using conductive textiles, Au−Te nanowires, and a multilayered TENG, which can eliminate harmful microorganisms and enhance H_2O_2 enrichment for effective electroporation-assisted disinfection.[35] The system was primarily made up of conductive textiles as electrodes and a multilayered triboelectric nanogenerator (m-TENG) for capturing biomechanical energy. Specifically, as shown in Figure 4b, the system included a shoe-integrated TENG power source, a full-wave diode bridge to rectify electric output from the TENG, and carbon fiber fabrics (CFFs) with/without surface modifications of one-dimensional (1D) nanomaterials as electrodes for sterilization. The proposed self-powered active disinfection system was readily adaptable for use in industrial textiles, allowing production of "smart garments" that can eliminate harmful microorganisms. Apart from this, one of the most impressive aspects of their work is the modification of Au−Te nanowires (Au−Te NWs) on the CFFs, whereas 1D Au−Te NWs can build up a much stronger electric field near the nanowire tip, as shown in Figure 4c. Moreover, micropatterned surfaces, which increased effective contact area and friction during contact and separation, were also a reasonable design for boosting triboelectrification efficiency. In order to evaluate how the m-power TENG's output affected the efficacy of its electro-

https://doi.org/10.1021/acsnano.3c01634
ACS Nano XXXX, XXX, XXX−XXX

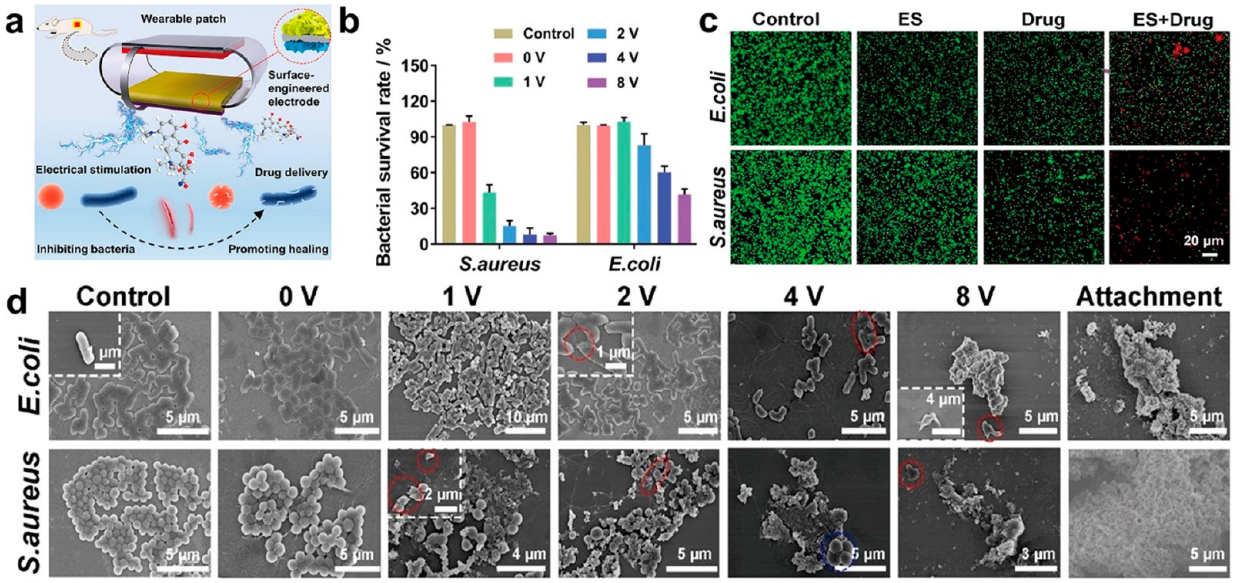

Figure 6. Functions of surface-engineered TENGs that inhibit bacterial growth. a) The suggested mechanism for boosting infected wound healing. b) Bacterial survival rate after 24 h under ES of various intensities produced by SETENG. c) Images of live (green) and dead (red) bacteria after 2 h of treatment with ES (2 V), minocycline (5 g), or both. d) SEM photos of bacteria and electrode attachments were taken at varied ES intensities. Reproduced with permission from ref.[37] Copyright 2021 Elsevier.

poration-assisted disinfection, a pair of metal plates was used, as shown in Figure 4d. The bacterial survival rate declined as the electric field intensity and treatment period increased. *S. aureus* and *E. coli* were monitored before and after being subjected to ES by scanning electron microscopy (SEM). After treatment, holes can be clearly observed on the bacterial surface, indicating that the electroporation disinfection mechanism contributes to the antibacterial effects of m-TENG-based ES, as shown in Figure 4f,g. To determine the concentration of generated H_2O_2, the hydrogen peroxide/peroxidase test was conducted by the researchers, which indicated that the H_2O_2 concentration increased linearly with operation time and was doubled with the help of Au−Te NWs, demonstrating the potential of their self-powered antibacterial system to enhance H_2O_2 enrichment and combine it with the electroporation process.

While miniaturizing therapeutic TENGs-based ES, incorporating antimicrobial materials in the construction of TENGs can achieve synergistic antibacterial effects. For instance, a biocompatible and high-performance wearable TENG was developed by genetically engineering recombinant spider silk proteins (RSSP) that exhibited strong bactericidal performance on *S. aureus* (antibacterial rate up to 58%) and *E. coli* (antibacterial rate up to 93%), with promising biocompatibility in cell culture and *in vivo* testing, as shown schematically in Figure 5.[36] The RSSP patch, which was triboelectrically charged, created a potential differential between the bacteria and the positive electrode surface, as shown in Figure 5a. After bacteria were charged, their morphology was altered due to extracellular electron transfer between the bacteria and the RSSP patch, which also caused a burst of reactive oxygen species inside the bacteria and ultimately led to their demise, as shown in Figure 5b.[93] To assess those intrinsic triboelectric characteristics of different RSSPs, a TENG apparatus with a vertical contact-separation mode was utilized. The surface would get electrified when the two contacted with one another and then separated, which resulted in a potential difference. As a result, the morphology of bacterial cell can be altered due to the extracellular electron transmission. Moreover, graphene (GR) or Ag nanoparticles were incorporated into the RSSP patch to offer synergetic antibacterial effects. Therefore, the developed system exhibited a strong bactericidal performance on both *S. aureus* (antibacterial rate up to 58%) and *E. coli* (antibacterial rate up to 93%), as illustrated in Figure 5c. Besides, antimicrobial efficacy and biocompatibility are both essential for applying TENGs in clinics. The cytotoxicity of the TENG was assessed by growing PC12 neurons on charged RSSP samples, with the results depicted in Figure 5d showing that the RSSP/graphene/Ag composite patch samples exhibited excellent biocompatibility in cell culture. In addition, as illustrated in Figure 5e, the developed TENG achieved an antibacterial rate of 67.4% in *S. aureus* infected mice, thus indicating its potent antibacterial capability *in vivo*.

As mentioned above, the therapeutic TENGs-based ES for antibacterial therapy typically operates at hundreds of volts, which may result in electroporation and harm normal cells. Therefore, to prevent damage to normal cells, TENGs-based ES with low intensity has been designed and generated. For instance, Du et al. developed a low-intensity electric impulse generating surface engineered TENG (SETENG) patch using a Mg−Al double hydroxides (LDH) friction layer that also acted as smart drug containers to obtain synergetic antibacterial effects and demonstrated the significant synergistic antibacterial effect of combining minocycline with ES, as shown in Figure 6.[37] The alternating low-intensity electric field (LIEF) can change membrane permeability and lead to hydrogen peroxide buildup. Specifically, the arch-shaped patch was composed of polytetrafluoroethylene (PTFE) (electronegative) and Mg−Al LDH@Al film (electropositive), as shown schematically in Figure 6a. *S. aureus* and *E. coli* were used as models to investigate how bacteria react to AC LIEF of varying volts produced by the developed TENG. As shown in Figure 6b, bacterial inhibition was enhanced when increasing the voltage. SEM was also employed to investigate the effects of ES over bacteria. As shown by the SEM images in Figure 6d, cell membranes were largely damaged after the ES treatment; when the voltage was raised to 8 V, fractured membranes can be observed. Moreover, minocycline

https://doi.org/10.1021/acsnano.3c01634
ACS Nano XXXX, XXX, XXX−XXX

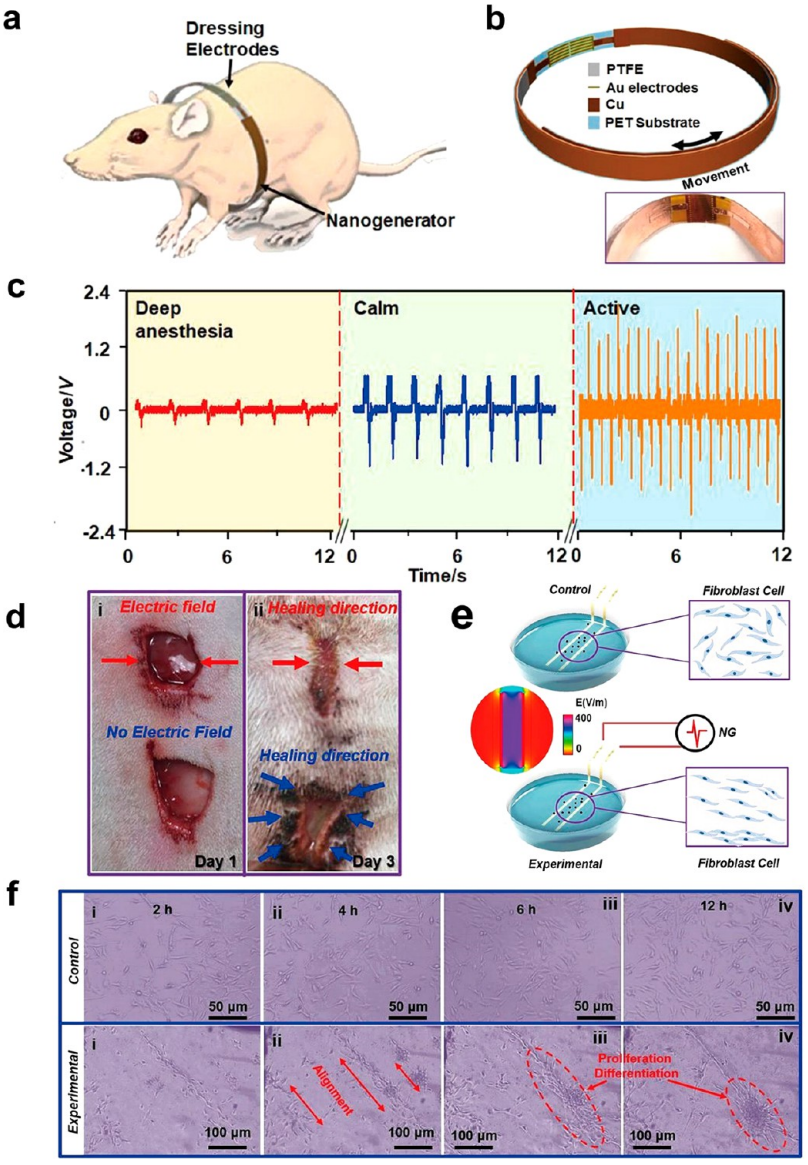

Figure 7. TENG-based electrical bandages that can offer ES for accelerated wound healing. a) Schematics illustrate the practical application of the TENG-based bandage. The SD rat's chest was covered in a bandage, which captured biomechanics energy from of the rat's breathing and transformed it into electrical energy. b) Diagram of the TENG-based bandage. c) Rat breathing at various frequencies can induce electrical activity in the TENG. d) Digital depictions of three-day healing progression for rectangular wounds with and without the treatment of ES generated by the developed bandage. e) A diagram shows a dish of grown cells with Au electrodes linked and disconnected to a pulse voltage created by TENG. f) Analysis of the morphology of cultured cells before and after being subjected to ES. Reprinted with permission under a Creative Commons ACS Author Choice License from ref.[38] Copyright 2018 Yin Long et al., published by American Chemical Society.

was used as the model drug to be encapsulated in the developed TENG. To assess the bactericidal effect of combining minocycline with ES, SYTO 9/PI staining was utilized. As shown by the fluorescent images in Figure 6c, the single treatment with ES (2 V) or minocycline showed modest bactericidal efficacy, while combining both produced a significant synergistic antibacterial effect.

APPLYING TENGS-BASED ES FOR PROMOTING WOUND HEALING

TENGs-Based ES for Directly Accelerating Wound Healing. The process of wound healing can be divided into three stages, which include inflammatory, proliferative, and remodeling.[94−98] In the early and entire phase of inflammation, the accelerated recruitment of cytokines and immune cells is very important. It has been shown that endogenous electric fields can promote the migration of macrophages, lymphocytes, and neutrophils to skin wound sites and ultimately promote wound healing.[63] Moreover, the rate of wound healing will be severely slowed by the prolonged inflammatory response. Interestingly, ES may reduce the quantity of immunocytes and cytokines, which can help with inflammation resolution. Besides, bacteria are often seen in wound healing. If bacteria are not cleared by inflammatory factors in a timely manner, they will induce bacterial infection and significantly delay wound healing.[99] As mentioned above, ES can be used as an antibacterial agent to minimize the emergence of sluggish wound healing caused by bacterial infection, thus indirectly assisting the wound healing. Moreover, ES can offer direction indications for cells, such as chemokines and cell migration

https://doi.org/10.1021/acsnano.3c01634
ACS Nano XXXX, XXX, XXX−XXX

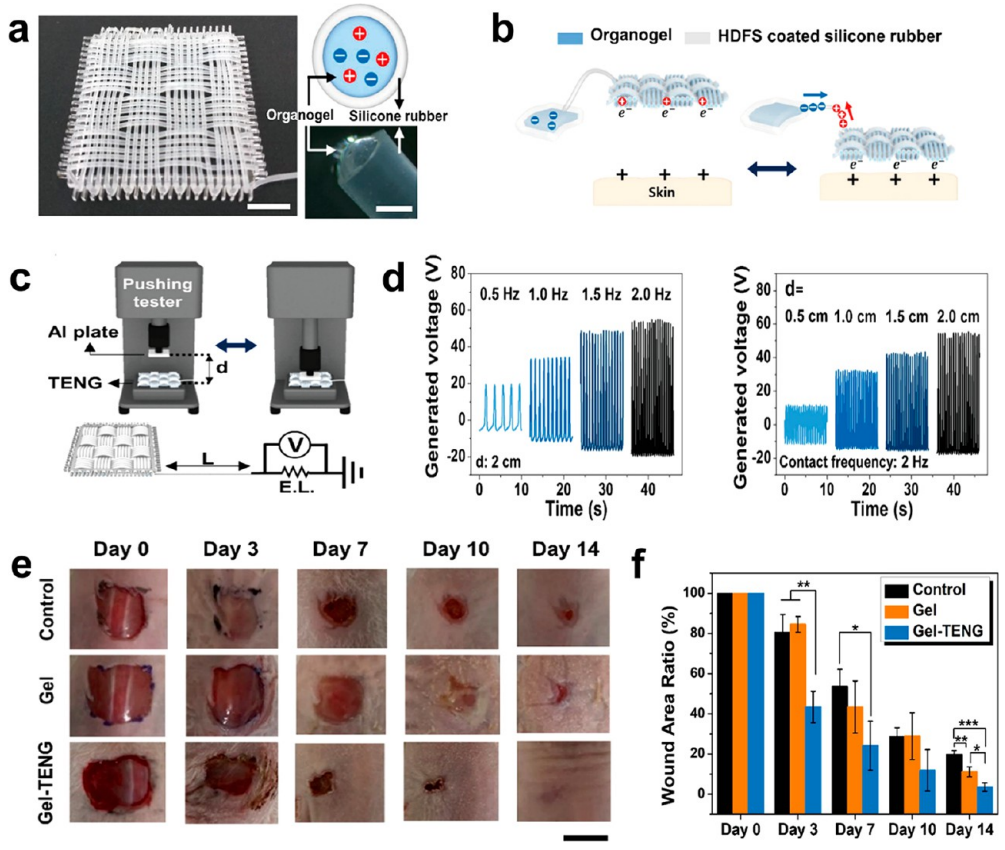

Figure 8. Application of an ionic TENG (iTENG) patch-based ES for wound healing. a) Optical image of the iTENG patch (scale bar: 1 cm) and schematic diagram of a cross section of the ionic fabric and magnified image of a fiber. b) A schematic depiction of the physiological power conversion mechanism of the iTENG. c) Schematics depicting the procedure for gauging the iTENG patch's electrical output performance. d) The contact frequency ranges from 0.5 to 2.0 Hz and separation between iTENG and contact material from 0.5 to 2.0 cm. e) Macroscopic wound healing progression in the untreated (control), ionic patch solely (Gel), and ionic patch coupled with TENG (Gel-TENG) groups over time, scale bar: 1 cm. f) The quantized percentage of wound area that has healed after 3, 7, 10, and 14 days of treatment. Reproduced with permission from ref.[39] Copyright 2020 Elsevier.

pressure, which can also significantly contribute to cell proliferation and facilitate the healing process.[6,10,66] Apart from all the benefits that ES can offer, TENGs-based ES has extra advantages of being microscaled and can be tailored depending on the specific size and location of the wound, by which it can provide consistent therapy to the damaged wound and promote the entire healing process.

For instance, a wearable TENG-based electrical bandage was developed to promote wound healing by creating an alternating electric field.[38] As shown in Figure 7b, Cu/PTFE (electronegative material) was layered on top of a poly(ethylene terephthalate) (PET) substrate, and then another Cu (electropositive material) layer was layered on top of that, creating the TENG. Wrapping the device around the torso of a Sprague–Dawley (SD) rat was shown to be the optimal strategy for achieving such a minute sliding displacement (Figure 7a). Therefore, the voltage produced by the dressing electrodes can be monitored at different points in the rat's day-to-day routine (Figure 7c). In order to explore electric stimulated wound healing, full thickness rectangular skin wounds were utilized. As shown in Figure 7d, the electric field was directed horizontally, with the proximal wound (top of the image) positioned between the two vertical line electrodes. The control wound, seen at the image's bottom, had the identical electrode configuration applied to it, but there was no electric field. Three days after the treatment, the top wound displayed a closed wound (image ii in Figure 7d). On the contrary, the control wound was not closed, and the healing was in a disorganized fashion. Fibroblasts are recognized to play a significant part in the complex biological process of cutaneous wound healing.[100] To pursue an explanation for the phenomenon of the very rapid wound recovery, the migration and proliferation of fibroblast cells was studied *in vitro*, as illustrated by the schematics in Figure 7e. Within 12 h, the fibroblasts of control groups showed no significant difference from the baseline. However, the cells subjected to TENG-based ES showed linear alignment in under 2 h (image i in Figure 7f). After 4 h, fibroblast cells showed obvious proliferation (Figure 7f, image ii). After 6 h, fibroblasts kept multiplying and differentiating in the direction of ES (Figure 7f, images iii and iv). The results *in vivo* on rats and *in vitro* on fibroblast cells exhibit that TENG-based ES can promote the differentiation of fibroblasts into muscle fibroblasts and then contribute to the rapid healing of wounds.

Despite advancements in TENG patch technology, metal or ceramic electrodes are still commonly required but lack the necessary mechanical adaptability for wound healing therapy.[101,102] Recently, fabric-based TENGs offer an alternative and hold promise for promoting wound healing through TENG-based electrical stimulation in real-life scenarios. For instance, Jeong et al. developed a flexible and wearable fabric ionic triboelectric nanogenerator (iTENG) patch using organogel fibers, which demonstrated improved wound healing capabilities

https://doi.org/10.1021/acsnano.3c01634
ACS Nano XXXX, XXX, XXX−XXX

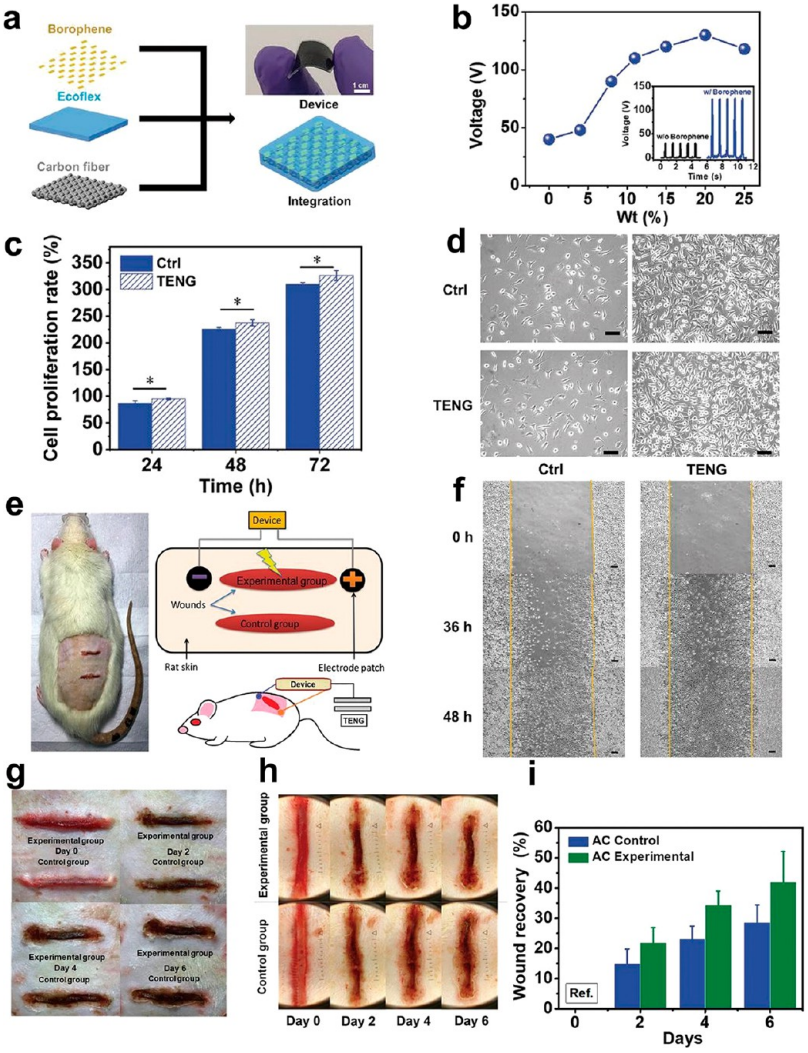

Figure 9. Developed B-TENG as a self-powered *in vitro* electrical stimulating patch for continuous wound healing. a) The fabrication of the B-TENG patch. b) Output voltage of B-TENG patch with different borophene concentrations. c) The proliferation rate of L929 cells with and without treatment by ES. d) Cell morphology at 0 and 72 h without (Ctrl) and with (TENG) ES, scale bars: 100 μm. e) A schematic system setup by B-TENG to induce ES for wound healing on rat models. f) L929 fibroblasts with scratched regions in the control and TENG stimulation groups at 0, 36, and 48 h, scale bars: 200 μm. g) Digital photographs of the wound healing process with ES. h) Wound recovery images taken by dermoscopy. (i) Quantized changes in wound closure status. Reprinted with permission under a Creative Commons Attribution 4.0 International (CC BY 4.0) License from ref.[54] Copyright 2022 Shuo-Wen Chen et al., published by Wiley-VCH GmbH.

in vivo, as shown in Figure 8.[39] A stretchy wire and a wearable generator were created when weaving ionically conductive organogel fibers in an elastic tubulin structure together like fabric (Figure 8a). The ionic patch, enclosed in an elastomeric film, can be used as a wound dressing and an electrode. A simplified diagram of the iTENG patch's inner workings is shown in Figure 8b. Because of the differing electron affinities of the two materials, contact electrification occurred when the TENG met the dermal surface.[103] Electrons attract cations and repel anions in the organogel as it traveled away from the skin. Repelled anions were collected in the patch, creating an electric field (EF). In order to evaluate the output performance of iTENG, mechanical motions were maintained with the help of a pushing tester (Figure 8c). The contact frequency and the maximum gap distance between the TENG and the contact material both affected the voltage produced. As shown in Figure 8d, when the contact frequency was raised from 0.5 to 2.0 Hz, the produced voltage also rose from 25 to 75 Vpp. Similarly, when the maximal spacing between the TENG and the contact material was increased from 0.5 to 2.0 cm, the produced voltage followed suit, climbing from 33 to 73 Vpp. These results showed that forceful motions, including making quick contact and then quickly separating the iTENG from the skin, may cause larger increasement in generated ES by the iTENG. Furthermore, the effectiveness of the iTENG patch-based ES in wound healing was evaluated *in vivo* using full-thickness wound animal models, where the ionic patch was placed vertically on top of the wound and ES was performed every 2 days, resulting in accelerated wound healing compared to control and Gel groups, indicating the potential of iTENG patch-based ES for promoting rapid wound recovery.

Apart from the above-mentioned organogel fibers, a borophene/ecoflex (Ecoflex-B) triboelectric material was developed and fabricated into a fabric-based triboelectric nanogenerator (B-TENG) for wound healing. Improved output performance with increasing borophene concentration, enhanced cell proliferation and migration, and successful wound healing in an animal model can be achieved by the developed B-

https://doi.org/10.1021/acsnano.3c01634
ACS Nano XXXX, XXX, XXX−XXX

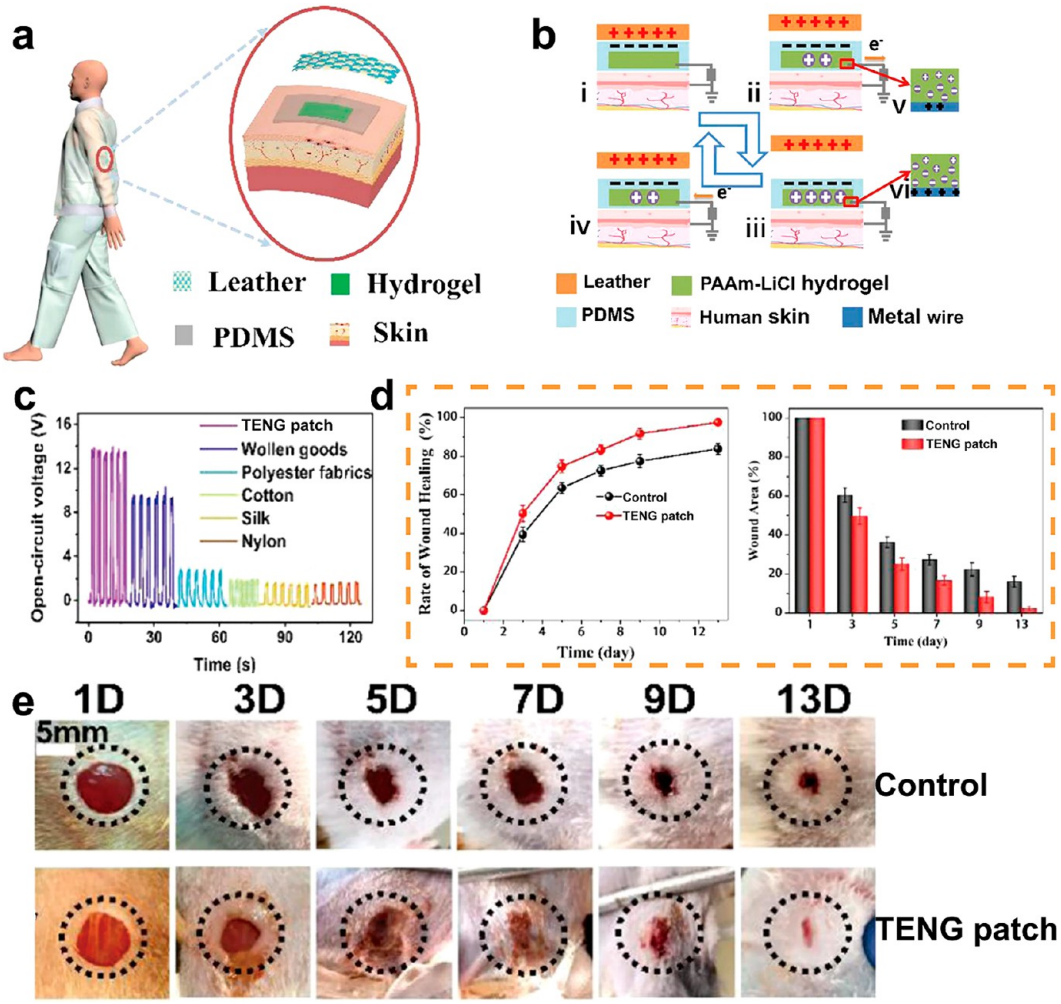

Figure 10. A flexible stretchable sandwich-structured triboelectric patch for accelerating wound healing. a) Device schematic and functional model. b) The diagram of working mechanism. c) The open-circuit voltage of the six cloths integrated with sandwich structure. d) The rates of wound healing of different test groups. e) Images depicting the treatment procedure for wounds in the TENG patch group and the control group on days 1, 3, 5, 7, 9, and 13. Reproduced with permission from ref.[55] Copyright 2021 Elsevier.

TENG-based ES, as shown in Figure 9.[54] As shown in Figure 9a, carbon fiber (CF) acted as the flexible electrode material in the Ecoflex-B, which was made up of layers of ecoflex, borophene nanosheets (NSs), and CF. The Ecoflex-B was further coupled with a nylon-coated cloth to create the B-TENG. Then the output performances of B-TENG under various mixed situations were investigated. As illustrated in Figure 9b, the output performance was improved with increasing the borophene NSs concentration. Particularly, the optimized output performance can be achieved when the concentration of borophene NSs was 20 wt %, where the output voltage and current were up to 120 V and 20 A, respectively. Under this condition, the developed B-TENG can fully meet the requirement of wound healing. Cell proliferation and migration are important indicators in assessing biological activity throughout the wound healing process. Herein, by performing cell proliferation and cell migration assays with ES by B-TENG, the cellular behaviors of L929 fibroblasts were examined. As shown in Figure 9c, at 24, 48, and 72 h, the proliferation rate of the control and stimulated cells showed statistical significance. The proliferation rate of the stimulated cells was greater than the proliferation rate of the control cells without ES. Figure 9d depicted the cell morphology of control and stimulated cells, further demonstrating that ES can promote cell proliferation. The migratory behavior of L929 fibroblasts driven by B-TENG is shown in Figure 9f. It was discovered that the cells in the electrical stimulated group migrated quicker than the cells without ES. The feasibility of using B-TENG for wound healing was demonstrated through animal model testing, where wounds treated with B-TENG showed significant healing compared to the control group, as depicted in Figure 9g. The wound area in the ES treated group was significantly smaller than that in the control group, and the wound shrinking rate was greater by day 2, day 4, and day 6, as quantified in Figure 9h,i.

An alternative approach to utilizing fabric-based TENG patches for wound healing is to introduce stretchable materials between the friction layers, thereby enhancing both tensile properties and patient comfort. For example, Wan et al. developed a wearable, flexible triboelectric patch for wound treatment, utilizing a conductive hydrogel, PDMS layer, and garment fabric to generate an electric field, resulting in accelerated wound healing in animal models.[55] As illustrated in Figure 10a, the developed TENG patch held a soft, wearable sandwich structure by combining a double-layer polydimethylsiloxane (PDMS) membrane with an embedded polyacrylamide-LiCl (PAAm-LiCl) hydrogel. The working mechanism of

https://doi.org/10.1021/acsnano.3c01634
ACS Nano XXXX, XXX, XXX−XXX

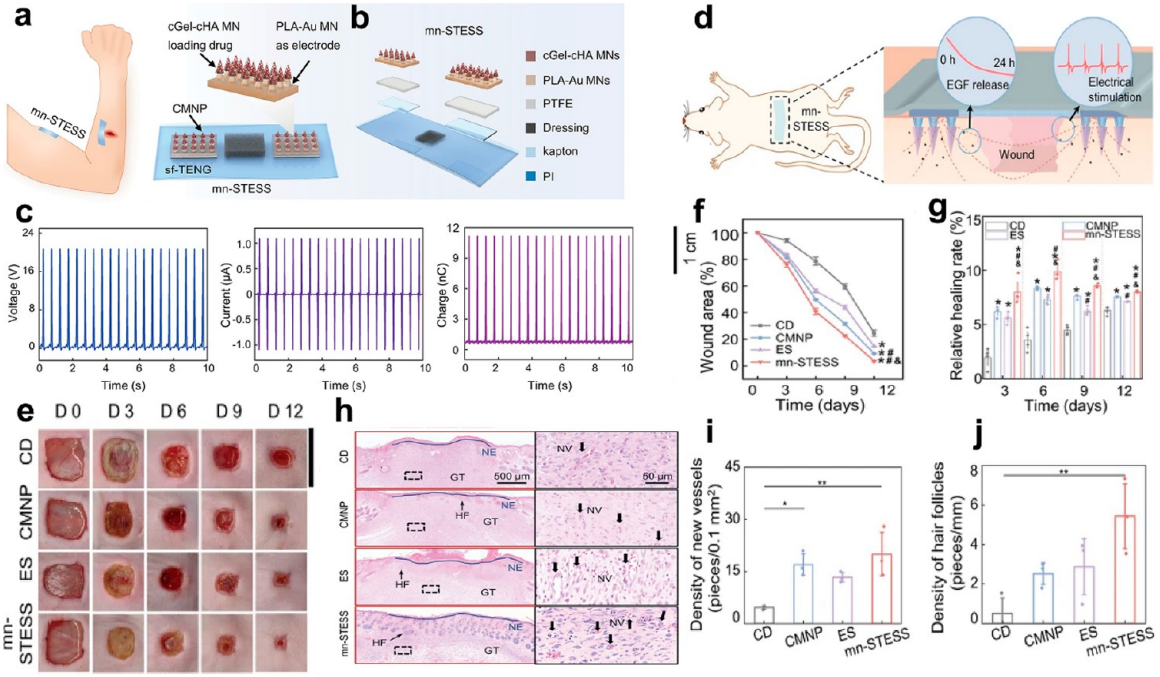

Figure 11. TENGs-based ES can be applied as the adjuvant to synergistically boost the healing effect of therapeutic drugs. a) The mn-STESS consisted of sf-TENG, CMNP, and dressing. The CMNP composed of cGel-cHAMNs loading drug and PLA-AuMNs as electrode. b) Three-dimensional structure of the mn-STESS. c) V_{OC}, I_{SC}, and Q_{SC} of the sf-TENG. d) Illustration of the mn-STESS wound-healing mechanism. e) Digital pictures showing wound regions on days 0, 3, 6, 9, and 12 after treatments by different tested groups. f, g) Quantitative comparison of wound area healed and relative healing rate from day 0 to days 3, 6, 9, and 12 across all groups. h) H&E staining of wound healing tissue showing the mn-STESS group can present better wound healing quality. (i) The proliferation of new vessels in quantitative form for the healing process treated by different tested groups. j) Quantitative statistics of new hair follicles in healing skin treated by different tested groups. Reprinted with permission under a Creative Commons Attribution 4.0 International (CC BY 4.0) License from ref.[104] Copyright 2022 Yuan Yang et al., published by Nature.

the developed TENG patch is illustrated in Figure 10b. Specifically, the conductive hydrogel acted as a single electrode, while the upper PDMS layer and garment fabric formed a frictional electric pair owing to their distinct triboelectric polarities. The leather would touch and detach from the hydrogel patch as the body moved to extract the biomechanical energy of a human body. When the leather came into contact with the TENG patch, a surface made of leather and PDMS would produce a charge of equal but opposing polarity (Figure 10b, image i). When the leather moved away from the TENG patch, the electrostatic charge on the PDMS surface promoted ionic mobility in the hydrogel, resulting in the formation of a layer of positive charge only at the interface. Simultaneously, the metal wires would be charged negatively and positively due to the polarization of the electric layer generated at the hydrogel interface (Figure 10b, image ii). When the moving leather got close enough to the PDMS, the electrostatic attraction between them was canceled out, and the system returned to its initial state of equilibrium (Figure 10b, image iv). As the potential difference increased, electrons would flow from the hydrogel to the body, which constructed an electric field between the TENG patch and the body's tissue, facilitating the wound healing process. As shown in Figure 10c, the output voltage is illustrated when leather, polyester fabrics, silk, woolen goods, and nylon periodically contact-separated from the device. Furthermore, to assess the performance of the developed TENG patch in wound healing, male mice wound healing experiments were conducted. The developed TENG patch was applied to the wound as well as control studies conducted under identical settings. As shown in Figure 10e, the wound area of the control group was not significantly reduced, but the TENG patch group mostly healed in 13th day. Following 0, 3, 5, 7, 9, and 13 days of therapy, the TENG patch group healed completely at 13 days, while the control group still had 13% of the wound area unhealed; the rates of wounds closure (Figure 10d) indicated that the application of the developed TENG patch can significantly accelerate the wound healing process. This study presents an opportunity for creating soft, wearable TENGs for wound treatment.

TENGs-Based ES Serves as an Adjuvant to Indirectly Promote Wound Healing. In addition to being used directly as a therapeutic agent, TENGs-based ES can also serve as an adjuvant to enhance the efficacy of therapeutic drugs in promoting wound healing. For instance, a microneedle-based self-powered transcutaneous electrical stimulation system (mn-STESS) utilizing a sliding free-standing TENG (sf-TENG) and two-stage composite microneedle patches (CMNPs) was shown to enhance the pharmacodynamics of epidermal growth factor (EGF) and accelerate wound healing in a mouse model.[104] As shown in Figure 11a, the mn-STESS was developed based on a sliding free-standing triboelectric nanogenerator (sf-TENG) and two-stage composite microneedle patches (CMNPs). The three components of TENG were the polyimide film as the triboelectric layer, the polytetrafluoroethylene (PTFE) film-coated Kapton adhesive acting as the dielectric layer, and the gold microelectrode array patch serving as the electrode (Figure 11b). A two-stage CMNP was made by covering the PLA-Au MNP with drug-loaded cross-linked gelatin and cross-linked hyaluronic acid microneedles (cGel-cHA MNs). The developed mn-STESS can enhance the EGF entry and absorption by

https://doi.org/10.1021/acsnano.3c01634
ACS Nano XXXX, XXX, XXX−XXX

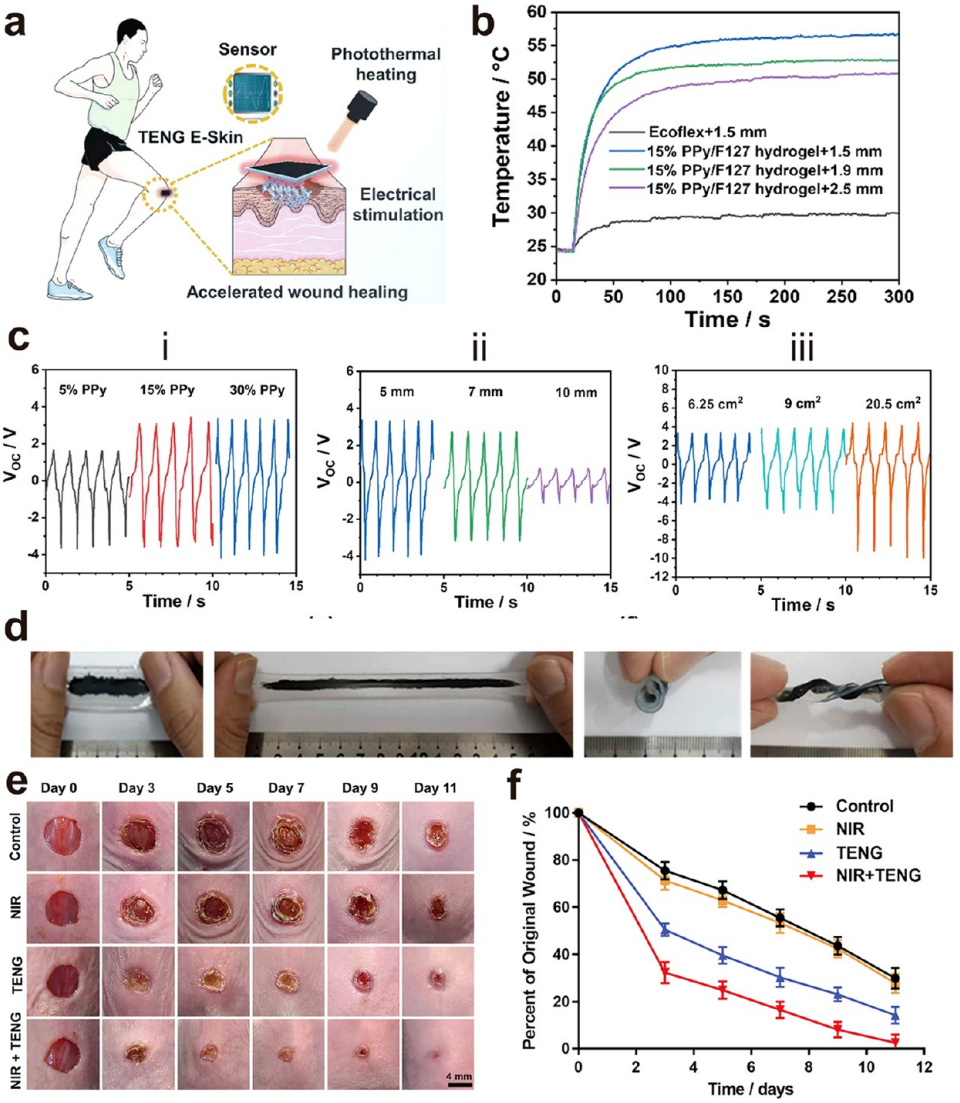

Figure 12. TENG-based electric skin patch for wound healing by synergistically combining ES and photothermal heating capability. a) Schematics showing the application of the developed dual-functional TENG-based E-skin patches on the wound. b) The photothermal capability of the developed TENG-based patches under an 808 nm NIR laser at 0.5 W cm^{-2}. c) The output performance of the developed patches with different concentrations of PPy, thickness, and hydrogel area. d) Photographs showing the developed patches in their natural, stretched, curled, and twisted forms. e) Photographs of the *in vivo* wound healing efficacy of different tested groups (control, NIR, TENG, and NIR+TENG) for 11 days. f) Quantification of wound closure rates of different tested groups. Reproduced with permission from ref.[40] Copyright 2021 Elsevier.

puncturing the stratum corneum with tiny needles. Moreover, the ES generated by the sf-TENG performed as a "protector" of EGF, which can effectively compensate for receptor desensitization by preventing glutathione's decrease of EGF and increasing the expression of its receptor in keratinocyte cells.[105−107] The sf-TENG was powered by a pigskin-encased mechanical linear motor, which resulted in an open-circuit voltage (V_{OC}) of approximately 20 V, a short-circuit current (I_{SC}) of about 1 A, and a short-circuit transmitted charge (Q_{SC}) of about 11 nC (Figure 11c). In order to assess the role of mn-STESS in enhancing the pharmacodynamics of EGF and wound healing, two CMNPs were attached on opposite sides of the wound to prevent further injury to the wound site and established the full-thickness mouse skin wound (Figure 11d). As shown in Figure 11e, all treated groups had better healing results than the pure EGF group (termed as CD in the figure) did. Among those shown in Figure 11f,g, the application of mn-STESS resulted in higher first 6-day healing rates (18% and 36% higher than in the CMNP and ES groups, respectively). Moreover, the results of a hematoxylin and eosin (H&E) staining test demonstrated that the mn-STESS group presented an even better wound healing quality, with more new vessels (NVs) and hair follicles (HFs) compared to the other groups. All the results demonstrated the potential of TENGs-based ES as an effective adjuvant to enhance the healing effect of therapeutic drugs.

Combination of TENGs-Based ES with Various Physiotherapeutic Approaches to Facilitate Wound Healing. In addition to utilizing TENG-based ES as a standalone approach for enhancing wound healing, several physiotherapeutic techniques, including light heating and active ROS elimination, have been combined with TENG-based ES to develop more precise and controllable methods with broader potential for accelerating wound healing.[14,108−110] For example, Du et al. developed a dual-functional TENG-based electric skin

https://doi.org/10.1021/acsnano.3c01634
ACS Nano XXXX, XXX, XXX−XXX

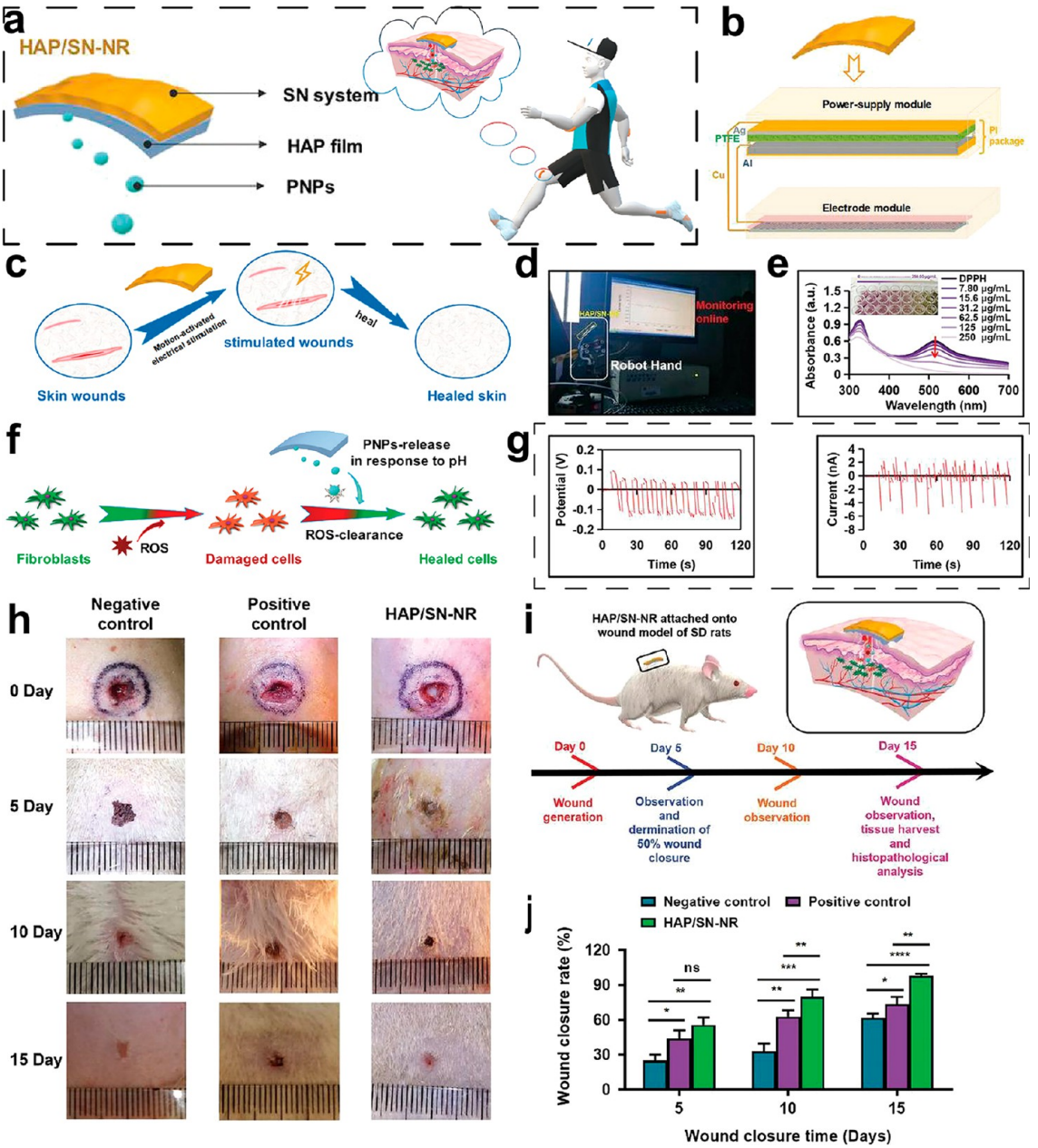

Figure 13. A TENG-based HAP/SN-NR skin patch capable of generating ES and removing ROS for accelerating wound healing. a) The composition of the developed TENG-based patch. b) Design of the TENG module. c) The work process of the patch for generating ES to facilitate wound healing. d) The motion-driven, online electrical signal monitoring schematic for the robot. e) PNPs with capability of removing excessive ROS by scavenging DPPH free radicals. f) The pH-responsiveness of the developed patch to release PNPs to perform ROS-clearance to repair injured human dermal fibroblasts. g) The potential and the current can be converted by the bending and stretching of the HAP/SN-NR patch on the robot hand. h) Images of SD rat wounds with no therapy (negative control), Tegaderm film (positive control), and HAP/SN-NR patch (experimental group) for 15 days. (i) Experimental chronology and a schematic of applying HAP/SN-NR patch to rat wounds. j) The quantized wound healing rate. Reproduced with permission from ref.[113] Copyright 2021 Wiley-VCH.

patch using ES and photothermal heating to accelerate the process of wound healing synergistically, which showed promising results in reducing wound area in a full-thickness wound model on mice.[11] As shown in Figure 12a, encapsulating conductive and photothermal composite hydrogels of polypyrrole (PPy) and aqueous F127 into silicone rubber resulted in the establishment of E-skin patches, which can exert high efficiency in converting light into heat, high conductivity, and shape adaptability. As shown in Figure 12d, the tensile strength of the packed TENG patches was comparable to that of the pure Ecoflex film, coming in at about 200 kPa with a strain at break of around 300%, which can meet the requirements of a wearable device for wound healing. The output voltage increased from 5.4 to 7.6 V with PPy percentage increased from 0 to 30%, which can be attributed to the decrease of e-skin patch electrolyte (Figure 12c, image i). Moreover, increasing Ecoflex sealant thickness resulted in a lower open-circuit voltage, and an expansion of the hydrogel's surface area leads to greater V_{OC} (Figure 12c, images ii & iii). Besides, as a dual-functional patch, another distinguishing feature is their photothermal capability. 0.5 W cm^{-2} of irradiation from an 808 nm Near Infra-Red (NIR) laser was adopted to measure TENG E-skin patch photothermal heating

https://doi.org/10.1021/acsnano.3c01634
ACS Nano XXXX, XXX, XXX−XXX

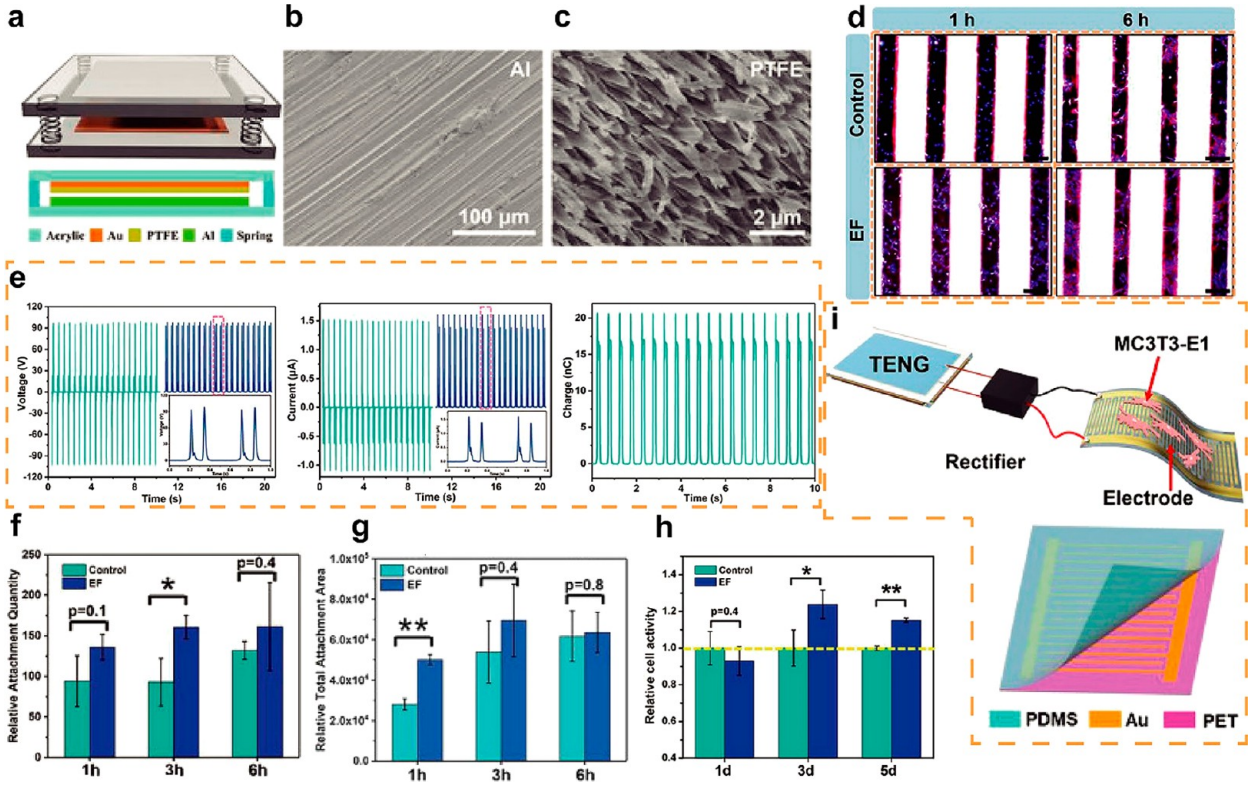

Figure 14. Implantable self-powered electrical stimulator for promoting bone tissue repairing. a) The structure of implanted TENG device. b, c) The SEM images of the linear structures on Al film and on PTFE film, the nanostructured arrays formed on PTFE were dense and homogeneous. d) After seeding for 1 and 6 h with and without TENGs-based ES, MC3T3-E1 cells were stained with phalloidin (red) and DAPI (blue), scale bar: 200 μm. e) The output voltage, current, and transferred charge of TENG with and without rectification; the inset image is the output performance after rectification. f) After stimulation for 1, 3, and 6 h, the relative quantity of attached MC3T3-E1 cells was 44.68%, 72.76%, and 22.22% greater than the control group, respectively ($*p < 0.05$, $n = 10$). g) After stimulation for 1, 3, and 6 h, the relative total attachment areas of MC3T3-E1 cells were determined. The TENGs-based ES treatment group outperformed the control group by 78.37%, 29.05%, and 3.06%, respectively ($**p < 0.01$, $n = 10$). h) After 3 and 5 days of stimulation, MC3T3-E1 cells proliferated 23.82% and 15.18% higher than the control group, respectively ($*p < 0.05$, $**p < 0.01$, $n = 4$). (i) The electrical stimulator and interdigitated electrode are shown schematically. Reproduced with permission from ref.[116] Copyright 2019 Elsevier.

curves. As shown by the plots in Figure 12b, the temperature of the patch quickly rose over time, and when compared to the patch without PPY, the temperature of the one with PPY was 26.5 $^{\circ}$C higher. As demonstrated in Figure 12e,f, a full-thickness wound model was established in mice to assess the efficacy of the dual-functional TENG-based electric skin patch on wound healing, with the TENG group showing significant reduction in wound area and the NIR+TENG group exhibiting the greatest results, proving that TENGs-based ES can be well-combined with other physiotherapeutic approaches to accelerate the wound healing process effectively.

The presence of reactive oxygen species (ROS) at wound sites can impede the healing process, cause intense inflammation, and reduce the ability of endogenous stem cells and macrophages to regenerate skin tissue. Consequently, the suppression of ROS levels at wound sites is essential for promoting wound healing.[111,112] TENGS-based ES can be combined with the active ROS elimination to obtain a better wound healing effect. Recently, Yuan et al. designed a dual-functional TENG-based patch that generates electric fields to promote angiogenesis and fast skin repair while also removing ROS using polydopamine nanoparticles, which was successfully tested on rats to accelerate wound healing.[113] As illustrated in Figure 13a, the developed HAP/SN-NR patch was constructed by layer-by-layer (LBL) self-assembling of 2-hydroxypropyltrimethylammonium chloride chitosan (HTCC), alginate (ALG), and polydopamine nanoparticles (PNPs), with self-powered nanogenerator (SN). The SN layer in the top of HAP/SN-SR can create an electric field with the necessary strength, which is advantageous for angiogenesis and fast active skin repair, as shown in Figure 13c. The self-powered nanogenerator contains a power-supply module and an electrode module. As shown in Figure 13b, the power-supply module's friction layers are made of polytetrafluorethylene (PTFE) and aluminum (Al) films since the triboelectric properties of these two materials are noticeably different. Moreover, the poly(vinyl chloride) (PVC) substrate was coated with the liquid metal (LM) composed of GaInSn for the electrode module. As shown in Figure 13d, the robot hand was utilized for continuously bending and stretching HAP/SN-NR patch to evaluate the output performance. When the robotic finger starts to bend, HAP/SN-NR, which is connected to an electrochemical workstation for online monitoring, can produce the normal voltage and current (Figure 13g). Besides, PNPs showed the capability of removing excessive ROS by scavenging 2,2-diphenyl-1-picrylhydrazyl (DPPH) free radicals (Figure 13e). Due to the electrostatic interactions between HTCC and ALG, the developed HAP/SN-NR patch showed pH-responsiveness that can release PNPs. Specifically, as the pH value of the wound environment changed from neutral to mildly acidic, PNPs in the bottom layer of the patch can be released into

https://doi.org/10.1021/acsnano.3c01634
ACS Nano XXXX, XXX, XXX−XXX

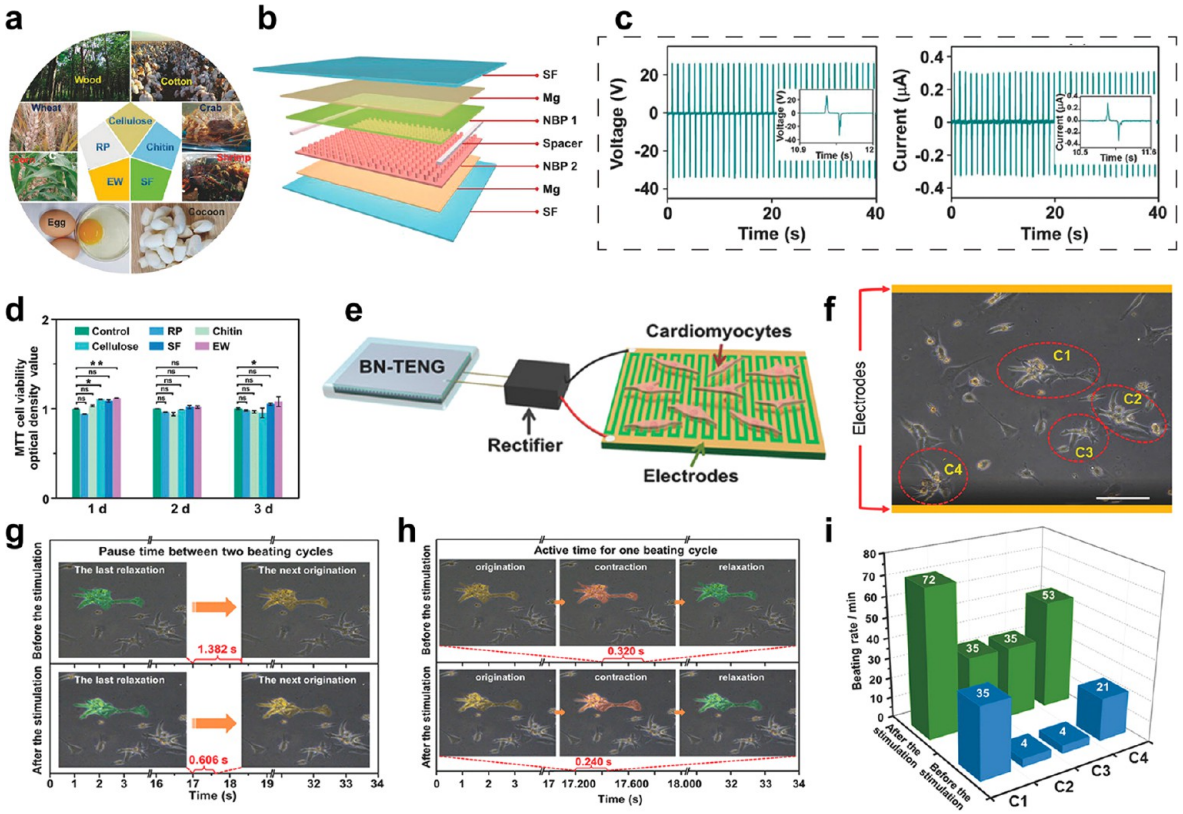

Figure 15. Fully bioabsorbable natural-materials-based triboelectric nanogenerators (BN-TENGs) accelerate the beating rates of cardiomyocyte clusters for cardiac disorders, such as bradycardia and arrhythmia. a) NBPs with diverse raw materials sources. b) Structure illustration of BN-TENG device. c) Output voltage and current of BN-TENG. d) Cell viability of L929 cells cultured on NBPs film for 3 days. e) Schematic diagram of the BN-TENG electric system. f) Image shows cardiomyocytes cultivated on the surface of an interdigital electrode. The four distinct cardiomyocyte clusters are shown by the red circles (C1, C2, C3, and C4). g) Before and after electric stimulation, pause duration between the two beating cycles of cardiomyocyte cluster. h) Active period for a cardiomyocyte cluster's one cycle of beating before and after electric stimulation. (i) Before and after BN-TENG electric stimulation, the beating rates of the four cardiomyocyte clusters. Reproduced with permission from ref.[117] Copyright 2018 Wiley-VCH.

the damaged areas to perform ROS-clearance capability to repair injured human dermal fibroblasts (Figure 13f). As demonstrated by the plots in Figure 13e, 2,2-diphenyl-1-picrylhydrazyl (DPPH) free radicals can be scavenged by the PNPs of different concentrations. The healing efficacy of the developed HAP/SN-NR patch was evaluated by creating 7 mm circular wounds on the backs of SD rats and monitoring the wound closure rates over time, as depicted in Figure 13i,j, which demonstrated that wounds treated with the patch healed nearly completely after 10 days, with significantly higher closure rates of 55.7%, 80.0%, and 99.6% at day 5, day 10, and day 15, respectively, compared to other tested groups, thus indicating the practical potential of the combination of TENG-based ES with ROS elimination for promoting wound healing.

TENGs-Based ES for Tissue Repair Promotion. As we discussed above, TENGs-based ES can accelerate wound healing on skin by enhancing migration and proliferation of fibroblast cells.[114] Interestingly, TENGs-based ES regulated cell modulation is also beneficial for tissue repairing, such as promoting cell pulsation, osteoblasts proliferation and adhesion, and proliferation and migration of fibroblasts.[50] Recently, utilizing TENGs-based ES for tissue therapeutic applications has also been developed with a number of achievements obtained. In this section, we briefly summarize the recent progress of TENGs-based ES for tissue repair promotion.

TENGs-Based ES for Promoting Proliferation of Osteoblasts. Osteoporosis, a metabolic bone disease characterized by low bone mass and bone tissue degeneration, can result in an increased risk of bone fractures in the hip, spine, and forearm.[115] A potential solution to this problem was proposed by Tian et al. in 2019, who introduced an implantable TENG device that promotes adhesion, differentiation, and proliferation of osteoblasts in the human body.[116] The TENG was composed of two triboelectric layers and electrodes, as shown in Figure 14a. Aluminum (Al) and polytetrafluoroethylene (PTFE) film serve as friction layers, as these materials possess markedly different triboelectric properties that enable high output performance. To enhance the device's output performance, the Al film was polished with sandpaper to achieve linear microstructures, as shown in Figure 14b. Furthermore, PTFE thin film was treated with ICP (inductively coupled plasma-reaction ion etching) to create nanostructure arrays that increase the effective contact area and contact electrification (Figure 14c). To measure the output performance of the TENG, a linear motor with constant vertically compressive force was used, and the device's output voltage, current, and transferred charge were measured. Without rectifying, the output voltage, current, and transferred charge were approximately 100 V, 1.5 μA, and 21 nC, respectively (Figure 14e). To create a self-powered electrical stimulator, as illustrated in Figure 14i, the TENG was combined with a rectifier bridge and flexible electrode. To maintain the device's

https://doi.org/10.1021/acsnano.3c01634
ACS Nano XXXX, XXX, XXX−XXX

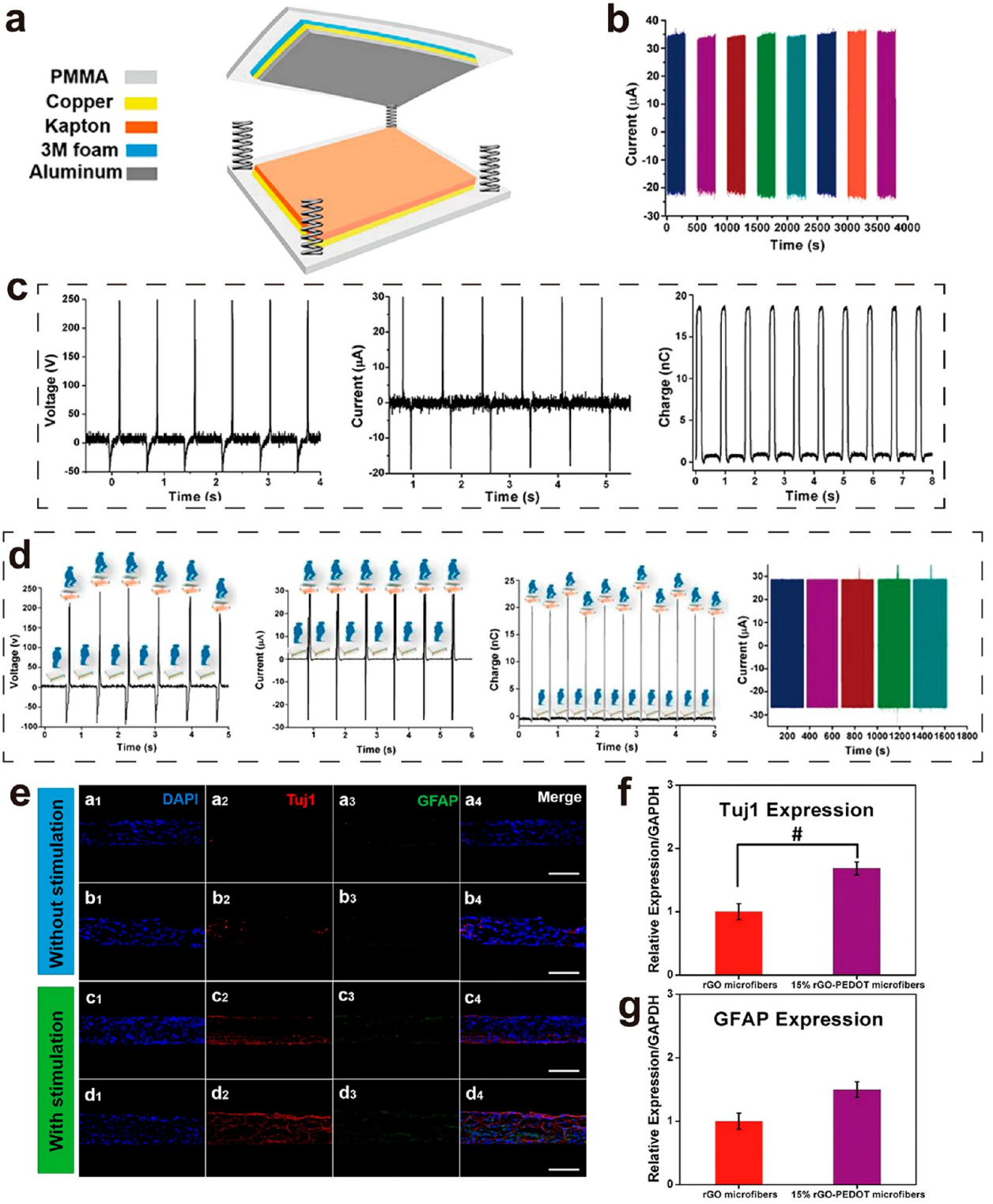

Figure 16. TENGs-based electric stimulation combined with engineered conductive scaffolds for neural differentiation of MSCs cells. a) Schematic illustration of TENGs construction. b) TENGs current output stability experiment in 4000 s (about 3360 pulses). c) The output performance of the TENG, including voltage, current, and transferred charge. d) The output performance of TENG driven by walking steps. e) After being cultured under electric stimulation (c, d) and conditions without TENG electrical stimulation (a, b), cells were immunostained with (1) DAPI (Blue), (2) Tuj1 (red, cy3), (3) GFAP (green, FITC) for the nucleus and neural-specific antibodies for 21 days on rGO-PEDOT microfiber (a, c) and 15% rGO-PEDOT hybrid microfiber (b, d). f, g) qPCR analysis of the cell expression levels of Tuj1 (f) and GFAP (g) neural-specific genes on rGO microfibers and 15% rGO-PEDOT hybrid microfibers. Reproduced with permission from ref.[120] Copyright 2016 American Chemical Society.

flexibility and stability, a poly(ethylene terephthalate) (PET) substrate was used for interdigitated electrodes, and a flexible PDMS layer was used to package the entire device. For the TENGs-based ES experiment, MC3T3-E1 cells were selected as

https://doi.org/10.1021/acsnano.3c01634
ACS Nano XXXX, XXX, XXX−XXX

the model cell to provide reliable support for the application in bone tissue regeneration. For the adhesion experiment, after being TENGs-based ES stimulated for 1, 3, and 6 h, phalloidin and 4′,6-diamidino-2-phenylindole (DAPI) were used to stain the cell cytoskeleton and nucleus to red and blue, respectively. The immunofluorescent staining pictures demonstrated that MT3T3-E1 adhered normally after seeding, as shown in Figure 14d. The statistical analysis of the areas and quantity of attached cells (Figure 14f,g) revealed that the quantity of attached cells was higher than the control group for 1, 3, and 6 h, respectively. Additionally, the whole spreading areas were greater after 1, 3, and 6 h of TENGs-based ES, respectively. These results suggest that TENGs-based ES can significantly impact the adhesion and spreading area of MC3T3-E1 immediately after seeding. Regarding proliferation activity, on day 1, there were no noticeable differences between the groups that received TENG-based ES and the control group. However, on days 3 and 5, the cell count in the TENG-based ES group was significantly higher than in the control group, as revealed in Figure 14h. These results clearly demonstrate the potential of TENG-based ES in promoting bone cell proliferation. Overall, these findings suggest that TENG-based ES could effectively promote bone tissue repair by enhancing adhesion, proliferation, and differentiation of osteoblast progenitor cells, thereby offering therapeutic avenues for osteoporosis treatment.

TENGs-Based ES for Promoting Beating Rates of Cardiomyocyte. In 2018, Jiang et al. introduced a natural-materials-based triboelectric nanogenerator (BN-TENGs) for the treatment of heart diseases such as arrhythmia and bradycardia.[117] The BN-TENGs system was designed to promote the beating rates of dysfunctional cardiomyocytes and enhance the consistency of cell contraction. To achieve this, natural bioresorbable polymers (NBPs), including silk fibroin (SF), chitin, cellulose, rice paper (RP), and egg white (EW), were utilized as triboelectric materials, as illustrated in Figure 15a. The friction layers were composed of any two NBPs, while the electrodes were made of ultrathin Mg films. Moreover, SF films were used as encapsulation layers to shield BN-TENG from the outside environment (Figure 15b). In order to measure the output performance of the TENG, SF and RP were chosen as the friction layers. The voltage and current generated by the BN-TENG were 34 V and 0.32 μA, respectively, as shown in Figure 15c. To evaluate the biocompatibility of the NBPs films, L929 cells and five NBPs films were cultured for 1 to 3 days. The results showed that the NBPs films did not affect the growth and proliferation of L929 cells, confirming their excellent biocompatibility (Figure 15d). To demonstrate the feasibility of utilizing BN-TENG for modulating the beating of cardiomyocytes, the BN-TENG was integrated with rectifier and interdigital electrode to fabricate a self-powered stimulation system, as shown in Figure 15e. Primary cardiomyocytes were cultured on the surface of the electrodes, which formed isolated cardiomyocyte clusters (C1, C2, C3, and C4) through gap junction protein interconnections, as depicted in Figure 15f. After 48 h of culture without BN-TENG-based electrical stimulation, the cardiomyocyte clusters exhibited slow beating with significant pauses. However, after the application of electrical stimulation by BN-TENG, the beating rates of the cardiomyocyte clusters (C1, C2, C3, and C4) increased significantly. In particular, the average cease duration between two beating cycles of the cardiomyocyte cluster reduced from 1.382 to 0.606 s in C1 cluster after electrical stimulation, as shown in Figure 15g. The average contraction duration in a single cycle was also reduced from 0.320 to 0.240 s, as illustrated in Figure 15h. These findings indicate that the BN-TENG electric stimulation can significantly increase the beating rates of cardiomyocytes. Figure 15i summarizes the beating rates of the four clusters after BN-TENG electric stimulation, demonstrating that the beating rates of all clusters were significantly increased, particularly for C2 and C3. These results suggested that the biocompatible BN-TENG can enhance the beating rates of dysfunctional cardiomyocyte clusters and improve the consistency of contraction, providing a promising and effective treatment for cardiac disorders, such as bradycardia and arrhythmia.

TENGs-Based ES for Promoting Neural Differentiation. Nerve injuries affect millions of people, resulting in significant financial burden and suffering.[118] One of the critical components in nerve tissue engineering (NTE) is the development of engineered conductive scaffolds, which play a crucial role in repairing and regenerating neural systems.[118,119] These scaffolds must have characteristics that promote mesenchymal stem cell (MSC) differentiation into neural cells. However, the differentiation effect mediated by the scaffold is limited. In 2016, Guo et al. developed a differentiation system, including a highly effective triboelectric nanogenerator (TENG) and a poly(3,4-ethylenedioxythiophene)-reduced graphene oxide (rGO) hybrid microfiber scaffold, for synergistically promoting MSC differentiation into neural lineage.[120] The rGO-poly(3,4-ethylenedioxythiophene (PEDOT) microfiber not only served as a scaffold for enhancing MSC differentiation but also acted as a medium to conduct electric stimulation generated by the TENG. Figure 16a shows the TENG device established on two PMMA substrates to achieve portability, low cost, and decent strength. The device operated in contact-separation mode by four springs with Kapton and aluminum as two friction layers. A layer of copper film was sandwiched between the Kapton film and the PMMA substrate on the bottom, while the copper film on the other side was fixed on the substrate with a buffer sponge to stabilize the TENG. The output performance of the TENG was evaluated using a Keithley 2400 system electrometer and an SR570 low-noise current amplifier. The TENG generated an induced voltage of approximately 300 V, a short-circuit current of +30 and −20 A, and a transferred charge of around 18 nC during one circuit (Figure 16c). Furthermore, the output performance remained stable after 3360 pulses, indicating that the TENG has excellent electric output performance stability, as shown in Figure 16b. In addition, the researchers examined the output performance of the TENG when driven by walking, as depicted in Figure 16d. The TENG generated a voltage of approximately 300 V (reaching up to 340 V), with a peak short-circuit current of +30 and −28 A and a transferred charge of roughly 20 nC per cycle. Moreover, the TENG output current remained stable without any degradation after 4500 pulses, indicating that the TENG driven by human walking has excellent stability. To assess the differentiation of MSCs in vitro, the researchers set up four groups: two control groups consisting of rGO microfibers and 15% rGO-PEDOT microfibers without TENG-based ES and two experimental groups of the same microfibers with stimulation treatment (3000 pulses/day). Before the experiment began, all MSCs were cultured under normal conditions to ensure proper adhesion to the microfibers. After attachment, the control and experimental groups were cultured, respectively, with normal conditions and TENG-based ES treatment for 21 days. To evaluate the density and distribution of MSCs cells, the

https://doi.org/10.1021/acsnano.3c01634
ACS Nano XXXX, XXX, XXX−XXX

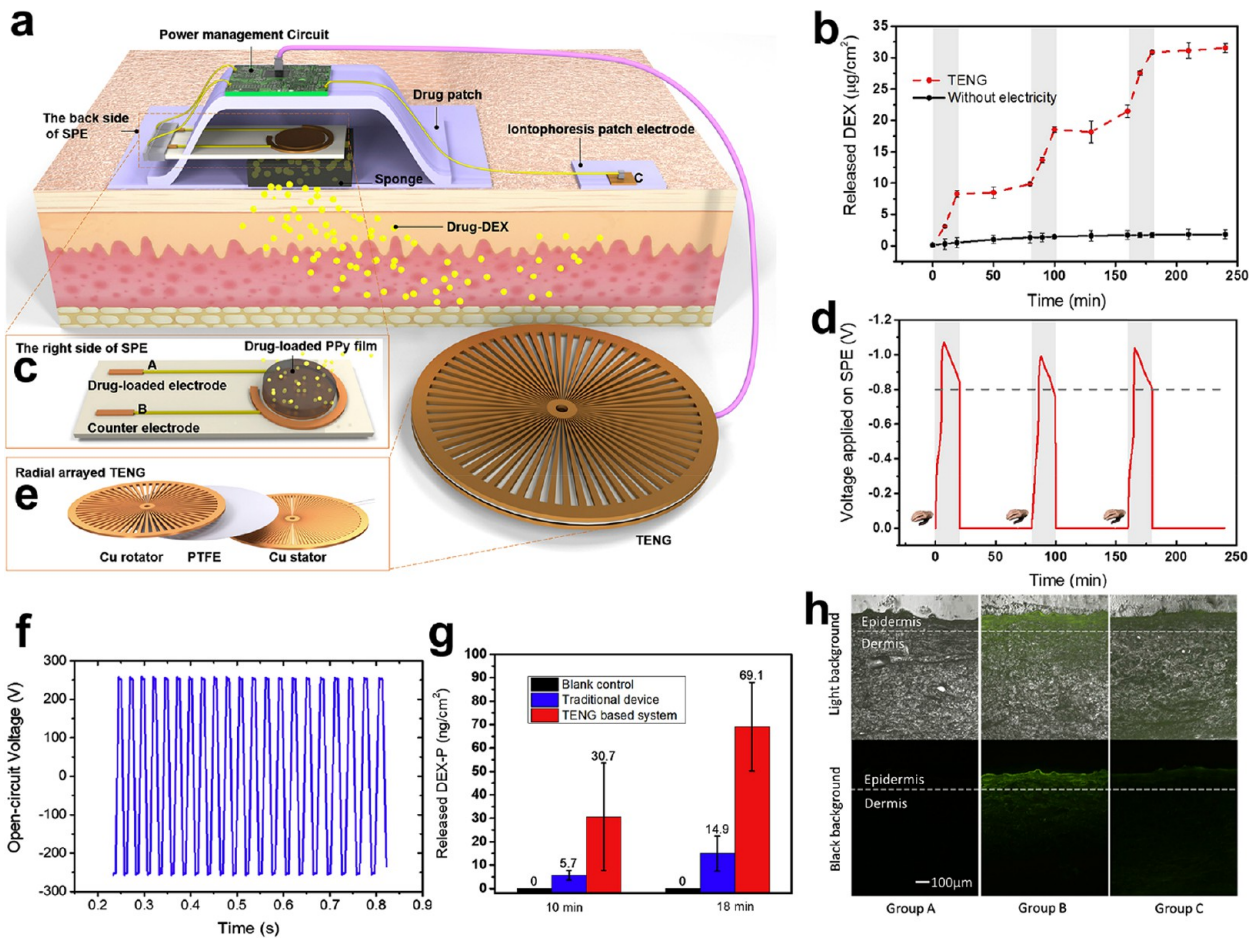

Figure 17. Applying TENGs-based ES for realizing iontophoretic TDD. a) Schematic illustration of the self-powered, on-demand transdermal drug delivery system based on TENG-based ES. b) The promoted drug release from the transdermal patch under the effect of TENG-based ES. c) The schematics of the proposed transdermal patch. d) Drug release can only be triggered under the effective voltages generated by TENG. e) The schematics of the rotary TENG. f) The output performance of TENG. g) Amount of drug that penetrates the porcine dermis after being released from the patch. h) Cross-section fluorescent images of the porcine skin demonstrating the TENG-based ES can induce the best transdermal drug behavior. Reproduced with permission from ref.[41] Copyright 2019 Elsevier.

samples were stained with DAPI, which revealed no significant differences between the rGO microfiber and the 15% rGO-PEDOT hybrid microfiber (Figure 16e-a1 to 16e-d1). To assess the effect of inherent materials characteristics and TENGs-based ES on neural differentiation, immunostaining was used to measure the expression of two neural special markers, Tuj1 for neuron cells and GFAP for glial cells. Without TENGs-based ES, Tuj1 expression was minimal in the cells attached to the rGO microfiber (Figure 16e-a2), whereas Tuj1 expression was moderate in the 15% rGO-PEDOT hybrid microfiber (Figure 16e-b2). However, GFAP expression on 15% rGO-PEDOT hybrid microfibers (Figure 16e-b3) and rGO microfibers (Figure 16e-a3) showed no significant distinction. The results suggested that the rGO-PEDOT microfiber can promote the expression of Tuj1, indicating that the 15% rGO-PEDOT microfiber can promote the neutral differentiation of MSCs cells. With TENGs-based ES, both Tuj1 and GFAP expression in cells on the 15% rGO-PEDOT microfiber increased considerably compared to rGO microfibers. Furthermore, gene expression levels of Tuj1 and GFAP were estimated to confirm the staining findings. The quantitative polymerase chain reaction (qPCR) results depicted in Figure 16f,g indicate that Tuj1 expression on the 15% rGO-PEDOT microfiber was 1.68-fold higher than that on the rGO microfiber, and there was a significant 1.5-fold increase in GFAP expression as well. These findings strongly suggested that TENGs-based ES can effectively promote the neural differentiation of MSCs cells.

APPLYING TENGS-BASED ES FOR ENHANCING TRANSDERMAL DRUG DELIVERY

Transdermal drug delivery (TDD) has gained recognition as a noninvasive, convenient, and painless medical technique for systemic therapy; however, the skin's barrier function limits its effectiveness.[3,121,122] ES, primarily in the form of iontophoresis and electroporation, has been shown to be effective in overcoming this barrier. Nevertheless, the requirement for significant and expensive energy sources has hindered ES's application.[123−125] Fortunately, TENGs have emerged as a promising and self-powered power source for offering ES to promote TDD due to their durability, portability, and cost-effectiveness.[29,126]

TENGs-Based ES for Realizing Iontophoresis Therapy. The TDD technique is limited by the skin's barrier function, hindering the delivery of medical compounds for systemic therapy. Iontophoresis, primarily using electric current, has been an effective strategy to enhance TDD, but the need for massive and pricey energy power has limited its application. Therefore, a more sustainable, portable, and cost-effective approach, such as

https://doi.org/10.1021/acsnano.3c01634
ACS Nano XXXX, XXX, XXX−XXX

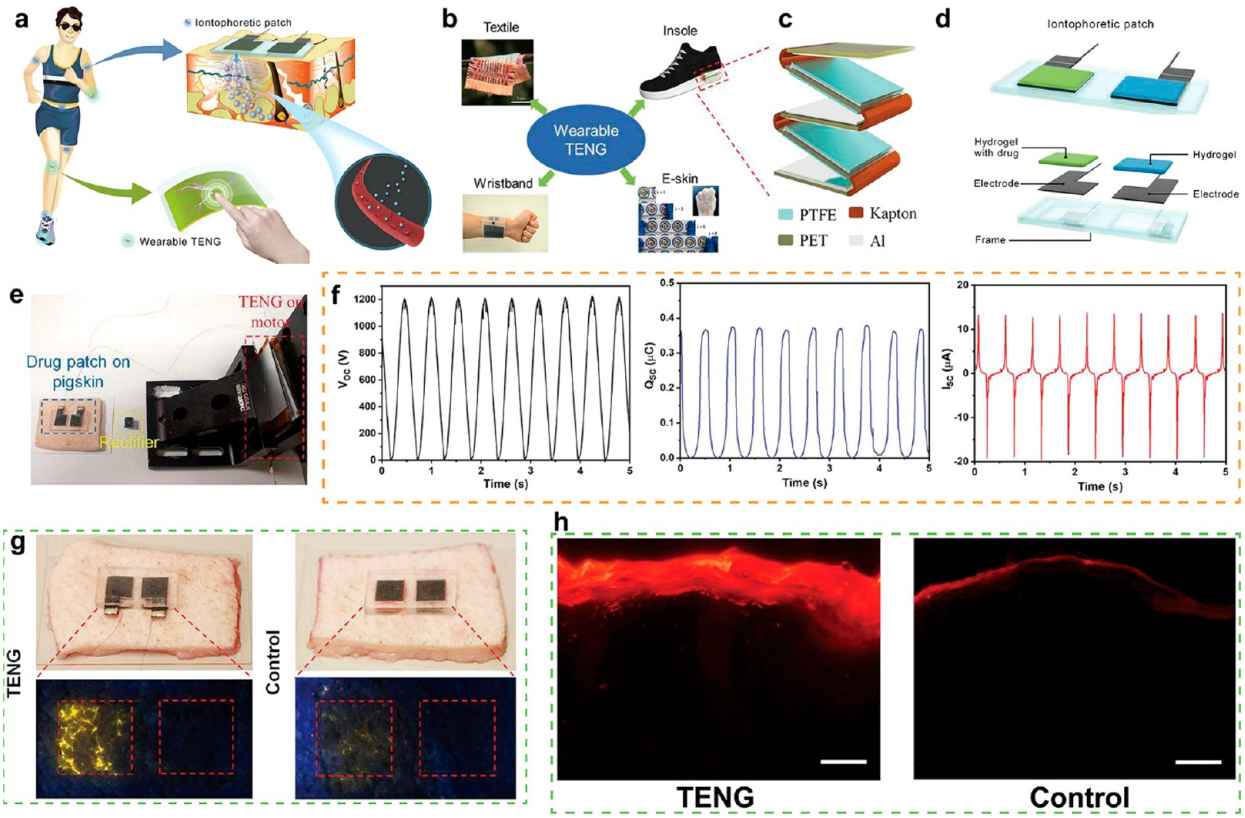

Figure 18. A wearable TENG-based drug iontophoresis patch for promoting TDD. a) Schematic of TENG-based TDD system composed of wearable TENG and iontophoresis patch. b) Examples of wearable TENGs. c) The structure of wearable insole TENG. d) Schematic of the hydrogel-based iontophoresis patch structure. e) Photograph of the experimental setup with a linear motor simulating the movement of the feet. f) Representative electrical outputs of the insole TENG. V_{OC} is open-circuit voltage, Q_{SC} is short-circuit charge transfer, and I_{SC} is short-circuit current. g) Photograph and fluorescence images of the R6G-containing hydrogel drug patch on skin with TENG and without TENG connection. h) Fluorescent cross-sectional histological images of skin after R6G delivery from the patch with TENG and without TENG connection, scale bar: 50 μm. Reproduced with permission from ref.[42] Copyright 2019 Wiley-VCH.

TENG-based ES, is necessary to overcome the limitations of iontophoresis and promote TDD. For instance, a TENG-based transdermal drug delivery system with enhanced delivery efficiency was proposed in 2019, employing TENG-based ES to trigger drug release and iontophoretic TDD, showing better drug release and transdermal ability compared with the control group and the conventional power group, as shown in Figure 17a.[41] Specifically, the system was composed of three parts: TENG, power management circuit, and transdermal patch (drug repository and iontophoresis patch). As shown in Figure 17c, the transdermal patch was a screen printed electrode (SPE) combing a round drug-loaded PPy-coated electrode A and an annular counter electrode B. In response to ES, the drug molecules that were originally incorporated in the PPy coating can be released. Simultaneously, the iontophoretic function of the transdermal patch can be activated under ES. The TENG consisted of a rotator and a stator (Figure 17e). When the TENG was driven by a motor, the resultant open-circuit voltage (as high as 250 V) could be converted by the power management circuit to desired DC voltage (within 0.8−1.5 V) for drug release and iontophoresis therapy (Figure 17f). When the rotary TENG was manually operated for 3 min, the adjusted DC voltage can be maintained for about 20 min. In order to evaluate the ES-triggered drug release from the patch, TENG was operated for 3 min each time. Thus, the drug-loaded transdermal patch had the effective voltage for 20 min and followed by a 60 min period with no voltage applied, as illustrated in Figure 17b. The results showed that the drug release can only be triggered when the effective voltages were generated by the TENG and applied on the transdermal patch (Figure 17d). Porcine skin was employed as an *ex vivo* model to evaluate the iontophoretic TDD performance. 6-Carboxyfluorescein (FLU) was loaded into PPy to facilitate the visualization of release behavior. The TENG-based ES group exhibited superior drug release and transdermal ability than the control and conventional power groups, as evidenced by fluorescent images. These results indicated the potential of TENGs-based ES for realizing iontophoresis therapy and promoting TDD.

While the above-mentioned TENG-based transdermal patch exhibited favorable transdermal properties, manually operating the rotary TENG may prove inconvenient for patients with limited mobility. To address this issue, Wu et al. developed a wearable TENG that can convert biomechanical motions into electricity using a hydrogel-based soft patch, thus facilitating iontophoretic TDD, as shown in Figure 18a.[42] The TENG can be constructed in a variety of form factors and installed on various body regions to harvest electrical energy from biomechanical actions and achieve maximal patient compliance (Figure 18b). As illustrated in Figure 18c, the four components of the TENG were Al as the triboelectric material and electrode, PTFE as another triboelectric material, poly(ethylene terephthalate) (PET) as the substrate, and Kapton as the bracket. The drug patch was comprised of two adjacent hydrogel cells and two carbon-cloth electrodes placed in a polydimethylsiloxane

https://doi.org/10.1021/acsnano.3c01634
ACS Nano XXXX, XXX, XXX−XXX

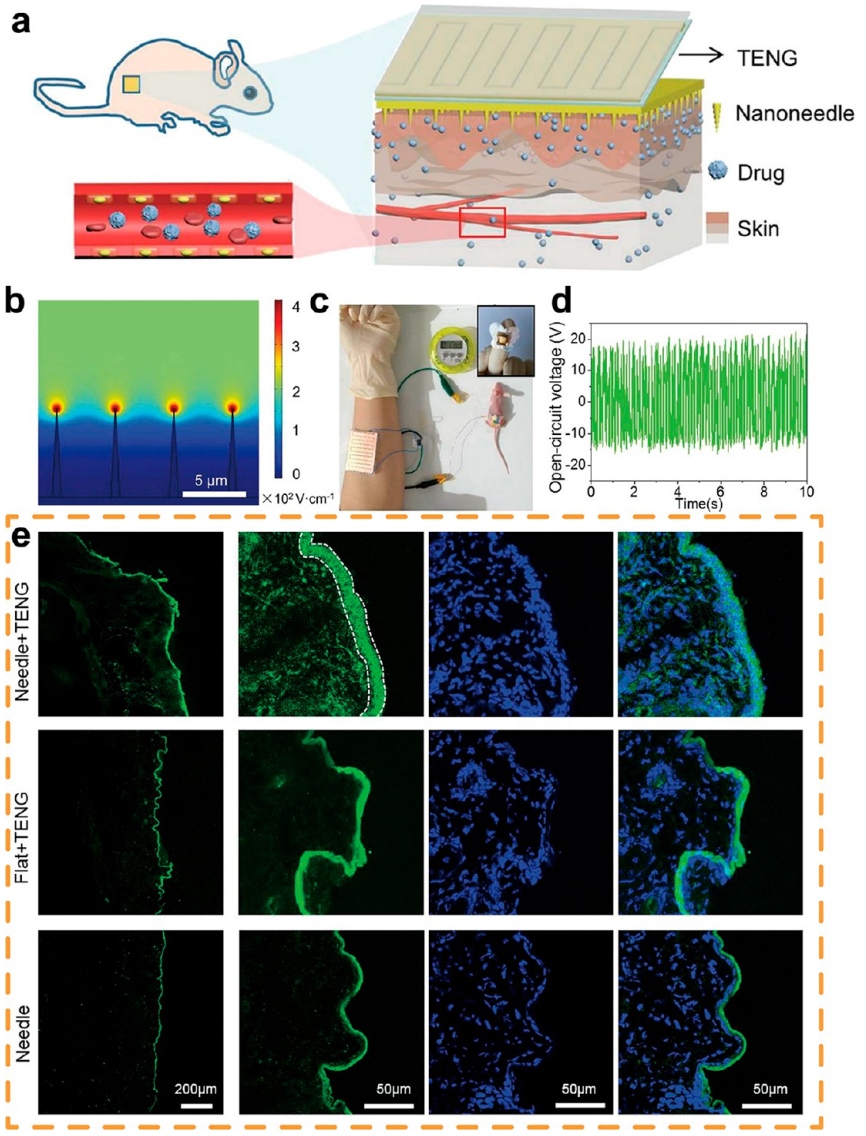

Figure 19. Electroporation TDD patch enabled by TENG-based ES. a) Schematic illustration of the proposed electroporation TDD system by employing TENG-based ES, which combined wearable TENG and the array of silicon nanoneedles electrode. b) The simulation of the electrical field distribution of the nanoneedle array when 20 V was applied. c) Photograph of the electroporation transdermal drug delivery system. d) The output performance of freestanding TENG driven by finger friction or hand clapping. e) Fluorescence images of cross-section tissue for drug-FITC delivery after different treatments. Reproduced with permission from ref.[33] Copyright 2019 Wiley-VCH.

(PDMS) framework (Figure 18d). For ankle injury, the drug patch was placed at the ankle, and a wearable TENG was put under the shoe. When the patient started walking, the TENG was able to generate electrical energy and transfer it to the patch, facilitating drug penetration through the skin. The typical output performance of the TENG was illustrated in Figure 18f. It had an open-circuit voltage of about 1200 V, a short-circuit charge transfer of about 370 nC per cycle, and a short-circuit current of about 20 A at 2 Hz. To evaluate the transdermal performance of the TENG-based iontophoresis patch, R6G was loaded as the model drug in the hydrogel patch and applied to pig skin (Figure 18e). The fluorescent images in Figure 18g demonstrated that the fluorescence of R6G transported to the skin from the TENG-based patch was more obvious compared to the control group. Cross-sectional histological pictures were also collected, providing stronger evidence that the TENG-based patch delivered more R6G into the skin with deeper penetration, as shown in Figure 18h. These results demonstrate that the developed wearable TENG-based iontophoresis patch has an excellent effect in enhancing iontophoresis therapy and TDD.

TENGs-Based ES for Inducing Electroporation for TDD. Electroporation is a promising method for achieving transdermal drug delivery and enabling active molecules to enter cells.[127] However, the high voltage required during electroporation can generate irreparable holes in cell membranes, causing permanent cell damage and death.[61] Therefore, there is a necessity to develop a more gentle and controllable electroporation method that can deliver drugs into cells effectively without causing permanent damage. This is where TENGs-based ES comes in as a potential solution that can provide a lower voltage alternative for electroporation therapy and allow for more precise control over the electric field to achieve optimal drug delivery without causing damage to the cells. Recently, Liu et al. proposed an electroporation TDD system by employing TENG-based ES, which combined wearable TENG and an array of silicon nanoneedles electrode

https://doi.org/10.1021/acsnano.3c01634
ACS Nano XXXX, XXX, XXX−XXX

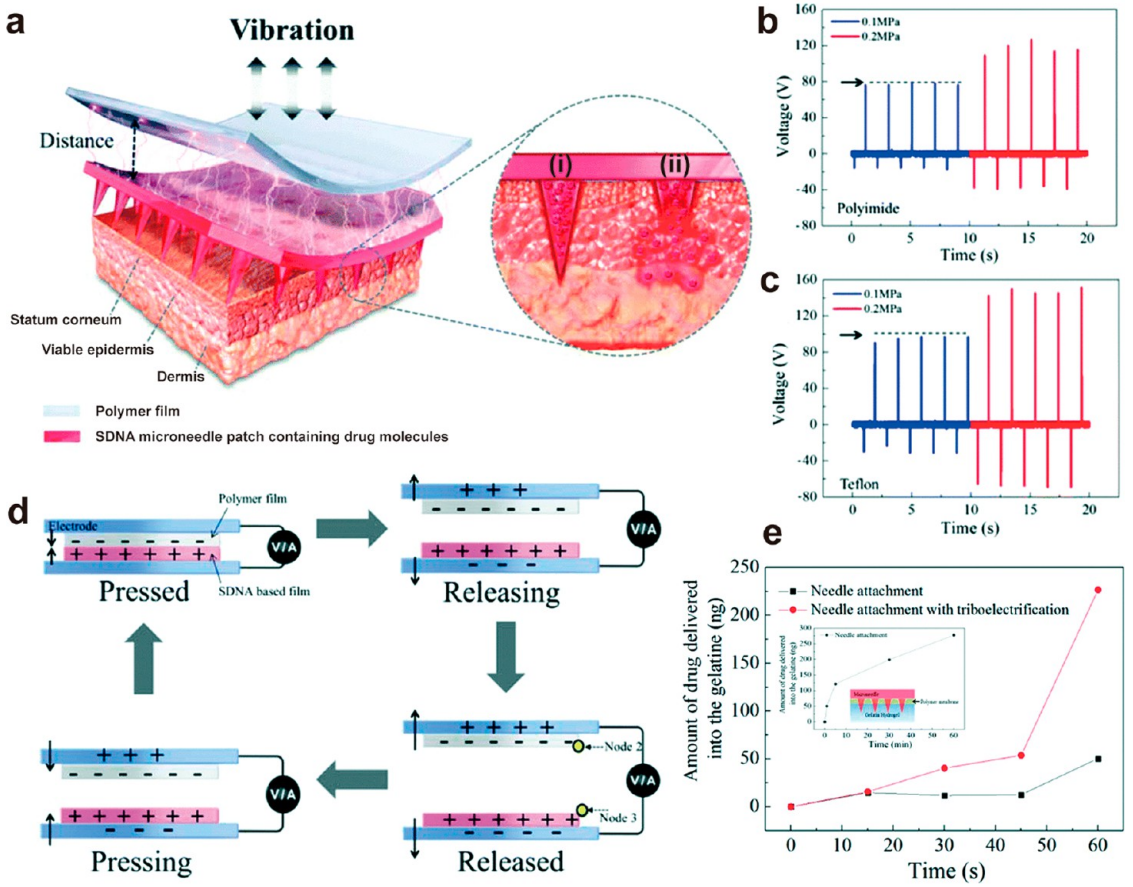

Figure 20. TENGs-based electrophoresis integrated with microneedles array can promote drug transdermal delivery. a) The coupling of the triboelectricity generated by vertical vibration with SDNA microneedles containing drug molecules. b) Output voltage of the TENG with Polyimide-SDNA. c) Output voltage of the TENG with Teflon-SDNA. d) Schematic illustration of the working mechanism of the SDNA-based TENG. e) Electrophoresis enabled by the TENG-based ES can improve the amount of the efficiency of TDD. Reproduced with permission from ref.[130] Copyright 2018 The Royal Society of Chemistry.

to reduce cell damage by enhancing the localized electric field.[33] As illustrated by the schematics in Figure 19a, a rectangular TENG in contact-separation mode was attached to human arm skin and driven by finger friction or hand slapping, and a array of silicon nanoneedles was attached to the skin of mice to realize transdermal drug delivery and penetration augmentation. The results of the electrical field in Figure 19b demonstrated that, when the wearable TENG output was 20 V, the enhanced electric field was limited to the tip of microneedles (up to about 2800 V cm^{-1}). *In vivo*, mice models were utilized to assess the performance of an integrated TENG patch designed for electroporation TDD, as depicted in Figure 19c. The fluorescent images of cross-sectional tissue (Figure 19e) showed that the drug-FITC (FITC = fluorescein isothiocyanate) was effectively delivered to the back skin of mice at a depth of approximately 23 μm, which was superior to that achieved by a flat electrode with ES based on TENG (11 μm) and a nanoneedle array without TENG-ES (6 μm). These results indicated that the TENG-based electroporation patch, which combined a freestanding TENG and an array of silicon nanoneedles, can efficiently induce electroporation TDD by facilitating drug penetration into deep skin while avoiding permanent cell damage and death.

Electrophoresis Enabled by TENGs-Based ES Integrating with Microneedles for TDD. The use of microneedles can enhance the efficiency of transdermal drug delivery by creating tiny holes in the skin. However, when used alone, microneedles have limited ability to deliver a wider variety of medications and biomolecules. Thus, combining microneedles with electrophoresis can further enhance the permeability of the lipid bilayer and facilitate the transport of a broader range of therapeutic agents into the skin. The addition of TENGs-based ES can further amplify the electric field and promote drug migration, enabling the realization of a more efficient and versatile electrophoresis therapy.[128,129] Recently, Bok et al. proposed an integrated system of salmon DNA (SDNA)-based microneedles and TENG-based electrophoresis for transdermal drug delivery, which demonstrated enhanced efficiency compared to the control group without TENG-based electrophoresis.[130] As illustrated in Figure 20a, the structure of this integrated system had two parts: the SDNA microneedles patch containing drug molecules and TENG (polymer film) for electrophoresis. When the drug-loaded SDNA microneedles reached the stratum corneum (Figure 20a, image i), they started to disintegrate and release the drug molecules into the skin (Figure 20a, image ii). Then, the ES generated by contact-separation mode TENG was coupled to a microneedles array for perturbating the lipid bilayer by electrophoresis. Figure 20d depicts the working mechanism of the TENG to help with understanding the triboelectrification based on the SDNA film. Specifically, in the initial state, there was a gap between the SDNA and polymer films. The SDNA and polymer films changed from neutral to positively and negatively charged, respectively, when the two films were pressed together.

https://doi.org/10.1021/acsnano.3c01634
ACS Nano XXXX, XXX, XXX−XXX

Table 1. A Summary of Current Skin Applications Enabled by TENGs-Based ES

Triboelectric materials	Operating modes	Type/intensity/frequency of ES	Features	Skin applications
PDMS and a gelatin/glycerol (G/G) film	Contact-separation	Bidirectional PC/Open circuit voltage: 100−500 V/Frequency: 1, 2, and 4 Hz	Synergistic effects of H_2O_2 generation and electroporation of ES	Antibacterial[35]
RSSP and PET	Contact-separation	Bidirectional PC/Open circuit voltage: 150 V/ Frequency: 1−20 Hz	Ag nanoparticles and electroporation offer synthetic effects	Antibacterial[36]
Polytetrafluoroethylene (PTFE) and Mg−Al LDH@Al film	Contact-separation	Bidirectional PC/Open circuit voltage: 6 V/ Frequency: 1−4 Hz	LIEF-induced membrane permeability change, hydrogen peroxide buildup, and drug release obtained synergetic effects	Antibacterial[37]
PTFE/Cu layer and another Cu layer	Lateral sliding	Bidirectional PC/Open circuit voltage: 0.2−2.2 V/ Frequency: 0.5−1.83 Hz	Promote the proliferation, migration and differentiation of fibroblasts	Wound healing[38]
Ionic patch and skin	Contact-separation	Bidirectional PC/Open circuit voltage: 10 V/ Frequency: 0.5−2.0 Hz	Promote the migration, proliferation and secretion of angiogenic growth factors of dermal fibroblasts	Wound healing[39]
Ecoflex-B and nylon-coated cloth	Contact-separation	Bidirectional PC/Open circuit voltage: 125 V/ Frequency: 2.5 Hz	Promote the proliferation, migration of fibroblasts	Wound healing[54]
Leather and PDMS	Contact-separation	Bidirectional PC/Open circuit voltage: 12 V	Induce cell proliferation, migration, and differentiation and stimulating granulation tissue growth	Wound healing[55]
Polyimide film as the triboelectric layer, the PTFE film as the dielectric layer	Freestanding triboelectric layer	Bidirectional PC/Open circuit voltage: 20 V/ Frequency: 2 Hz	Improve pharmacodynamics of epidermal growth factor (EGF)	Wound healing[104]
The human skin and Ecoflex	Contact-separation	Bidirectional PC/Open circuit voltage: 15−75 V/ Frequency: 1−10 Hz	Enhance the expression of TGF-β and VEGF, promote more re-epithelialization and angiogenesis	Wound healing[40]
PTFE and aluminum	Contact-separation	Bidirectional PC/Open circuit voltage: 1.5−8.8 V	Induce the proliferation and migration of fibroblasts, remove ROS free radicals, and instruct cell behavior	Wound healing[113]
Al film and PTFE	Contact-separation	Bidirectional PC/Open circuit voltage: 100 V/ Frequency: 2 Hz	Promote adhesion, differentiation, and proliferation of osteoblasts	Bone tissue repairing[116]
Natural bioresorbablepolymers (NBPs)	Contact-separation	Bidirectional PC/Open circuit voltage: 34 V/ Frequency: 1 Hz	Promote the beating rates of cardiomyocyte clusters	Myocardial tissue repairing[117]
Al film and Kapton	Contact-separation	Bidirectional PC/Open circuit voltage: 300 V/ Frequency: 1.4−3 Hz	Promote neural differentiation of MSCs cells	Neural tissue repairing[120]
PTFE and copper	Lateral sliding	DC/Open circuit voltage: 0.8−1.2 V	Iontophoresis and electro-induced drug release	Transdermal drug delivery[41]
PTFE and aluminum	Contact-separation	PC/Open circuit voltage: 4 V	Iontophoresis	Transdermal drug delivery[42]
Al film and Fluorinated ethylene propylene (FEP) film	Contact-separation	Bidirectional PC/Open circuit voltage: 20 V/ Frequency: 20 Hz	Electroporation	Transdermal drug delivery[33]
Polymer film and SDNA film	Contact-separation	Bidirectional PC/Open circuit voltage: 95 V/ Frequency: 2 Hz	Synthetic effects of microneedles array and electrophoresis	Transdermal drug delivery[130]

https://doi.org/10.1021/acsnano.3c01634
ACS Nano XXXX, XXX, XXX−XXX

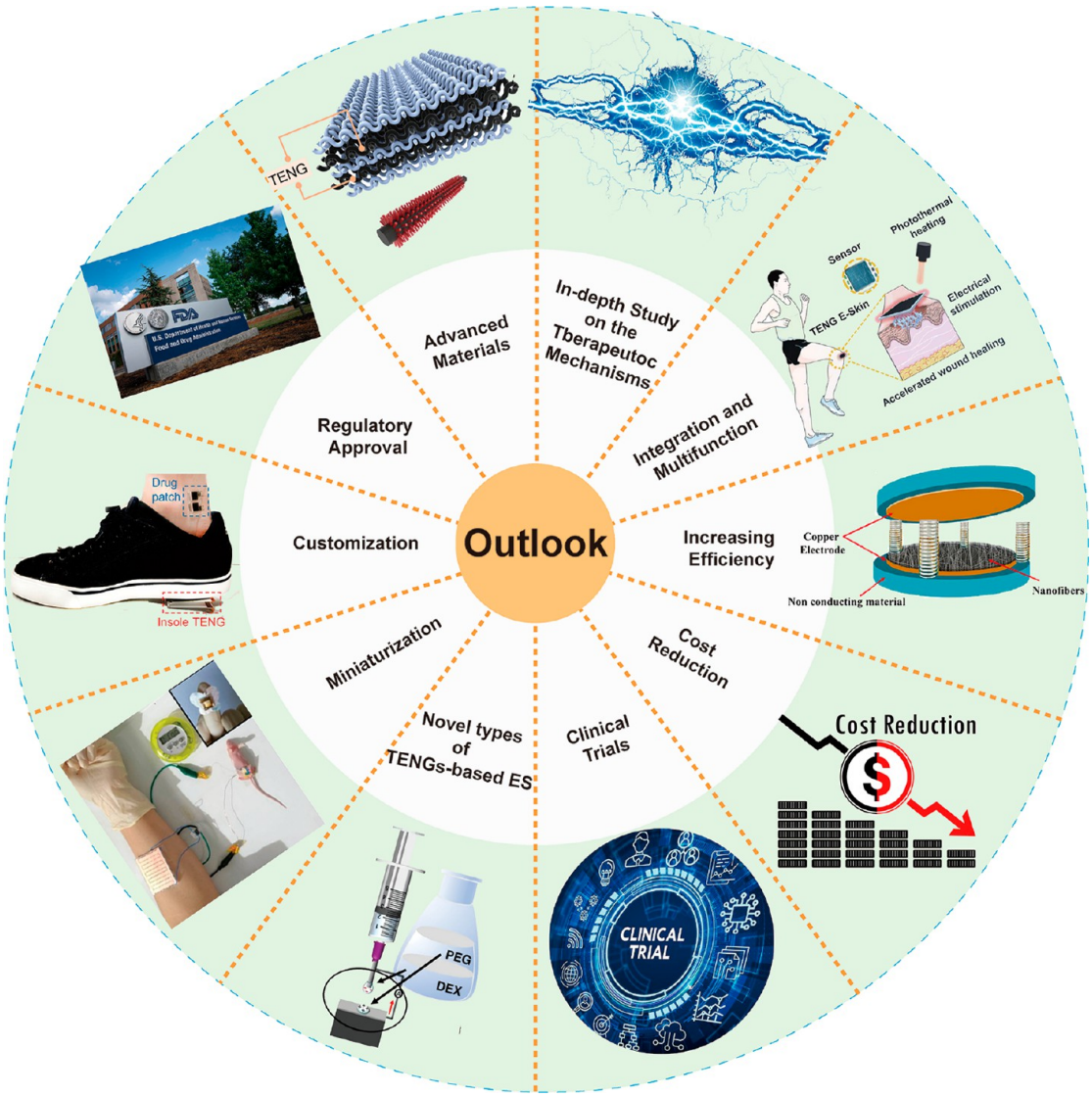

Figure 21. Outlook, challenges, and future research opportunities. Reproduced with permission from ref.[35] Copyright 2018 Elsevier. Reproduced with permission from ref.[40] Copyright 2021 Elsevier. Reproduced with permission from ref.[131] Copyright 2018 Society of Plastics Engineers. Reprinted with permission under a Creative Commons Attribution 4.0 International (CC BY 4.0) License from ref.[132] Copyright 2022 Ye Lu et al., published by Nature. Reproduced with permission from ref.[33] Copyright 2019 Wiley-VCH. Reproduced with permission from ref.[42] Copyright 2019 Wiley-VCH.

When the contact surface started to separate, a potential difference was created between the two pieces. Then when the two films were drawn closer once again, the potential difference was eliminated. AC voltage can be generated by repeating the above process. To assess the output performance of TENG, SDNA-polyimide and SDNA-Teflon films were utilized. As shown in Figure 20b,c, the polyimide-SDNA film had an output voltage of 80 V and the Teflon film had an output voltage of 100 V when subjected to an external force of 0.1 MPa. The transdermal drug delivery performance of an integrated system consisting of hydrogel derived from bovine skin as a model tissue, SDNA-based microneedles, and TENG-based electrophoresis was evaluated, and the results showed that, after 60 min of TENG-ES microneedle administration, 220 ng of the drug was delivered, indicating that the combination of TENGs-based ES with other techniques can greatly improve the efficiency of TDD.

CONCLUSION AND PROSPECTS

In summary, we have outlined the recent progress in applying TENGs-based ES as a versatile strategy for achieving comprehensive therapeutic effects on multiple skin applications (Table 1). The concepts of self-power and biocompatibility of the TENGs-based ES will lead to better understanding in fundamental science and propel advancements in biomedical devices and applications. A plethora of emerging opportunities, together with challenges, are briefly presented below (Figure 21).

In-Depth Study on the Therapeutic Mechanisms. Despite the impressive therapeutic outcomes demonstrated by TENGs-based ES in various skin applications, the underlying biological mechanisms remain largely unexplored. The electric conduction behavior of TENGs-based ES in a humoral environment is more complex than in a metal environment due to the presence of an electrochemical interface between the electrode and the skin surface, and further investigation into this

https://doi.org/10.1021/acsnano.3c01634
ACS Nano XXXX, XXX, XXX−XXX

phenomenon is crucial for understanding the basic mechanisms of TENGs-based ES.[133,134] Additionally, although the antibacterial effects of traditional ES have been well-established through the induction of electroporation and other mechanisms, the antibacterial mechanisms of TENGs-based ES have not yet been thoroughly explored.[35−37] Moreover, while TENGs-based ES has been shown to enhance wound healing, the exact mechanisms by which it stimulates fibroblast proliferation and differentiation remain unclear.[135] Furthermore, the mechanisms by which TENGs-based ES modulates skin structure and permeability to facilitate transdermal drug delivery are also largely unaddressed, indicating the need for further research in this area.[51] Therefore, to advance our understanding of the therapeutic effects of TENGs-based ES, it is important to undertake further studies to investigate the biological mechanisms involved. This may involve developing more sophisticated experimental systems and integrating techniques from multiple scientific disciplines to achieve a more in-depth characterization of the relationship between biological therapeutic factors and the electrical properties of TENGs-based ES.

Integration and Multifunction. The potential for synergistic effects can be achieved by combining TENGs-based ES with other methods. For example, the combination of TENGs-based ES and Ag nanowires has been shown to enhance antibacterial performance and photothermal heating capability, leading to improved expression of EGF, re-epithelialization, angiogenesis, and accelerated wound healing.[36] This inspires the integration of TENGs-based ES with other therapeutic techniques such as ultrasonication in physiotherapeutic strategies and photodynamic therapy in chemotherapeutic strategies.[136] Exploring synergistic effects through the combination of therapeutic techniques and TENGs-based ES has significant implications for not only skin but also other biomedical applications.

Moreover, the integration of TENGs-based ES with other technologies, such as sensors and wireless communication, can enable more advanced applications. For instance, TENGs-based ES can be combined with sensors to monitor the healing of wounds and provide real-time feedback to medical professionals.[137] TENGs-based ES can also be integrated with wireless communication technologies to enable remote monitoring and control of the therapeutic treatment.[138] Integration with other technologies requires the development of advanced control systems and communication protocols that enable seamless integration of the different technologies.

Increasing Efficiency. The efficiency of electricity generation in TENGs is a crucial factor that will determine their practical applications. Researchers are exploring various approaches to improve the efficiency of TENGs-based electricity generation systems. One approach involves optimizing the design of the TENG structure, including the materials used and the pattern of the electrodes.[36] Another approach involves exploring the use of advanced materials, such as nanomaterials and composites, to enhance electricity generation efficiency.[35] Additionally, researchers are exploring the use of hybrid electricity generation systems that combine TENGs with other technologies, such as piezoelectric and thermoelectric generators, to increase the overall efficiency of the system.[131]

Miniaturization. Miniaturization of TENGs is another area of active research. To be useful for therapeutic ES, TENGs need to be small and lightweight, making them suitable for wearable and implantable applications. Miniaturization of TENGs requires the development of fabrication techniques and the use of advanced materials to reduce the size of the device while maintaining its efficiency. The use of flexible and stretchable materials, such as polymers and elastomers, is also critical for the miniaturization of TENGs, as they enable the devices to conform to the skin surface and provide comfortable and unobtrusive stimulation.[39,54,55]

Customization. One of the key advantages of TENGs-based ES is its ability to provide personalized and customized treatment.[139] TENGs can be designed to match the specific requirements of individual patients, enabling the development of tailored therapeutic treatments. Researchers are exploring various approaches to customize TENGs, including the use of machine learning algorithms to optimize the design of the TENGs for specific patients.[140] In addition, the use of flexible and stretchable materials in the fabrication of TENGs enables customization by allowing the device to conform to the skin surface.[36]

Advanced Materials. The development of advanced materials is critical for improving the performance and durability of TENGs. Researchers are exploring the use of various materials, such as polymers, composites, and nanomaterials, to improve the properties of TENGs.[37] For instance, the use of high-performance polymers, such as polyimides and polyurethanes, can improve the mechanical and thermal properties of TENGs, making them more durable and reliable.[54] The use of composites, such as carbon fiber composites and metal−polymer composites, can also improve the electricity generation efficiency and mechanical properties of TENGs devices.[35] Additionally, the use of nanomaterials, such as graphene and carbon nanotubes, can improve the electrical properties of TENGs, making them more efficient and sensitive.[141]

Liquid−Liquid TENGs-Based ES. The utilization of traditional TENGs for the generation of ES has typically been based on a solid−solid interface. Despite their success, such TENGs present several limitations including limited charge transfer and concerns regarding biocompatibility. These factors hinder the practical application of these TENGs in biomedical applications. In response, the development of TENGs that feature improved charge transfer and biocompatibility is of utmost importance. Recently, the design of TENGs based on solid−liquid interfaces has gained considerable attention.[142] However, challenges such as limited contact area and biocompatibility concerns remain. Recently, liquid−liquid TENGs based on the immiscible interface of an aqueous two-phase system (ATPS) have been developed with 100% contact area and improved charge transfer.[132] In addition, the ATPS can avoid the use of oily phases, organic solvents, strong acids, and alkalis with poor biocompatibility. Thus, it can provide a green all-aqueous environment and endow superior biocompatibility for the entire process, which enables the generation of ES in a biocompatible manner. This type of TENG represents a significant shift in the scientific study of TENGs-based ES. Further investigation is needed to determine the best application of these TENGs in skin and other biomedical applications.

Regulatory Approval. The regulatory approval of TENG-based ES is critical for their widespread adoption in clinical settings. To gain regulatory approval, TENGs need to be tested and evaluated for their safety and efficacy.[143] This requires the development of standardized testing protocols and procedures that enable consistent and reproducible evaluation of TENGs. Additionally, regulatory approval requires the development of manufacturing processes and quality control procedures that ensure the safety and reliability of TENGs-based ES.

https://doi.org/10.1021/acsnano.3c01634
ACS Nano XXXX, XXX, XXX−XXX

Cost Reduction. One of the challenges in the widespread adoption of TENGs-based ES for skin applications is the cost of production. The cost of materials and fabrication processes can be significant, particularly for customized or miniaturized devices. Therefore, researchers are exploring various approaches to reduce the cost of TENGs.[144] One approach is to use low-cost and abundant materials, such as polymers and metals, to fabricate TENGs. Another approach is to develop scalable and high-throughput manufacturing processes that can reduce the cost of production. For example, researchers are exploring the use of 3D printing and roll-to-roll printing to manufacture TENGs at a lower cost.[145,146] In addition, the integration of TENGs with other technologies, such as sensors and wireless communication, can also reduce the overall cost of the system by enabling more efficient and targeted treatment.[138]

Clinical Trials. Clinical trials are critical for evaluating the safety and efficacy of TENGs-based ES for skin applications. The results of clinical trials can inform the development of TENGs and guide their use in clinical settings.[49] Clinical trials also provide an opportunity to validate the personalized and customized nature of TENGs-based treatments. Currently, there are only a limited number of clinical trials involving TENGs-based ES for skin applications. Therefore, there is a need for more extensive and rigorous clinical trials to evaluate the safety and efficacy of TENGs. These trials should involve a diverse range of patients, including those with different skin conditions, ages, and medical histories. Additionally, the trials should evaluate the long-term safety and efficacy of TENGs, particularly in the context of wearables and implants. The results of these trials can provide valuable insights into the effectiveness of TENG-based treatments and inform the development of devices and treatment protocols.

AUTHOR INFORMATION

Corresponding Authors

Hongfei Xiang − *Department of Orthopedic Surgery, the Affiliated Hospital of Qingdao University, Qingdao 266000, China*; Email: zli@binn.cas.cn

Xiaoxiong Wang − *College of Physics, Qingdao University, Qingdao 266071, China*; orcid.org/0000-0001-9375-4829; Email: wangxiaoxiong69@163.com

Yong Sun − *Department of Pharmaceutics, School of Pharmacy, Qingdao University, Qingdao 266021, China*; Email: sunyongqdu@163.com

Zhou Li − *CAS Center for Excellence in Nanoscience, Beijing Key Laboratory of Micro−Nano Energy and Sensor, Beijing Institute of Nanoenergy and Nanosystems, Chinese Academy of Sciences, Beijing 100083, China; School of Nanoscience and Technology, University of Chinese Academy of Sciences, Beijing 100049, China*; orcid.org/0000-0002-9952-7296; Email: xianghf@qdu.edu.cn

Qingming Ma − *School of Pharmacy, Qingdao University, Qingdao 266021, China; The Shandong Consortium in the Yellow River Basin for Prevention, Treatment and Drug Development for Primary Diseases Related to Alcoholism, Qingdao University, Qingdao 266021, China*; orcid.org/0000-0001-9026-2706; Email: qma@qdu.edu.cn

Authors

Weijiang Wang − *School of Pharmacy, Qingdao University, Qingdao 266021, China*

Wentao Sun − *School of Health and Life Sciences, University of Health and Rehabilitation Sciences, Qingdao 266113, China*

Yanfeng Du − *College of Physics, Qingdao University, Qingdao 266071, China*

Wenbin Zhao − *School of Pharmacy, Qingdao University, Qingdao 266021, China*

Lijun Liu − *School of Pharmacy, Qingdao University, Qingdao 266021, China*

Dejuan Kong − *Tongliao Market Detection and Testing Center, Tongliao 028000, China*

Complete contact information is available at: https://pubs.acs.org/10.1021/acsnano.3c01634

Author Contributions

ΦW.W. and W.S. contributed equally to this work. The manuscript was written through contributions of all authors. All authors have given approval to the final version of the manuscript.

Notes

The authors declare no competing financial interest.

ACKNOWLEDGMENTS

This study was supported by the Shandong Provincial Natural Science Foundation (ZR2022QH234), National Natural Science Foundation of China (12104249, 22008130, 82200440), the China Postdoctoral Science Foundation (2020M682124), the Qingdao Science and Technology Demonstration and Guidance Project (21-1-4-rkjk-10 nsh), and the financial support from The Shandong Consortium in the Yellow River Basin for Prevention, Treatment and Drug Development for Primary Diseases Related to Alcoholism.

ABBREVIATIONS

ES, electric stimulation; TENG, triboelectric nanogenerator; G/G, gelatin/glycerol; PTFE, polytetrafluoroethylene; EGF, epidermal growth factor; FEP, fluorinated ethylene propylene; TDDS, transdermal drug delivery system; TE, triboelectricity; S. aureus, *Staphylococcus aureus*; *E. coli*, *Escherichia coli*; CuONW, copper oxide nanowire; m-TENG, multilayered triboelectric nanogenerator; CFFs, carbon fiber fabrics; Au−Te NWs, Au−Te nanowires; SEM, scanning electron microscopy; RSSP, recombinant spider silk proteins; SETENG, surface engineered TENG; LDH, Mg−Al double hydroxides; LIEF, low-intensity electric field; PET, poly(ethylene terephthalate); SD, Sprague−Dawley; EF, electric field; iTENG, ionic TENG; Ecoflex-B, borophene/ecoflex; B-TENG, fabric-based triboelectric nanogenerator; CF, carbon fiber; PDMS, polydimethylsiloxane; PAAm-LiCl, polyacrylamide-LiCl; mn-STESS, microneedle-based self-powered transcutaneous ES system; sf-TENG, sliding free-standing triboelectric nanogenerator; CMNPs, composite microneedle patches; cGel-cHA MNs, cross-linked gelatin and cross-linked hyaluronic acid microneedles; NVs, new vessels; HFs, hair follicles; PPy, polypyrrole; NIR, Near Infra-Red; ROS, reactive oxygen species; LBL, layer-by-layer; HTCC, 2-hydroxypropyltrimethylammonium chloride chitosan; ALG, alginate; PNPs, polydopamine nanoparticles; SN, self-powered nanogenerator; Al, aluminum; PVC, polyvinyl chloride; LM, liquid metal; DPPH, 2,2-diphenyl-1-picrylhydrazyl; TDD, transdermal drug delivery; SPE, screen printed electrode; FLU, 6-carbox-yfluorescein; PET, poly(ethylene terephthalate); PDMS, polydimethylsiloxane; SDNA, salmon DNA; ATPS, aqueous two-phase system

https://doi.org/10.1021/acsnano.3c01634
ACS Nano XXXX, XXX, XXX−XXX

VOCABULARY

Triboelectric nanogenerators (TENGs), are a class of energy harvesting devices that convert mechanical energy, typically generated by human motion or environmental vibrations, into electrical energy using the triboelectric effect. TENGs utilize the contact and separation of materials with different electrostatic properties to induce a flow of electrons, creating an electric potential and generating usable electrical power. They offer a promising avenue for self-powered systems, wearable electronics, and the integration of energy harvesting capabilities into various devices and structures; **Electrical stimulation (ES)**, is a type of physical therapy modality or treatment used to accomplish various tasks in physical therapy. It involves the application of an electrical current through electrodes that are either placed in close proximity to a wound on the skin or inserted directly into the wound itself. This technique enables medical professionals to administer external electrical signals to wound tissue, which replicates the intrinsic bioelectrical response to injury that occurs naturally within the body; **Transdermal drug delivery (TDD)**, refers to the administration of therapeutic substances through the skin for systemic distribution in the body. It involves the application of specially formulated pharmaceutical products, such as patches or gels, that enable the active drug molecules to permeate the outer layers of the skin and enter the bloodstream. This route of drug administration bypasses the gastrointestinal tract and provides controlled, sustained release of the medication, allowing for consistent therapeutic levels in the body over an extended period; **Antibacterial**, refers to the property or characteristic of a substance, treatment, or agent that is effective in inhibiting or killing bacteria, which are microorganisms that can cause infections and diseases. An antibacterial agent targets bacteria by disrupting their growth, metabolism, or vital cellular processes, thereby preventing their proliferation or directly causing their death. This term encompasses a wide range of compounds, including antibiotics, disinfectants, antiseptics, and other antimicrobial substances, which are employed in various medical, pharmaceutical, and hygiene applications to combat bacterial infections and maintain cleanliness; **Wound healing**, refers to the complex biological process by which the body repairs and restores damaged or injured tissues. It involves a series of coordinated events and cellular responses aimed at closing the wound, restoring tissue integrity, and promoting tissue regeneration. The process typically includes hemostasis (blood clot formation), inflammation, proliferation (cellular growth and migration), and remodeling (restructuring of the healed tissue). Various factors, such as the type and severity of the wound, the individual's overall health, and external interventions, can influence the speed and effectiveness of the wound healing process

REFERENCES

(1) Xu, Z.; Chen, D.; Hu, Y.; Jiang, K.; Huang, H.; Du, Y.; Wu, W.; Wang, J.; Sui, J.; Wang, W.; et al. Anatomically Distinct Fibroblast Subsets Determine Skin Autoimmune Patterns. *Nature* **2022**, *601* (7891), 118−124.

(2) Nizet, V.; Ohtake, T.; Lauth, X.; Trowbridge, J.; Rudisill, J.; Dorschner, R. A.; Pestonjamasp, V.; Piraino, J.; Huttner, K.; Gallo, R. L. Innate Antimicrobial Peptide Protects the Skin from Invasive Bacterial Infection. *Nature* **2001**, *414* (6862), 454−457.

(3) Prausnitz, M. R.; Langer, R. Transdermal Drug Delivery. *Nature biotechnology* **2008**, *26* (11), 1261−1268.

(4) Carter, P.; Narasimhan, B.; Wang, Q. Biocompatible Nanoparticles and Vesicular Systems in Transdermal Drug Delivery for Various Skin Diseases. *International journal of pharmaceutics* **2019**, *555*, 49−62.

(5) Velnar, T.; Bailey, T.; Smrkolj, V. The Wound Healing Process: An Overview of the Cellular and Molecular Mechanisms. *Journal of international medical research* **2009**, *37* (5), 1528−1542.

(6) Hu, W.; Wei, X.; Zhu, L.; Yin, D.; Wei, A.; Bi, X.; Liu, T.; Zhou, G.; Qiang, Y.; Sun, X.; et al. Enhancing Proliferation and Migration of Fibroblast Cells by Electric Stimulation Based on Triboelectric Nanogenerator. *Nano Energy* **2019**, *57*, 600−607.

(7) Biranje, S. S.; Madiwale, P. V.; Patankar, K. C.; Chhabra, R.; Bangde, P.; Dandekar, P.; Adivarekar, R. V. Cytotoxicity and Hemostatic Activity of Chitosan/Carrageenan Composite Wound Healing Dressing for Traumatic Hemorrhage. *Carbohydr. Polym.* **2020**, *239*, 116106.

(8) Peng, X.; Dong, K.; Ye, C.; Jiang, Y.; Zhai, S.; Cheng, R.; Liu, D.; Gao, X.; Wang, J.; Wang, Z. L. A Breathable, Biodegradable, Antibacterial, and Self-Powered Electronic Skin Based on All-Nanofiber Triboelectric Nanogenerators. *Science Advances* **2020**, *6* (26), No. eaba9624.

(9) Chopra, V.; Thomas, J.; Kaushik, S.; Rajput, S.; Guha, R.; Mondal, B.; Naskar, S.; Mandal, D.; Chauhan, G.; Chattopadhyay, N. Injectable Bone Cement Reinforced with Gold Nanodots Decorated Rgo-Hydroxyapatite Nanocomposites, Augment Bone Regeneration. *Small* **2023**, *19*, 2204637.

(10) Zhao, M.; Song, B.; Pu, J.; Wada, T.; Reid, B.; Tai, G.; Wang, F.; Guo, A.; Walczysko, P.; Gu, Y.; et al. Electrical Signals Control Wound Healing through Phosphatidylinositol-3-Oh Kinase-Γ and Pten. *Nature* **2006**, *442* (7101), 457−460.

(11) Qu, J.; Zhao, X.; Ma, P. X.; Guo, B. Injectable Antibacterial Conductive Hydrogels with Dual Response to an Electric Field and Ph for Localized "Smart" Drug Release. *Acta biomaterialia* **2018**, *72*, 55−69.

(12) Panwar, V.; Babu, A.; Sharma, A.; Thomas, J.; Chopra, V.; Malik, P.; Rajput, S.; Mittal, M.; Guha, R.; Chattopadhyay, N.; et al. Tunable, Conductive, Self-Healing, Adhesive and Injectable Hydrogels for Bioelectronics and Tissue Regeneration Applications. *J. Mater. Chem. B* **2021**, *9* (31), 6260−6270.

(13) Peters, E. J.; Lavery, L. A.; Armstrong, D. G.; Fleischli, J. G. Electric Stimulation as an Adjunct to Heal Diabetic Foot Ulcers: A Randomized Clinical Trial. *Archives of physical medicine and rehabilitation* **2001**, *82* (6), 721−725.

(14) Luo, R.; Dai, J.; Zhang, J.; Li, Z. Accelerated Skin Wound Healing by Electrical Stimulation. *Adv. Healthcare Mater.* **2021**, *10* (16), 2100557.

(15) Jain, S.; Sharma, A.; Basu, B. Vertical Electric Field Induced Bacterial Growth Inactivation on Amorphous Carbon Electrodes. *Carbon* **2015**, *81*, 193−202.

(16) Dauben, T. J.; Ziebart, J.; Bender, T.; Zaatreh, S.; Kreikemeyer, B.; Bader, R. A Novel *in Vitro* System for Comparative Analyses of Bone Cells and Bacteria under Electrical Stimulation. *BioMed. Research International* **2016**, *2016*, 5178640.

(17) Foldvari, M.; Babiuk, S.; Badea, I. DNA Delivery for Vaccination and Therapeutics through the Skin. *Curr. Drug Delivery* **2006**, *3* (1), 17−28.

(18) Sieg, A.; Guy, R. H.; Delgado-Charro, M. B. Noninvasive and Minimally Invasive Methods for Transdermal Glucose Monitoring. *Diabetes technology & therapeutics* **2005**, *7* (1), 174−197.

(19) Stupp, R.; Taillibert, S.; Kanner, A.; Read, W.; Steinberg, D. M.; Lhermitte, B.; Toms, S.; Idbaih, A.; Ahluwalia, M. S.; Fink, K.; et al. Effect of Tumor-Treating Fields Plus Maintenance Temozolomide Vs Maintenance Temozolomide Alone on Survival in Patients with Glioblastoma: A Randomized Clinical Trial. *Jama* **2017**, *318* (23), 2306−2316.

(20) Zhang, Q.; Li, H.; Poh, M.; Xia, F.; Cheng, Z.-Y.; Xu, H.; Huang, C. An All-Organic Composite Actuator Material with a High Dielectric Constant. *Nature* **2002**, *419* (6904), 284−287.

https://doi.org/10.1021/acsnano.3c01634
ACS Nano XXXX, XXX, XXX−XXX

(21) Majerus, S. J.; Garverick, S. L.; Suster, M. A.; Fletter, P. C.; Damaser, M. S. Wireless, Ultra-Low-Power Implantable Sensor for Chronic Bladder Pressure Monitoring. *ACM Journal on Emerging Technologies in Computing Systems (JETC)* **2012**, *8* (2), 1−13.
(22) Ko, W. H. Early History and Challenges of Implantable Electronics. *ACM Journal on Emerging Technologies in Computing Systems (JETC)* **2012**, *8* (2), 1−9.
(23) Sharma, A.; Panwar, V.; Mondal, B.; Prasher, D.; Bera, M. K.; Thomas, J.; Kumar, A.; Kamboj, N.; Mandal, D.; Ghosh, D. Electrical Stimulation Induced by a Piezo-Driven Triboelectric Nanogenerator and Electroactive Hydrogel Composite, Accelerate Wound Repair. *Nano Energy* **2022**, *99*, 107419.
(24) Song, P.; Kuang, S.; Panwar, N.; Yang, G.; Tng, D. J. H.; Tjin, S. C.; Ng, W. J.; Majid, M. B. A.; Zhu, G.; Yong, K. T.; et al. A Self-Powered Implantable Drug-Delivery System Using Biokinetic Energy. *Adv. Mater.* **2017**, *29* (11), 1605668.
(25) Fan, F.-R.; Tian, Z.-Q.; Lin Wang, Z. Flexible Triboelectric Generator. *Nano energy* **2012**, *1* (2), 328−334.
(26) Wang, Z. L. Triboelectric Nanogenerators as New Energy Technology for Self-Powered Systems and as Active Mechanical and Chemical Sensors. *ACS Nano* **2013**, *7* (11), 9533−9557.
(27) Zeng, W.; Shu, L.; Li, Q.; Chen, S.; Wang, F.; Tao, X. M. Fiber-Based Wearable Electronics: A Review of Materials, Fabrication, Devices, and Applications. *Advanced materials* **2014**, *26* (31), 5310−5336.
(28) Asadi, M. R.; Torkaman, G. Bacterial Inhibition by Electrical Stimulation. *Advances in wound care* **2014**, *3* (2), 91−97.
(29) Ita, K. Transdermal Iontophoretic Drug Delivery: Advances and Challenges. *J. Drug Targeting* **2016**, *24* (5), 386−391.
(30) Stewart, M. P.; Langer, R.; Jensen, K. F. Intracellular Delivery by Membrane Disruption: Mechanisms, Strategies, and Concepts. *Chem. Rev.* **2018**, *118* (16), 7409−7531.
(31) Wolcott, L. E.; et al. Accelerated Healing of Skin Ulcer by Electrotherapy: Preliminary Clinical Results. *South Med. J.* **1969**, *62*, 795−801.
(32) Xiao, X.; Xiao, X.; Nashalian, A.; Libanori, A.; Fang, Y.; Li, X.; Chen, J. Triboelectric Nanogenerators for Self-Powered Wound Healing. *Adv. Healthcare Mater.* **2021**, *10* (20), 2100975.
(33) Liu, Z.; Nie, J.; Miao, B.; Li, J.; Cui, Y.; Wang, S.; Zhang, X.; Zhao, G.; Deng, Y.; Wu, Y.; et al. Self-Powered Intracellular Drug Delivery by a Biomechanical Energy-Driven Triboelectric Nanogenerator. *Adv. Mater.* **2019**, *31* (12), 1807795.
(34) Song, P.; Yang, G.; Lang, T.; Yong, K.-T. Nanogenerators for Wearable Bioelectronics and Biodevices. *J. Phys. D: Appl. Phys.* **2019**, *52* (2), 023002.
(35) Chiu, C.-M.; Ke, Y.-Y.; Chou, T.-M.; Lin, Y.-J.; Yang, P.-K.; Wu, C.-C.; Lin, Z.-H. Self-Powered Active Antibacterial Clothing through Hybrid Effects of Nanowire-Enhanced Electric Field Electroporation and Controllable Hydrogen Peroxide Generation. *Nano energy* **2018**, *53*, 1−10.
(36) Zhang, Y.; Zhou, Z.; Sun, L.; Liu, Z.; Xia, X.; Tao, T. H. Genetically Engineered" Biofunctional Triboelectric Nanogenerators Using Recombinant Spider Silk. *Adv. Mater.* **2018**, *30* (50), 1805722.
(37) Du, S.; Zhou, N.; Xie, G.; Chen, Y.; Suo, H.; Xu, J.; Tao, J.; Zhang, L.; Zhu, J. Surface-Engineered Triboelectric Nanogenerator Patches with Drug Loading and Electrical Stimulation Capabilities: Toward Promoting Infected Wounds Healing. *Nano Energy* **2021**, *85*, 106004.
(38) Long, Y.; Wei, H.; Li, J.; Yao, G.; Yu, B.; Ni, D.; Gibson, A. L.; Lan, X.; Jiang, Y.; Cai, W.; et al. Effective Wound Healing Enabled by Discrete Alternative Electric Fields from Wearable Nanogenerators. *ACS Nano* **2018**, *12* (12), 12533−12540.
(39) Jeong, S.-H.; Lee, Y.; Lee, M.-G.; Song, W. J.; Park, J.-U.; Sun, J.-Y. Accelerated Wound Healing with an Ionic Patch Assisted by a Triboelectric Nanogenerator. *Nano Energy* **2021**, *79*, 105463.
(40) Du, S.; Suo, H.; Xie, G.; Lyu, Q.; Mo, M.; Xie, Z.; Zhou, N.; Zhang, L.; Tao, J.; Zhu, J. Self-Powered and Photothermal Electronic Skin Patches for Accelerating Wound Healing. *Nano Energy* **2022**, *93*, 106906.
(41) Ouyang, Q.; Feng, X.; Kuang, S.; Panwar, N.; Song, P.; Yang, C.; Yang, G.; Hemu, X.; Zhang, G.; Yoon, H. S.; et al. Self-Powered, on-Demand Transdermal Drug Delivery System Driven by Triboelectric Nanogenerator. *Nano Energy* **2019**, *62*, 610−619.
(42) Wu, C.; Jiang, P.; Li, W.; Guo, H.; Wang, J.; Chen, J.; Prausnitz, M. R.; Wang, Z. L. Self-Powered Iontophoretic Transdermal Drug Delivery System Driven and Regulated by Biomechanical Motions. *Adv. Funct. Mater.* **2020**, *30* (3), 1907378.
(43) Jiao, J.; Lu, Q.; Wang, Z.; Qin, Y.; Cao, X. Sandwich as a Triboelectric Nanogenerator. *Nano Energy* **2021**, *79*, 105411.
(44) Chen, H.; Lu, Q.; Cao, X.; Wang, N.; Wang, Z. L. Natural Polymers Based Triboelectric Nanogenerator for Harvesting Biomechanical Energy and Monitoring Human Motion. *Nano Research* **2022**, *15* (3), 2505−2511.
(45) Wang, Z. L.; Wang, A. C. On the Origin of Contact-Electrification. *Mater. Today* **2019**, *30*, 34−51.
(46) Zi, Y.; Niu, S.; Wang, J.; Wen, Z.; Tang, W.; Wang, Z. L. Standards and Figure-of-Merits for Quantifying the Performance of Triboelectric Nanogenerators. *Nat. Commun.* **2015**, *6* (1), 8376.
(47) Wang, Z. L. Triboelectric Nanogenerators as New Energy Technology and Self-Powered Sensors-Principles, Problems and Perspectives. *Faraday Discuss.* **2014**, *176*, 447−458.
(48) Chen, S.; Zheng, J.; Yu, L.; Ren, X.; Engelhard, M. H.; Niu, C.; Lee, H.; Xu, W.; Xiao, J.; Liu, J.; et al. High-Efficiency Lithium Metal Batteries with Fire-Retardant Electrolytes. *Joule* **2018**, *2* (8), 1548−1558.
(49) Liu, Z.; Li, H.; Shi, B.; Fan, Y.; Wang, Z. L.; Li, Z. Wearable and Implantable Triboelectric Nanogenerators. *Adv. Funct. Mater.* **2019**, *29* (20), 1808820.
(50) Khandelwal, G.; Maria Joseph Raj, N. P.; Kim, S.-J. Triboelectric Nanogenerator for Healthcare and Biomedical Applications. *Nano Today* **2020**, *33*, 100882.
(51) Li, X.; Tat, T.; Chen, J. Triboelectric Nanogenerators for Self-Powered Drug Delivery. *Trends in Chemistry* **2021**, *3* (9), 765−778.
(52) Tian, J.; Feng, H.; Yan, L.; Yu, M.; Ouyang, H.; Li, H.; Jiang, W.; Jin, Y.; Zhu, G.; Li, Z.; et al. A Self-Powered Sterilization System with Both Instant and Sustainable Anti-Bacterial Ability. *Nano Energy* **2017**, *36*, 241−249.
(53) Liu, C.; Xie, X.; Zhao, W.; Yao, J.; Kong, D.; Boehm, A. B.; Cui, Y. Static Electricity Powered Copper Oxide Nanowire Microbicidal Electroporation for Water Disinfection. *Nano Lett.* **2014**, *14* (10), 5603−5608.
(54) Chen, S. W.; Huang, S. M.; Wu, H. S.; Pan, W. P.; Wei, S. M.; Peng, C. W.; Ni, I. C.; Murti, B. T.; Tsai, M. L.; Wu, C. I.; et al. A Facile, Fabric Compatible, and Flexible Borophene Nanocomposites for Self-Powered Smart Assistive and Wound Healing Applications. *Adv. Sci. (Weinh)* **2022**, *9* (22), No. 2201507.
(55) Wan, D.; Yang, J.; Cui, X.; Ma, N.; Wang, Z.; Li, Y.; Li, P.; Zhang, Y.; Lin, Z.-H.; Sang, S. Human Body-Based Self-Powered Wearable Electronics for Promoting Wound Healing Driven by Biomechanical Motions. *Nano Energy* **2021**, *89*, 106465.
(56) Sharma, A.; Panwar, V.; Salaria, N.; Ghosh, D. Protease-Responsive Hydrogel, Cross-Linked with Bioactive Curcumin-Derived Carbon Dots, Encourage Faster Wound Closure. *Biomaterials Advances* **2022**, *139*, 212978.
(57) Chen, J.; Wang, Z. L. Reviving Vibration Energy Harvesting and Self-Powered Sensing by a Triboelectric Nanogenerator. *Joule* **2017**, *1* (3), 480−521.
(58) Ita, K.; Banga, A. In Vitro Transdermal Iontophoretic Delivery of Penbutolol Sulfate. *Drug Delivery* **2009**, *16* (1), 11−14.
(59) Sieg, A.; Jeanneret, F.; Fathi, M.; Hochstrasser, D.; Rudaz, S.; Veuthey, J.-L.; Guy, R. H.; Begona Delgado-Charro, M. Extraction of Amino Acids by Reverse Iontophoresis in Vivo. *Eur. J. Pharm. Biopharm.* **2009**, *72* (1), 226−231.
(60) Raiman, J.; Koljonen, M.; Huikko, K.; Kostiainen, R.; Hirvonen, J. Delivery and Stability of Lhrh and Nafarelin in Human Skin: The Effect of Constant/Pulsed Iontophoresis. *European journal of pharmaceutical sciences* **2004**, *21* (2−3), 371−377.

https://doi.org/10.1021/acsnano.3c01634
ACS Nano XXXX, XXX, XXX−XXX

(61) Guo, Y.; Zhang, Y.; Klein, R.; Nijm, G. M.; Sahakian, A. V.; Omary, R. A.; Yang, G.-Y.; Larson, A. C. Irreversible Electroporation Therapy in the Liver: Longitudinal Efficacy Studies in a Rat Model of Hepatocellular Carcinomairreversible Electroporation of Liver Tumors. *Cancer research* **2010**, *70* (4), 1555−1563.
(62) Caprettini, V.; Cerea, A.; Melle, G.; Lovato, L.; Capozza, R.; Huang, J.-A.; Tantussi, F.; Dipalo, M.; De Angelis, F. Soft Electroporation for Delivering Molecules into Tightly Adherent Mammalian Cells through 3d Hollow Nanoelectrodes. *Sci. Rep.* **2017**, *7* (1), 8524.
(63) Leppik, L.; Oliveira, K. M. C.; Bhavsar, M. B.; Barker, J. H. Electrical Stimulation in Bone Tissue Engineering Treatments. *European Journal of Trauma and Emergency Surgery* **2020**, *46* (2), 231−244.
(64) Luo, R.; Dai, J.; Zhang, J.; Li, Z. Accelerated Skin Wound Healing by Electrical Stimulation. *Adv. Healthc Mater.* **2021**, *10* (16), No. 2100557.
(65) Costerton, J. W.; DeMeo, P. Discussion: The Role of Biofilms: Are We Hitting the Right Target? *Plastic and reconstructive surgery* **2011**, *127*, 36S−37S.
(66) Zhao, M. Electrical Fields in Wound Healing—An Overriding Signal That Directs Cell Migration. In *Seminars in cell & developmental biology;* Elsevier, 2009; Vol. *20*, pp 674−682.
(67) Huttenlocher, A.; Horwitz, A. R. Wound Healing with Electric Potential. *New England Journal of Medicine* **2007**, *356* (3), 303−304.
(68) Jaffe, L. F.; Vanable Jr, J. W. Electric Fields and Wound Healing. *Clinics in dermatology* **1984**, *2* (3), 34−44.
(69) Mertz, P. Electrical Stimulation: Acceleration of Soft Tissue Repair by Varying the Polarity. *Wounds* **1993**, *5*, 153−159.
(70) Nishimura, K. Y.; Isseroff, R. R.; Nuccitelli, R. Human Keratinocytes Migrate to the Negative Pole in Direct Current Electric Fields Comparable to Those Measured in Mammalian Wounds. *Journal of cell science* **1996**, *109* (1), 199−207.
(71) Dunn, M. G.; Doillon, C. J.; Berg, R. A.; Olson, R. M.; Silver, F. H. Wound Healing Using a Collagen Matrix: Effect of Dc Electrical Stimulation. *J. Biomed. Mater. Res.* **1988**, *22* (S13), 191−206.
(72) Denker, S. P.; Barber, D. L. Cell Migration Requires Both Ion Translocation and Cytoskeletal Anchoring by the Na-H Exchanger Nhe1. *J. Cell Biol.* **2002**, *159* (6), 1087−1096.
(73) Konstantinou, E.; Zagoriti, Z.; Pyriochou, A.; Poulas, K. Microcurrent Stimulation Triggers Mapk Signaling and Tgf-B1 Release in Fibroblast and Osteoblast-Like Cell Lines. *Cells* **2020**, *9* (9), 1924.
(74) Bao, P.; Kodra, A.; Tomic-Canic, M.; Golinko, M. S.; Ehrlich, H. P.; Brem, H. The Role of Vascular Endothelial Growth Factor in Wound Healing. *Journal of Surgical Research* **2009**, *153* (2), 347−358.
(75) Reza Asadi, M.; Torkaman, G.; Hedayati, M. Effect of Sensory and Motor Electrical Stimulation in Vascular Endothelial Growth Factor Expression of Muscle and Skin in Full-Thickness Wound. *J. Rehabil Res. Dev* **2011**, *48* (3), 195−201.
(76) Kanno, S.; Oda, N.; Abe, M.; Saito, S.; Hori, K.; Handa, Y.; Tabayashi, K.; Sato, Y. Establishment of a Simple and Practical Procedure Applicable to Therapeutic Angiogenesis. *Circulation* **1999**, *99* (20), 2682−2687.
(77) Chen, Y.; Liang, Y.; Liu, J.; Yang, J.; Jia, N.; Zhu, C.; Zhang, J. Optimizing Microenvironment by Integrating Negative Pressure and Exogenous Electric Fields Via a Flexible Porous Conductive Dressing to Accelerate Wound Healing. *Biomaterials science* **2021**, *9* (1), 238−251.
(78) Hill, K. E.; Malic, S.; McKee, R.; Rennison, T.; Harding, K. G.; Williams, D. W.; Thomas, D. W. An in Vitro Model of Chronic Wound Biofilms to Test Wound Dressings and Assess Antimicrobial Susceptibilities. *J. Antimicrob. Chemother.* **2010**, *65* (6), 1195−1206.
(79) Monack, D. M.; Mueller, A.; Falkow, S. Persistent Bacterial Infections: The Interface of the Pathogen and the Host Immune System. *Nature Reviews Microbiology* **2004**, *2* (9), 747−765.
(80) Jarvis, W. R.; Martone, W. J. Predominant Pathogens in Hospital Infections. *Journal of antimicrobial chemotherapy* **1992**, *29* (supA), 19−24.
(81) Kaper, J. B.; Nataro, J. P.; Mobley, H. L. Pathogenic Escherichia Coli. *Nature reviews microbiology* **2004**, *2* (2), 123−140.
(82) Tong, S. Y.; Davis, J. S.; Eichenberger, E.; Holland, T. L.; Fowler Jr, V. G. Staphylococcus Aureus Infections: Epidemiology, Pathophysiology, Clinical Manifestations, and Management. *Clin. Microbiol. Rev.* **2015**, *28* (3), 603−661.
(83) Yuan Gao; Cranston, R. Recent Advances in Antimicrobial Treatments of Textiles. *Text. Res. J.* **2008**, *78* (1), 60−72.
(84) Van der Borden, A.; Van Der Mei, H.; Busscher, H. Electric Block Current Induced Detachment from Surgical Stainless Steel and Decreased Viability of Staphylococcus Epidermidis. *Biomaterials* **2005**, *26* (33), 6731−6735.
(85) Hong, S. H.; Jeong, J.; Shim, S.; Kang, H.; Kwon, S.; Ahn, K. H.; Yoon, J. Effect of Electric Currents on Bacterial Detachment and Inactivation. *Biotechnology and bioengineering* **2008**, *100* (2), 379−386.
(86) Liu, W.-K.; Brown, M.; Elliott, T. Mechanisms of the Bactericidal Activity of Low Amperage Electric Current (Dc). *Journal of antimicrobial chemotherapy* **1997**, *39* (6), 687−695.
(87) Gusbeth, C.; Frey, W.; Volkmann, H.; Schwartz, T.; Bluhm, H. Pulsed Electric Field Treatment for Bacteria Reduction and Its Impact on Hospital Wastewater. *Chemosphere* **2009**, *75* (2), 228−233.
(88) Rubinsky, L.; Guenther, E.; Mikus, P.; Stehling, M.; Rubinsky, B. Electrolytic Effects During Tissue Ablation by Electroporation. *Technology in cancer research & treatment* **2016**, *15* (5), NP95−NP103.
(89) Martínez-Huitle, C. A.; Brillas, E. Electrochemical Alternatives for Drinking Water Disinfection. *Angew. Chem., Int. Ed.* **2008**, *47* (11), 1998−2005.
(90) Qiang, Z.; Chang, J.-H.; Huang, C.-P. Electrochemical Generation of Hydrogen Peroxide from Dissolved Oxygen in Acidic Solutions. *Water Res.* **2002**, *36* (1), 85−94.
(91) Liu, C.; Xie, X.; Zhao, W.; Yao, J.; Kong, D.; Boehm, A. B.; Cui, Y. Static Electricity Powered Copper Oxide Nanowire Microbicidal Electroporation for Water Disinfection. *Nano Lett.* **2014**, *14* (10), 5603−5608.
(92) Shi, R.; Zhang, J.; Tian, J.; Zhao, C.; Li, Z.; Zhang, Y.; Li, Y.; Wu, C.; Tian, W.; Li, Z. An Effective Self-Powered Strategy to Endow Titanium Implant Surface with Associated Activity of Anti-Biofilm and Osteogenesis. *Nano Energy* **2020**, *77*, 105201.
(93) Wang, G.; Feng, H.; Hu, L.; Jin, W.; Hao, Q.; Gao, A.; Peng, X.; Li, W.; Wong, K.-Y.; Wang, H.; et al. An Antibacterial Platform Based on Capacitive Carbon-Doped Tio2 Nanotubes after Direct or Alternating Current Charging. *Nat. Commun.* **2018**, *9* (1), 2055.
(94) Gao, Y.; Sun, W.; Zhang, Y.; Liu, L.; Zhao, W.; Wang, W.; Song, Y.; Sun, Y.; Ma, Q. All-Aqueous Microfluidics Fabrication of Multifunctional Bioactive Microcapsules Promotes Wound Healing. *ACS Appl. Mater. Interfaces* **2022**, *14* (43), 48426−48437.
(95) Zhao, W.; Zhang, Y.; Liu, L.; Gao, Y.; Sun, W.; Sun, Y.; Ma, Q. Microfluidic-Based Functional Materials: New Prospects for Wound Healing and Beyond. *J. Mater. Chem. B* **2022**, *10* (41), 8357−8374.
(96) Gao, Y.; Ma, Q. Bacterial Infection Microenvironment-Responsive Porous Microspheres by Microfluidics for Promoting Anti-Infective Therapy. *Smart Medicine* **2022**, *1*
(97) Xu, F.; Wang, S.; Cao, C.; Ma, W.; Zhang, X.; Du, J.; Sun, W.; Ma, Q. Microfluidic Generation of Multifunctional Core-Shell Microfibers Promote Wound Healing. *Colloids Surf., B* **2022**, *219*, 112842.
(98) Liang, S.; Hofman, K.; Friedrich, M.; Keller, J.; Manolikakes, G. Recent Progress and Emerging Technologies Towards a Sustainable Synthesis of Sulfones. *ChemSusChem* **2021**, *14* (22), 4878−4902.
(99) Howell-Jones, R.; Wilson, M.; Hill, K. E.; Howard, A.; Price, P. E.; Thomas, D. W. A Review of the Microbiology, Antibiotic Usage and Resistance in Chronic Skin Wounds. *J. Antimicrob. Chemother.* **2005**, *55* (2), 143−149.
(100) Gosain, A.; DiPietro, L. A. Aging and Wound Healing. *World journal of surgery* **2004**, *28*, 321−326.
(101) Yu, L.; Yeo, J. C.; Soon, R. H.; Yeo, T.; Lee, H. H.; Lim, C. T. Highly Stretchable, Weavable, and Washable Piezoresistive Microfiber Sensors. *ACS Appl. Mater. Interfaces* **2018**, *10* (15), 12773−12780.
(102) Jo, A.; Seo, Y.; Ko, M.; Kim, C.; Kim, H.; Nam, S.; Choi, H.; Hwang, C. S.; Lee, M. J. Textile Resistance Switching Memory for Fabric Electronics. *Adv. Funct. Mater.* **2017**, *27* (15), 1605593.

https://doi.org/10.1021/acsnano.3c01634
ACS Nano XXXX, XXX, XXX−XXX

(103) Zou, H.; Zhang, Y.; Guo, L.; Wang, P.; He, X.; Dai, G.; Zheng, H.; Chen, C.; Wang, A. C.; Xu, C.; et al. Quantifying the Triboelectric Series. *Nat. Commun.* **2019**, *10* (1), 1427.
(104) Yang, Y.; Luo, R.; Chao, S.; Xue, J.; Jiang, D.; Feng, Y. H.; Guo, X. D.; Luo, D.; Zhang, J.; Li, Z.; et al. Improved Pharmacodynamics of Epidermal Growth Factor Via Microneedles-Based Self-Powered Transcutaneous Electrical Stimulation. *Nat. Commun.* **2022**, *13* (1), 6908.
(105) Zhao, M.; Dick, A.; Forrester, J. V.; McCaig, C. D. Electric Field-Directed Cell Motility Involves up-Regulated Expression and Asymmetric Redistribution of the Epidermal Growth Factor Receptors and Is Enhanced by Fibronectin and Laminin. *Molecular biology of the cell* **1999**, *10* (4), 1259−1276.
(106) Mukherjee, R.; Rivers, W. T.; Ruddy, J. M.; Matthews, R. G.; Koval, C. N.; Plyler, R. A.; Chang, E. I.; Patel, R. K.; Kern, C. B.; Stroud, R. E.; et al. Long-Term Localized High-Frequency Electric Stimulation within the Myocardial Infarct: Effects on Matrix Metalloproteinases and Regional Remodeling. *Circulation* **2010**, *122* (1), 20−32.
(107) Liu, Q.; Song, B. Electric Field Regulated Signaling Pathways. *international journal of biochemistry & cell biology* **2014**, *55*, 264−268.
(108) Ma, T.; Zhai, X.; Huang, Y.; Zhang, M.; Zhao, X.; Du, Y.; Yan, C. A Smart Nanoplatform with Photothermal Antibacterial Capability and Antioxidant Activity for Chronic Wound Healing. *Adv. Healthcare Mater.* **2021**, *10* (13), 2100033.
(109) Wang, X.; Yao, M.; Ma, L.; Yu, P.; Lu, T.; Zhang, L.; Yuan, X.; Zhang, Y.; Ye, J. Nir-Responsive Ti3c2Mxene Colloidal Solution for Curing Purulent Subcutaneous Infection through the "Nanothermal Blade" Effect. *Adv. Healthcare Mater.* **2021**, *10* (14), 2100392.
(110) Xie, G.; Zhou, N.; Gao, Y.; Du, S.; Du, H.; Tao, J.; Zhang, L.; Zhu, J. On-Demand Release of Co2 from Photothermal Hydrogels for Accelerating Skin Wound Healing. *Chemical Engineering Journal* **2021**, *403*, 126353.
(111) Zhao, H.; Huang, J.; Li, Y.; Lv, X.; Zhou, H.; Wang, H.; Xu, Y.; Wang, C.; Wang, J.; Liu, Z. Ros-Scavenging Hydrogel to Promote Healing of Bacteria Infected Diabetic Wounds. *Biomaterials* **2020**, *258*, 120286.
(112) Song, S.; Wang, J.; Cheng, Z.; Yang, Z.; Shi, L.; Yu, Z. Directional Molecular Sliding Movement in Peptide Hydrogels Accelerates Cell Proliferation. *Chemical science* **2020**, *11* (5), 1383−1393.
(113) Yuan, R.; Yang, N.; Fan, S.; Huang, Y.; You, D.; Wang, J.; Zhang, Q.; Chu, C.; Chen, Z.; Liu, L.; et al. Biomechanical Motion-Activated Endogenous Wound Healing through Lbl Self-Powered Nanocomposite Repairer with Ph-Responsive Anti-Inflammatory Effect. *Small* **2021**, *17* (50), 2103997.
(114) Adhikary, P.; Mahmud, M. P.; Solaiman, T.; Wang, Z. L. Recentadvances on Biomechanical Motion-Driven Triboelectric Nanogenerators for Drug Delivery. *Nano Today* **2022**, *45*, 101513.
(115) Priemel, M.; von Domarus, C.; Klatte, T. O.; Kessler, S.; Schlie, J.; Meier, S.; Proksch, N.; Pastor, F.; Netter, C.; Streichert, T.; et al. Bone Mineralization Defects and Vitamin D Deficiency: Histomorphometric Analysis of Iliac Crest Bone Biopsies and Circulating 25-Hydroxyvitamin D in 675 Patients. *J Bone Miner Res* **2010**, *25* (2), 305−312.
(116) Tian, J.; Shi, R.; Liu, Z.; Ouyang, H.; Yu, M.; Zhao, C.; Zou, Y.; Jiang, D.; Zhang, J.; Li, Z. Self-Powered Implantable Electrical Stimulator for Osteoblasts' Proliferation and Differentiation. *Nano Energy* **2019**, *59*, 705−714.
(117) Jiang, W.; Li, H.; Liu, Z.; Li, Z.; Tian, J.; Shi, B.; Zou, Y.; Ouyang, H.; Zhao, C.; Zhao, L.; et al. Fully Bioabsorbable Natural-Materials-Based Triboelectric Nanogenerators. *Adv. Mater.* **2018**, *30* (32), No. e1801895.
(118) Schmidt, C. E.; Leach, J. B. Neural Tissue Engineering: Strategies for Repair and Regeneration. *Annu. Rev. Biomed. Eng.* **2003**, *5* (1), 293−347.
(119) Willerth, S. M.; Sakiyama-Elbert, S. E. Approaches to Neural Tissue Engineering Using Scaffolds for Drug Delivery. *Advanced drug delivery reviews* **2007**, *59* (4−5), 325−338.
(120) Guo, W.; Zhang, X.; Yu, X.; Wang, S.; Qiu, J.; Tang, W.; Li, L.; Liu, H.; Wang, Z. L. Self-Powered Electrical Stimulation for Enhancing Neural Differentiation of Mesenchymal Stem Cells on Graphene-Poly(3,4-Ethylenedioxythiophene) Hybrid Microfibers. *ACS Nano* **2016**, *10* (5), 5086−5095.
(121) Yang, R.; Wei, T.; Goldberg, H.; Wang, W.; Cullion, K.; Kohane, D. S. Getting Drugs across Biological Barriers. *Adv. Mater.* **2017**, *29* (37), 1606596.
(122) Fenton, O. S.; Olafson, K. N.; Pillai, P. S.; Mitchell, M. J.; Langer, R. Advances in Biomaterials for Drug Delivery. *Adv. Mater.* **2018**, *30* (29), 1705328.
(123) Kalia, Y. N.; Naik, A.; Garrison, J.; Guy, R. H. Iontophoretic Drug Delivery. *Advanced drug delivery reviews* **2004**, *56* (5), 619−658.
(124) Yi, Y.; Sun, J.; Lu, Y.; Liao, Y. Programmable and on-Demand Drug Release Using Electrical Stimulation. *Biomicrofluidics* **2015**, *9* (2), 022401.
(125) Ita, K. Transdermal Delivery of Heparin: Physical Enhancement Techniques. *Int. J. Pharm.* **2015**, *496* (2), 240−249.
(126) Pandey, P. C.; Shukla, S.; Skoog, S. A.; Boehm, R. D.; Narayan, R. J. Current Advancements in Transdermal Biosensing and Targeted Drug Delivery. *Sensors* **2019**, *19* (5), 1028.
(127) Langer, R. Drug Delivery and Targeting. *Nature* **1998**, *392*, 5−10.
(128) Prausnitz, M. R. Microneedles for Transdermal Drug Delivery. *Advanced drug delivery reviews* **2004**, *56* (5), 581−587.
(129) Henry, S.; McAllister, D. V.; Allen, M. G.; Prausnitz, M. R. Microfabricated Microneedles: A Novel Approach to Transdermal Drug Delivery. *Journal of pharmaceutical sciences* **1998**, *87* (8), 922−925.
(130) Bok, M.; Lee, Y.; Park, D.; Shin, S.; Zhao, Z.-J.; Hwang, B.; Hwang, S. H.; Jeon, S. H.; Jung, J.-Y.; Park, S. H.; et al. Microneedles Integrated with a Triboelectric Nanogenerator: An Electrically Active Drug Delivery System. *Nanoscale* **2018**, *10* (28), 13502−13510.
(131) Khalifa, M.; Mahendran, A.; Anandhan, S. Durable, Efficient, and Flexible Piezoelectric Nanogenerator from Electrospun Pani/Hnt/Pvdf Blend Nanocomposite. *Polym. Compos.* **2019**, *40* (4), 1663−1675.
(132) Lu, Y.; Jiang, L.; Yu, Y.; Wang, D.; Sun, W.; Liu, Y.; Yu, J.; Zhang, J.; Wang, K.; Hu, H.; et al. Liquid-Liquid Triboelectric Nanogenerator Based on the Immiscible Interface of an Aqueous Two-Phase System. *Nat. Commun.* **2022**, *13* (1), 5316.
(133) van der Vliet, D. F.; Wang, C.; Li, D.; Paulikas, A. P.; Greeley, J.; Rankin, R. B.; Strmcnik, D.; Tripkovic, D.; Markovic, N. M.; Stamenkovic, V. R. Unique Electrochemical Adsorption Properties of Pt-Skin Surfaces. *Angew. Chem., Int. Ed.* **2012**, *51* (13), 3139−3142.
(134) Stamenkovic, V. R.; Mun, B. S.; Mayrhofer, K. J.; Ross, P. N.; Markovic, N. M. Effect of Surface Composition on Electronic Structure, Stability, and Electrocatalytic Properties of Pt-Transition Metal Alloys: Pt-Skin Versus Pt-Skeleton Surfaces. *J. Am. Chem. Soc.* **2006**, *128* (27), 8813−8819.
(135) Shi, X.; Chen, Y.; Zhao, Y.; Ye, M.; Zhang, S.; Gong, S. Ultrasound-Activable Piezoelectric Membranes for Accelerating Wound Healing. *Biomaterials Science* **2022**, *10* (3), 692−701.
(136) Bok, M.; Zhao, Z. J.; Jeon, S.; Jeong, J. H.; Lim, E. Ultrasonically and Iontophoretically Enhanced Drug-Delivery System Based on Dissolving Microneedle Patches. *Sci. Rep* **2020**, *10* (1), 2027.
(137) Chen, J.; Zhu, G.; Yang, W.; Jing, Q.; Bai, P.; Yang, Y.; Hou, T. C.; Wang, Z. L. Harmonic-Resonator-Based Triboelectric Nanogenerator as a Sustainable Power Source and a Self-Powered Active Vibration Sensor. *Advanced materials* **2013**, *25* (42), 6094−6099.
(138) Zhao, H.; Xu, M.; Shu, M.; An, J.; Ding, W.; Liu, X.; Wang, S.; Zhao, C.; Yu, H.; Wang, H.; et al. Underwater Wireless Communication Via Teng-Generated Maxwell's Displacement Current. *Nat. Commun.* **2022**, *13* (1), 3325.
(139) Conta, G.; Libanori, A.; Tat, T.; Chen, G.; Chen, J. Triboelectric Nanogenerators for Therapeutic Electrical Stimulation. *Adv. Mater.* **2021**, *33* (26), No. 2007502.
(140) Zhang, W.; Wang, P.; Sun, K.; Wang, C.; Diao, D. Intelligently Detecting and Identifying Liquids Leakage Combining Triboelectric

https://doi.org/10.1021/acsnano.3c01634
ACS Nano XXXX, XXX, XXX−XXX

Nanogenerator Based Self-Powered Sensor with Machine Learning. *Nano Energy* **2019**, *56*, 277−285.
(141) Wang, X.; Yang, B.; Liu, J.; He, Q.; Guo, H.; Yang, C.; Chen, X. Flexible Triboelectric and Piezoelectric Coupling Nanogenerator Based on Electrospinning P (Vdf-Trfe) Nanowires. In *2015 28th IEEE International Conference on Micro Electro Mechanical Systems (MEMS)*, 2015; IEEE: pp 110−113.
(142) Xu, W.; Zheng, H.; Liu, Y.; Zhou, X.; Zhang, C.; Song, Y.; Deng, X.; Leung, M.; Yang, Z.; Xu, R. X.; et al. A Droplet-Based Electricity Generator with High Instantaneous Power Density. *Nature* **2020**, *578* (7795), 392−396.
(143) Sun, M.; Li, Z.; Yang, C.; Lv, Y.; Yuan, L.; Shang, C.; Liang, S.; Guo, B.; Liu, Y.; Li, Z.; et al. Nanogenerator-Based Devices for Biomedical Applications. *Nano Energy* **2021**, *89*, 106461.
(144) Kim, I.; Roh, H.; Yu, J.; Jeon, H.; Kim, D. A Triboelectric Nanogenerator Using Silica-Based Powder for Appropriate Technology. *Sensors and Actuators A: Physical* **2018**, *280*, 85−91.
(145) Seol, M.-L.; Han, J.-W.; Moon, D.-I.; Yoon, K. J.; Hwang, C. S.; Meyyappan, M. All-Printed Triboelectric Nanogenerator. *Nano Energy* **2018**, *44*, 82−88.
(146) Lin, L.; Xie, Y.; Niu, S.; Wang, S.; Yang, P.-K.; Wang, Z. L. Robust Triboelectric Nanogenerator Based on Rolling Electrification and Electrostatic Induction at an Instantaneous Energy Conversion Efficiency of∼ 55%. *ACS Nano* **2015**, *9* (1), 922−930.

https://doi.org/10.1021/acsnano.3c01634
ACS Nano XXXX, XXX, XXX−XXX